Intercalation du lithium dans FeWO4C1 ; intercalation d'entités vanadates dans des hydroxydes doubles lamellaires dérivés de Ni(OH)2

Kyoo-Seung Han

N° d'ordre : 1477

T 96 17

THESE

PRESENTEE A

L'UNIVERSITE BORDEAUX I

ECOLE DOCTORALE DES SCIENCES CHIMIQUES

par **HAN KYOO - SEUNG**

POUR OBTENIR LE GRADE DE

DOCTEUR

SPECIALITE : **CHIMIE DU SOLIDE, SCIENCES DES MATERIAUX**

Titre : - Intercalation du lithium dans $FeWO_4Cl$
- Intercalation d'entités vanadates dans des hydroxydes doubles lamellaires dérivés de $Ni(OH)_2$

Soutenue le **30 Janvier 1996**

Après avis de :

MM. J. P. BESSE ----------] Rapporteurs
D. GUYOMARD ----------]

Devant la commission d'examen formée de :

MM.	J. ETOURNEAU	Professeur ----------	Président
	J. P. BESSE	Directeur de Recherche au CNRS ----]	
	D. GUYOMARD	Directeur de Recherche au CNRS ----]	Examinateurs
Mme	L. GUERLOU-DEMOURGUES	Maître de conférences ----------]	
M.	C. DELMAS	Directeur de Recherche au CNRS ----]	

- 1996 -

A ma famille.

REMERCIEMENTS

Ce travail a été réalisé au sein du Groupe Ionique du Solide, Interface entre l'Institut de Chimie de la Matière Condensée de Bordeaux du CNRS, dirigé par Monsieur le Professeur **J. ETOURNEAU** et l'Ecole Nationale Supérieure de Chimie et Physique de Bordeaux, dirigée par Monsieur le Professeur **H. GASPAROUX**. Qu'ils veuillent agréer l'expression de ma profonde reconnaissance pour l'accueil qu'ils m'ont réservé. Je tiens à remercier tout particulièrement Monsieur **J. ETOURNEAU** d'avoir accepté de présider le jury de ma thèse.

Monsieur **J. P. BESSE**, Directeur de Recherche au Laboratoire de Physico-Chimie des Matériaux de Clermont-Ferrand, a bien voulu mobiliser son temps et sa compétence pour être rapporteur de ma thèse et membre du jury. Qu'il soit assuré de ma profonde reconnaissance.

Monsieur **D. GUYOMARD**, Directeur de Recherche au Institut des Matériaux de Nantes, me fait l'honneur de juger ce travail en tant que rapporteur. Qu'il en soit vivement remercié.

Madame **L. GUERLOU-DEMOURGUES**, Maître de Conférences à l'Ecole Nationale Supérieure de Chimie et Physique de Bordeaux, me fait l'honneur de participer à ce jury. Elle a été d'une complète disponibilité et m'a beaucoup apporté par ses nombreux conseils et sa gentillesse. Qu'elle soit assurée de ma profonde reconnaissance et de ma sincère amitié.

Monsieur **C. DELMAS**, Directeur de Recherche au CNRS, a suivi et dirigé mes travaux. Il m'a fait partager son enthousiasme pour la recherche et m'a fait bénéficier de ses conseils avisés et de son expérience. Je voudrais lui exprimer ma profonde reconnaissance et l'en remercier très sincèrement.

Je remercie Monsieur le Professeur **A. LEVASSEUR**, co-responsable du groupe, pour ses conseils amicaux.

Monsieur **J. H. CHOY**, Professeur à "Seoul National University" en Corée du Sud, m'a permis de bénéficier d'une initiation en Chimie du Solide et de ses conseils humains et amicaux. Je tiens à lui exprimer toute ma reconnaissance et ma sincère amitié.

Monsieur **P. GRAVEREAU**, Professeur à l'Université de Bordeaux I, a pris une part active à la première partie de ce travail et m'a fait profiter avec beaucoup de gentillesse et de son expérience dans le domaine de la cristallographie.

Monsieur **M. MENETRIER**, Ingénieur de Recherche au CNRS, a su m'initier avec une grande patience à la Résonance Magnétique Nucléaire. Il m'a fait bénéficier de ses nombreux conseils et a fait preuve à mon égard de beaucoup de gentillesse.

Je remercie **A. DEMOURGUES**, Chargé de Recherche au CNRS, pour sa compétence lors de l'étude EXAFS et XANES. Je remercie également **E. DUGUET**, Maître de Conférences à l'Université de Bordeaux I, pour sa gentillesse, son étroite collaboration et sa compétence lors de l'étude de la polymérisation interfeuillet des matériaux organiques.

Je remercie tous les chercheurs et techniciens du laboratoire pour leur aide scientifique et en particulier, **J. P. CAZORLA**, **M. DUPEYRON** et **L. TRUT**.

C. DENAGE, **H. DUJARRIC** et **S. GOMA** m'ont aidé quotidiennement à la réalisation de ce travail. Ils m'ont été d'une aide précieuse, tant au point de vue technique qu'humain. Je tiens à les en remercier très sincèrement.

Mes remerciements les plus vifs s'adressent à **A. ROUGIER** pour sa disponibilité, sa sympathie et son esprit de collaboration. Qu'elle soit assurée de ma reconnaissance et de mon amitié.

Je remercie tous mes collègues pour leur soutien et leur amitié, en particulier : **A. AATIQ, M. BUTEL, F. CAPITAINE, S. H. CHANG, H. COGNAC, C. DUSSARRAT, C. ESTOURNES, C. FAURE, O. GASET, L. GAUTIER, M. HESS, D. Y. JUNG, B. Y. KIM, C. LAMBERT, E. LEBRAUD, C. LEGER, M. MALLACE, H. MOUDDEN, J. P. PERES, V. PREVOST, A. POTTIER, I. SAADOUNE, E. SCHMIDT, D. Y. SEUNG, Y. J. SHIN, K. S. SUH, P. VINATIER**.

Je ne saurais oublier de saluer mes copains **H. S. AHN, S. Y. AHN, H. M. CHAI, E. S. CHOI, O. S. HONG, H. S. KIM, S. J. KIM, S. J. KWON, G. O. LEE, H. J. LEE, J. R. PARK, D. Y. WANG**.

Enfin un remerciement particulier s'adresse à **J. H. GONG** qui m'a apporté un très grand réconfort moral par ses qualités humaines. Je lui exprime ma profonde amitié.

SOMMAIRE

NOTE AU LECTEUR

Ce travail entre dans le cadre des études générales réalisées sur les matériaux d'intercalation au sein du Groupe Ionique du Solide.

Nos travaux ont porté sur l'intercalation de deux types d'espèces dans des structures lamellaires : d'une part, le lithium dans l'oxychlorure de fer et de tungstène $FeWO_4Cl$ et d'autre part, des ions complexes vanadate dans des hydroxydes doubles lamellaires.

Ce travail a donné lieu à quatre publications qui sont présentées en fin de mémoire. Nous proposons en début de mémoire un résumé visant à donner au lecteur une vue générale et plus homogène de ce travail.

RESUMES

I. INSERTION DU LITHIUM DANS $FeWO_4Cl$

I. 1. INTRODUCTION

L'étude des réactions d'intercalation d'éléments alcalins connaît un succès considérable depuis plus d'une décennie en relation avec les problèmes de stockage électrochimique de l'énergie.

Les réactions d'intercalation et de désintercalation des ions lithium peuvent être effectuées par voie chimique ou électrochimique. La figure 1 représente schématiquement le fonctionnement d'un générateur électrochimique réversible ayant du lithium comme électrode négative et le matériau étudié comme électrode positive.

Les réactions d'intercalation ou de désintercalation électrochimique peuvent être simulées par des réactions chimiques avec des systèmes oxydants ou réducteurs ayant un ion lithium comme contre ion.

Récement plusieurs groupes de recherche ont étudié l'intercalation du lithium dans le composé bidimensionnel $FeMoO_4Cl$ [1-3]. La réaction d'intercalation du lithium dans $FeMoO_4Cl$ est réversible dans le domaine de composition ($FeMoO_4Cl$-$LiFeMoO_4Cl$) [1]. Ayant obtenu la phase $FeWO_4Cl$ isotype de $FeMoO_4Cl$, nous avons entrepris l'étude de l'intercalation du lithium dans ce matériau.

I. 2. PREPARATION DES MATERIAUX

Le composé lamellaire $FeWO_4Cl$ a été préparé par la technique du transport chimique en phase vapeur (CVT) à partir d'un mélange de WO_3, Fe_2O_3 et $FeCl_3$.

La phase $LiFeWO_4Cl$ peut être obtenue par intercalation électrochimique ou chimique du lithium dans $FeWO_4Cl$.

Ces procédés sont schématisés à la figure 2.

I. 3. COMPORTEMENT ELECTROCHIMIQUE

La figure 3 représente la courbe donnant la variation du potentiel en fonction de la quantité du lithium intercalée (décharge avec relaxation jusqu'à une pente $\Delta V/\Delta t \leq 0.1 mV/h$). Cette courbe montre que seul le premier plateau de potentiel ($0.00 < x < 0.85$) correspond à un vrai domaine biphasé entre la phase $FeWO_4Cl$ et $Li_{0.85}FeWO_4Cl$. Par contre, pour les deux autres plateaux, les valeurs du potentiel en fin

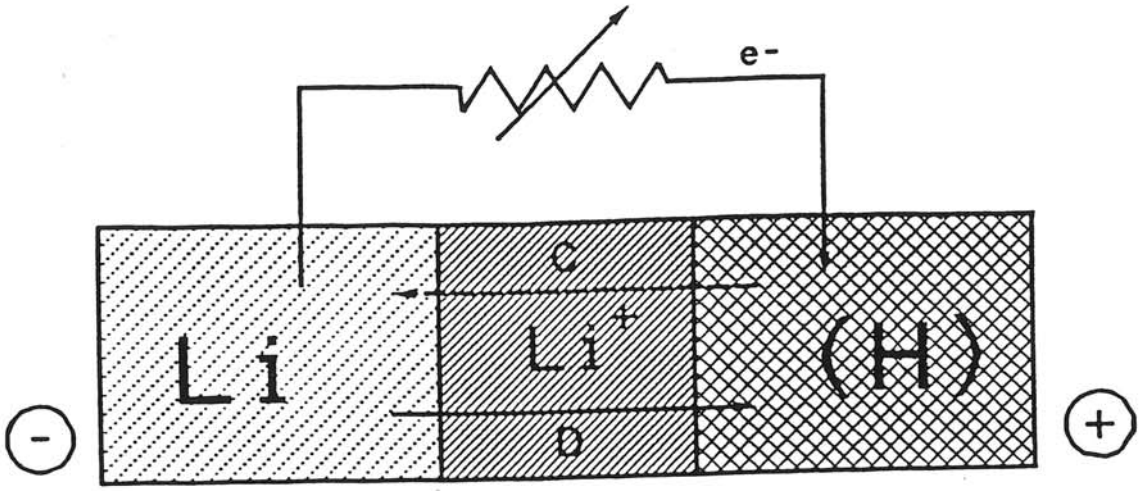

$$D : DISCHARGE \begin{cases} xLi \longrightarrow xLi^{+} + xe^{-} \\ (H) + xLi^{+} + xe^{-} \longrightarrow Li_x(H) \end{cases}$$

$$C : CHARGE \begin{cases} Li_x(H) \longrightarrow xLi^{+} + xe^{-} + (H) \\ xLi^{+} + xe^{-} \longrightarrow xLi \end{cases}$$

Fig. 1 : Représentation schématique d'une batterie au lithium.

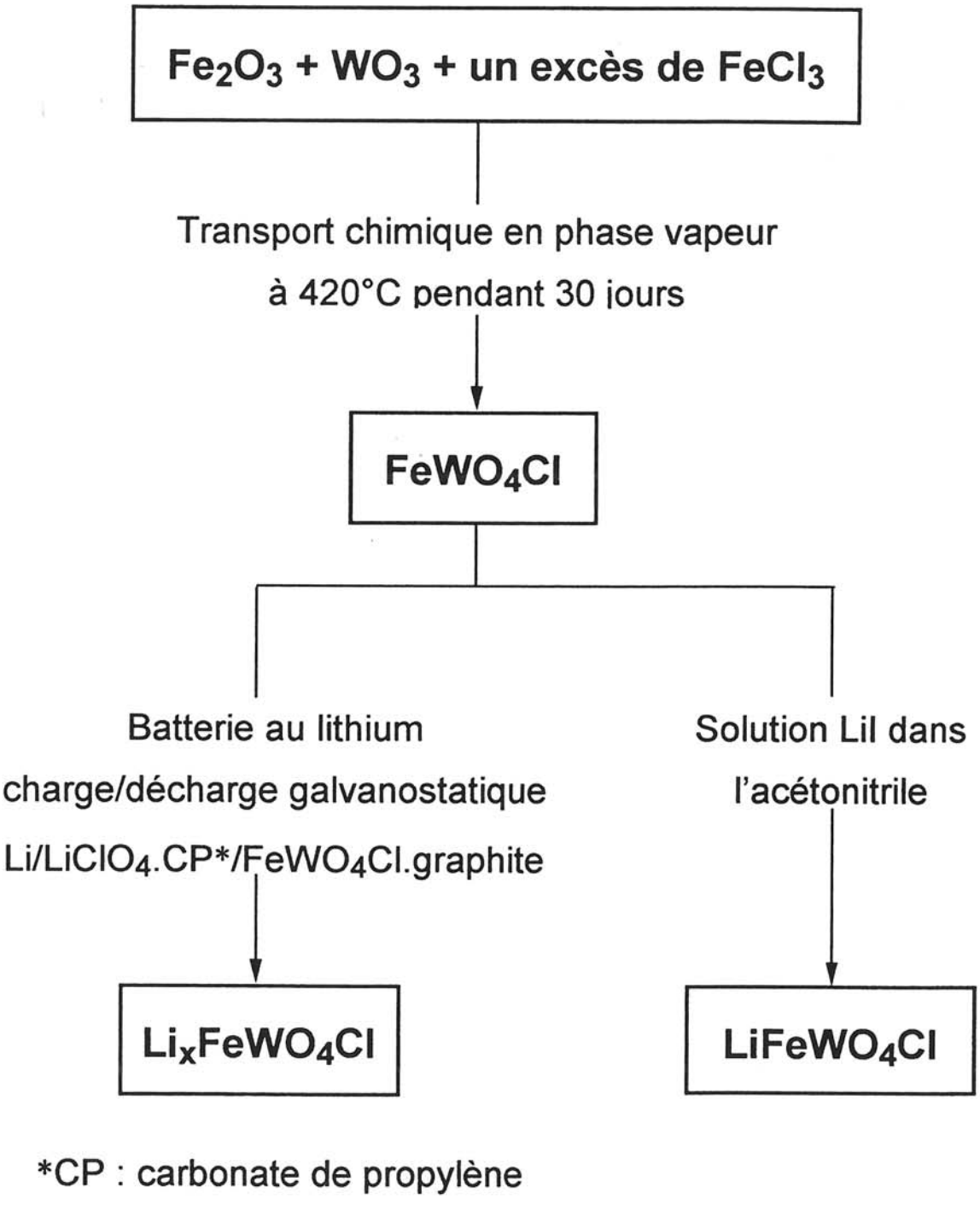

Fig. 2 : Schéma de préparation des matériaux étudiés.

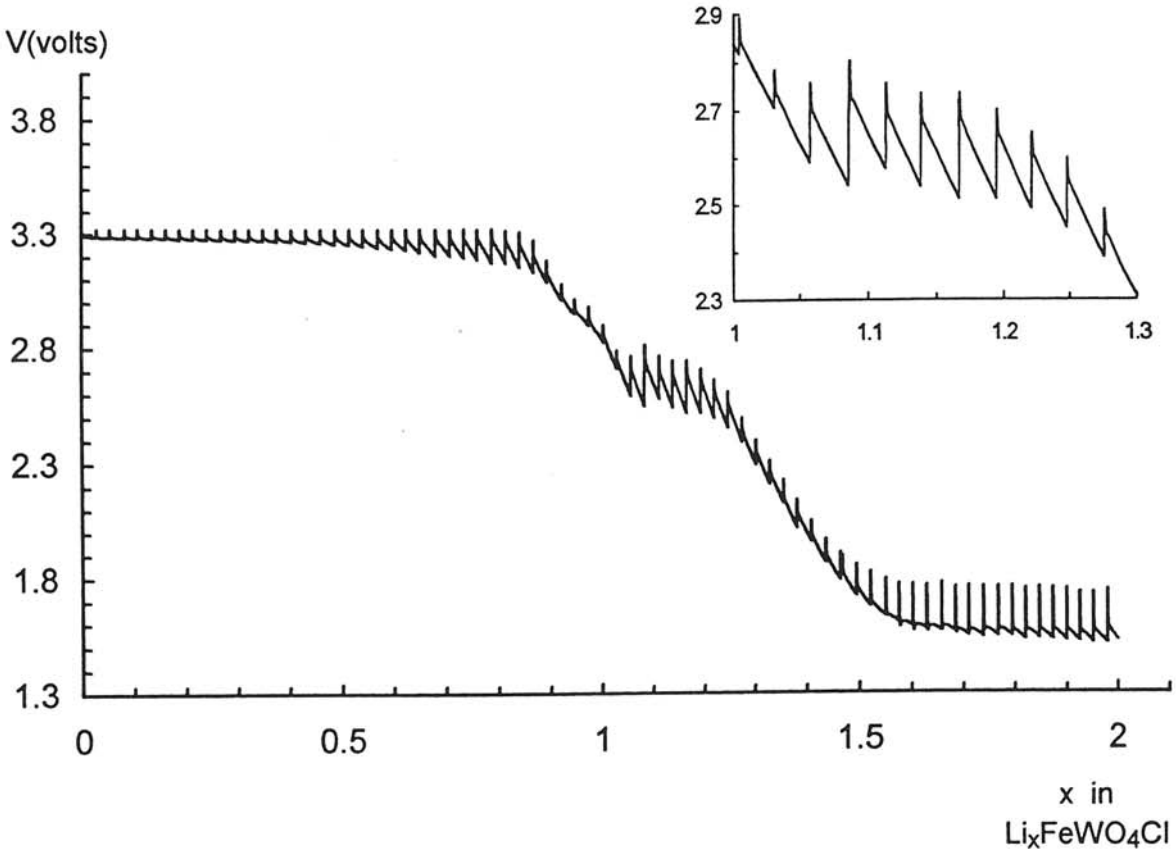

Fig. 3 : Courbe de première décharge d'un générateur Li//$FeWO_4Cl$ entrecoupée de périodes de relaxation.

de relaxation varient légèrement d'une composition à une autre indiquant qu'un processus irréversible apparaît. Pour le dernier plateau, cette hypothèse est confirmée par l'étude par diffraction des rayons X faite sur le matériau obtenu après l'intercalation de deux ions lithium. Au voisinage de la composition $LiFeWO_4Cl$, un domaine de solution solide a été mis en évidence ($0.85 \leq x \leq 1.05$). L'intercalation est complètement réversible dans le domaine $0 \leq x \leq 1.05$.

I. 4. CARACTERISATION DES STRUCTURES

La phase $FeWO_4Cl$ cristallise dans le système quadratique (Groupe d'espace : P4/nmm) et la phase $LiFeWO_4Cl$ dans le système monoclinique (Groupe d'espace : $P2_1/m$). Leurs paramètres des mailles sont montrés au tableau I.

L'analyse structurale sur monocristal de la phase $FeWO_4Cl$ et l'affinement par la méthode de Rietveld de la structure de la phase $LiFeWO_4Cl$ effectué à l'aide du programme FULLPROF [4] ont été réalisés en collaboration avec P. Gravereau.

Après divers cycles d'affinement, l'analyse sur monocristal de $FeWO_4Cl$ conduit aux facteurs de reliabilité $R = 0.026$ et $R_w = 0.032$ tandis que l'affinement Rietveld de $LiFeWO_4Cl$ conduit à $R_I = 0.056$ et $R_{wp} = 0.171$.

La figure 4 représente les vues en perspective de la structure de $FeWO_4Cl$ et de $LiFeWO_4Cl$ (programme CERIUS). La structure de $FeWO_4Cl$ peut être décrite comme un empilement de couches constituées de tétraèdres WO_4 partageant leurs sommets avec les oxygènes des pyramides à base carrée FeO_4Cl. Chaque atome de chlore n'est lié qu'à un atome de fer et les atomes de chlore pointent alternativement vers le haut et le bas.

La très grande différence entre la distance Fe-Cl au sein d'une couche (2.18 Å) et la distance Fe-Cl′ entre deux couches successives (3.03 Å) illustre clairement le caractère 2D de la structure de $FeWO_4Cl$. Cette structure est très voisine de celle de $FeMoO_4Cl$.

L'augmentation des distances Fe-O lors de l'intercalation du lithium montre que le fer est réduit à l'état divalent.

Paramètres de maille	a (Å)	b (Å)	c (Å)	β (°)
$FeWO_4Cl$	6.631(9)	6.631(9)	5.223(9)	90.00
$LiFeWO_4Cl$	7.071(3)	6.947(1)	5.060(0)	91.5(2)

Tableau I : Valeurs des paramètres de maille de $FeWO_4Cl$ et de $LiFeWO_4Cl$.

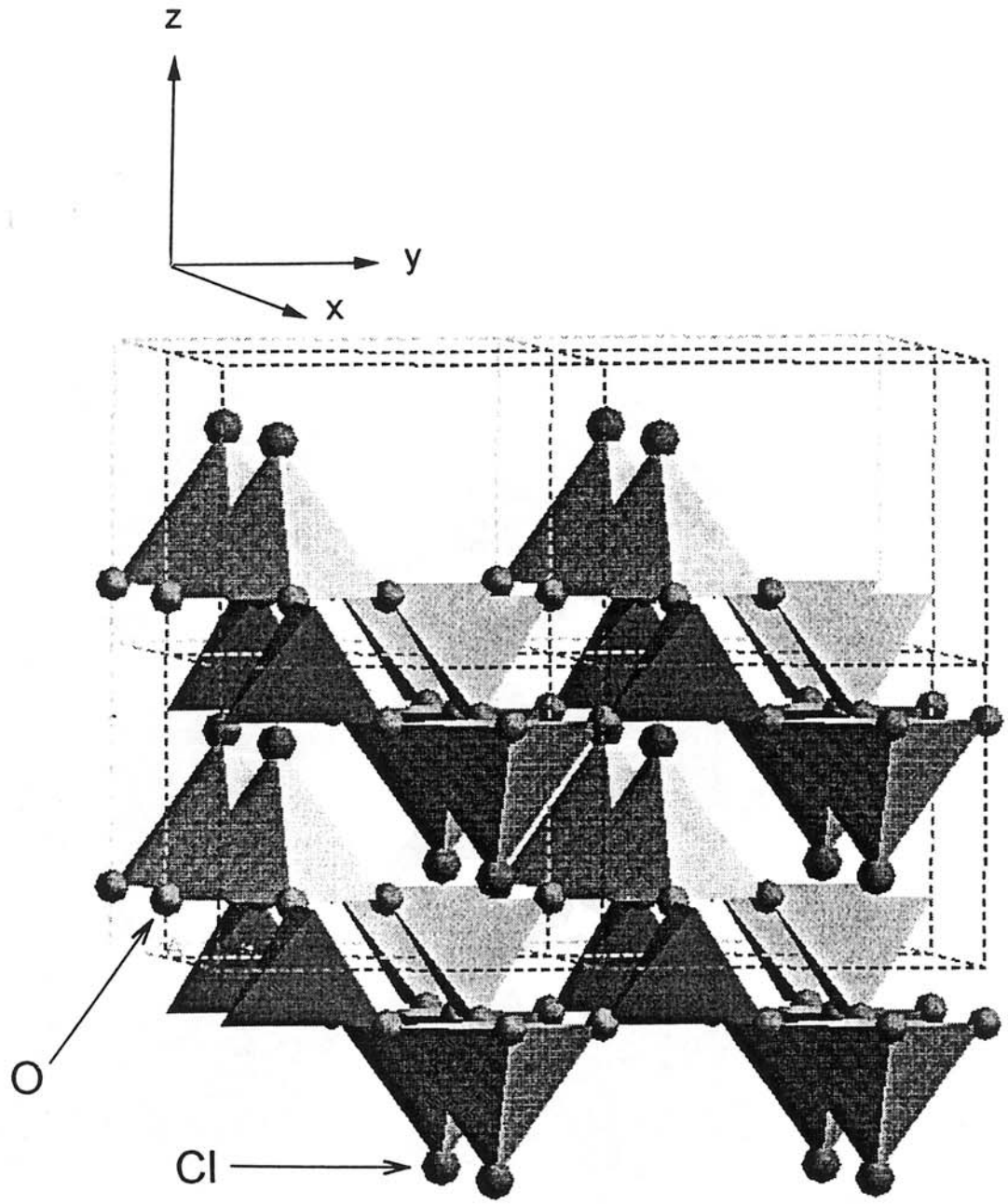

Fig. 4 (a) : Vue en perspective de la structure de $FeWO_4Cl$.

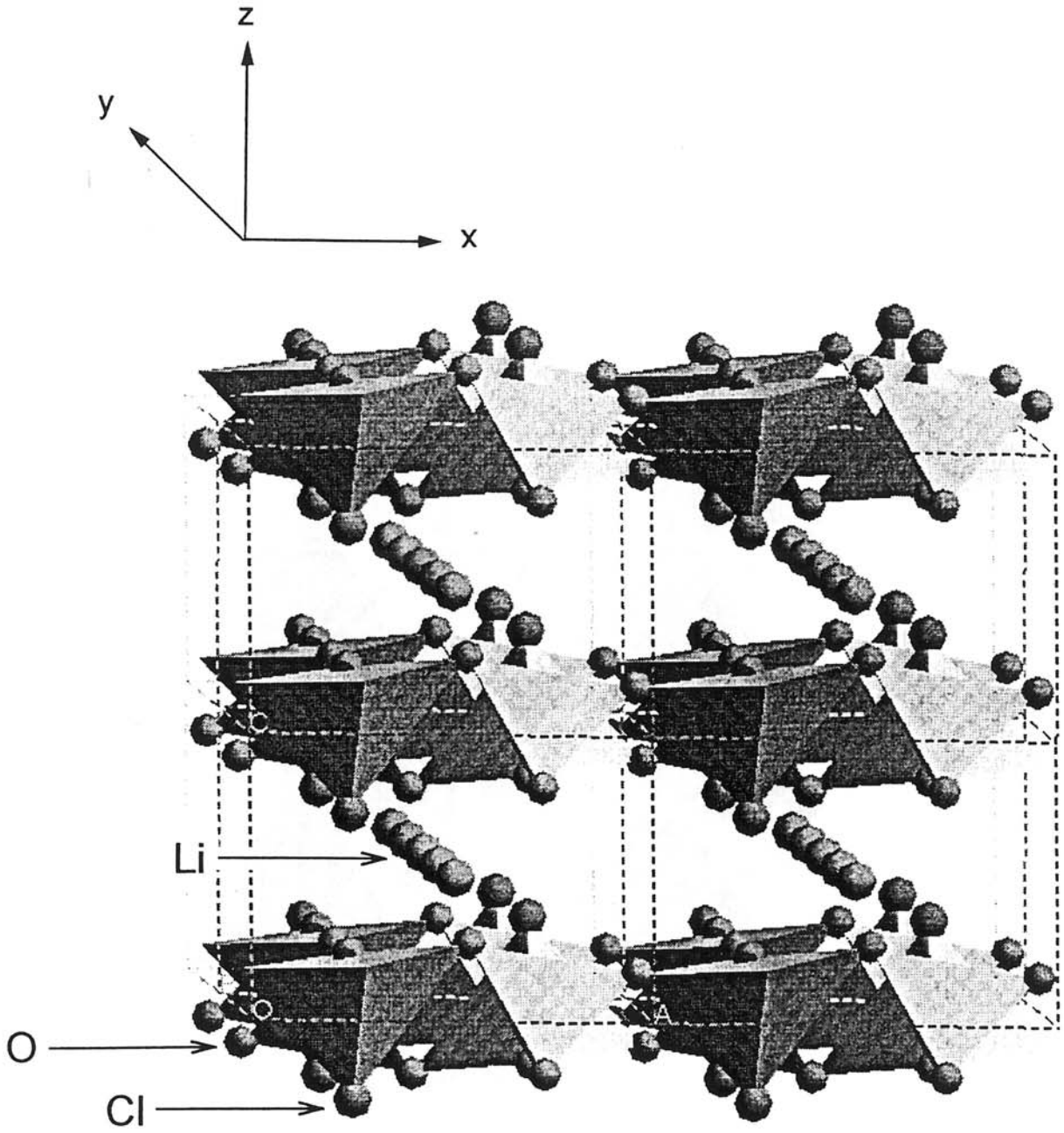

Fig. 4 (b) : Vue en perspective de la structure de $LiFeWO_4Cl$.

Lors de l'intercalation du lithium, la distance Fe-Cl s'allonge alors que la distance Fe-Cl′ diminue considérablement de telle sorte que l'on doit considérer la pyramide à base carrée FeO_4Cl' comme environnement du fer (Fig. 5). Dans le cas du système $LiFeMoO_4Cl$, les distances Fe-Cl et Fe-Cl′ étant plus proche, l'on était plutôt amené à considérer les structures comme tridimensionelles [3].

Il faut remarquer que dans tous les cas la forte diminution du paramètre c traduit une forte contraction du réseau perpendiculairement aux feuillets. Ce comportement montre que l'effet attractif électrostatique l'emporte sur l'effet stérique répulsif.

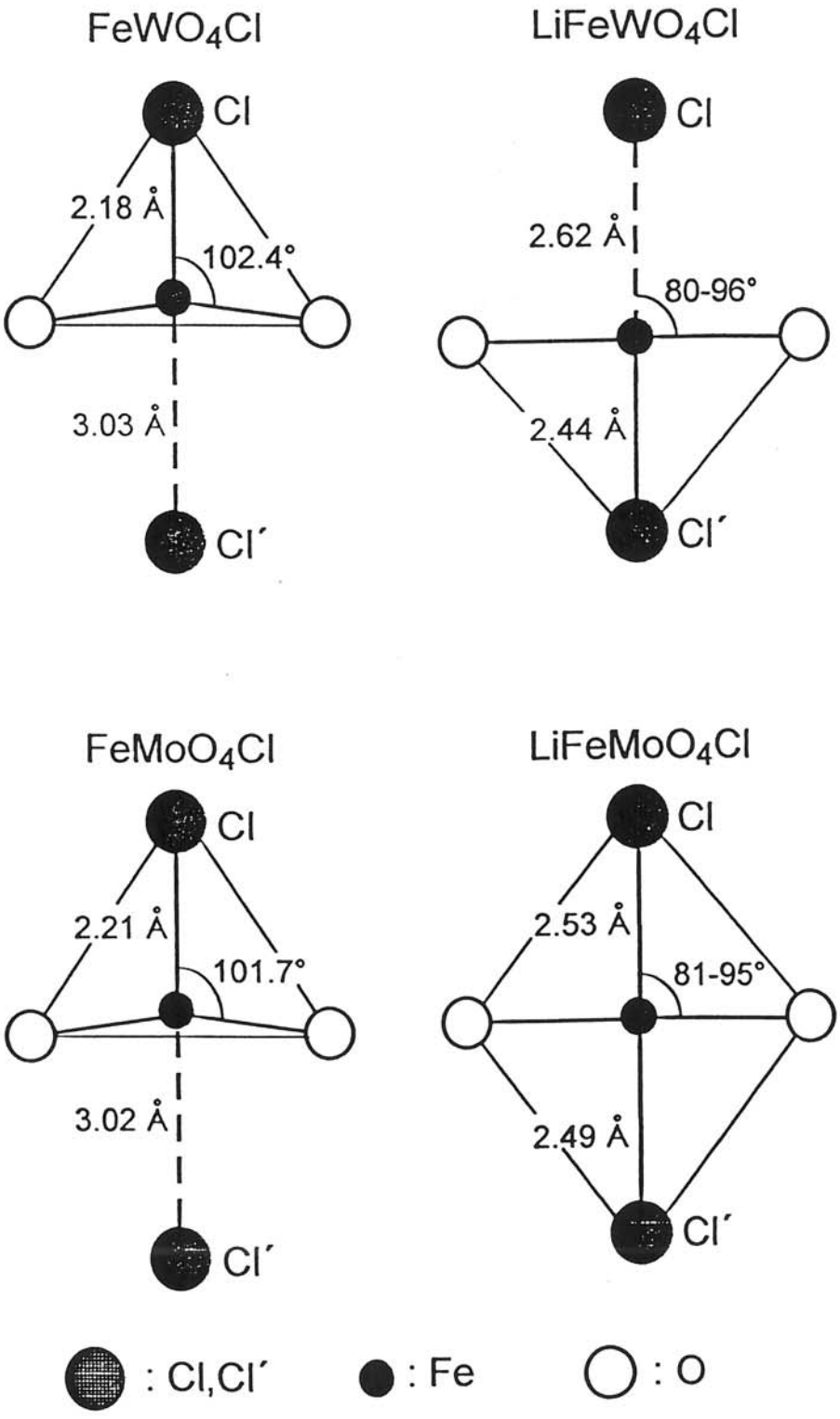

Fig. 5 : Modifications de l'environnement du fer dans $FeW(Mo)O_4Cl$ lors de l'intercalation du lithium.

BIBLIOGRAPHIE

[1] C. Delmas, S. H. Chang, D. Y. Dnoh and J. H. Choy, Solid State Ionics, 40/41 (1990) 563.

[2] J. H. Choy, D. Y. Noh, S. H. Chang and C. Delmas, Eur. J. Solid State Inorg. Chem., 27 (1990) 391.

[3] C. C. Torardi, W. M. Reiff, K. Lazar and E. Prince, J. Phys. Chem. Solids, 47(8) (1986) 741.

[4] J. Rodriguez-Carvajal, Collected Abstracts of Powder Diffraction Meeting, Toulouse (France) (1990) 127.

II. INSERTION DES IONS COMPLEXES VANADATE DANS DES HYDROXYDES DOUBLES LAMELLAIRES

II. 1. INTRODUCTION

L'intérêt des hydroxydes doubles lamellaires (notés usuellement LDHs comme "Layered Double Hydroxides") réside dans leurs propriétés d'échange anioniques, utilisables dans de très nombreuses applications pratiques (électrodes positives de batterie, adsorbants, tamis moléculaires, retardateurs de flamme, échangeurs d'ions, etc.), ainsi que dans leur potentialité d'utilisation comme précurseurs de nouveaux matériaux catalytiques [1,2].

Ces hydroxydes sont soit des minéraux naturels soit des phases synthétiques. Leur formule générale est la suivante : $[M^{II}_{1-y}\ L^{III}_{y}\ (OH)_2]^{y+}\ X^{p-}_{y/p}\ [H_2O]_z$ où

- M désigne un cation divalent tel que Mg, Ni, Zn, Fe, Co, Cu,
- L désigne un cation trivalent tel que Al, Cr, Mn, Fe, Co,
- X^{p-} un anion tel que NO_3^-, OH^-, Cl^-, CO_3^{2-}, SO_4^{2-}, etc.

La structure de ces matériaux consiste en un empilement de feuillets de type brucite, $\left[M^{II}_{1-y}\ L^{III}_{y}\ (OH)_2\right]$, entre lesquels s'intercalent des molécules d'eau et des anions X^{p-} [2], ainsi que le schématise la figure 1. La maille cristalline est constituée soit de deux feuillets par maille hexagonale (type structural P2, observé dans les "sjögrenites") soit de trois feuillets par maille en symétrie rhomboédrique (type structural P3, observé dans les "pyroaurites" ou les "hydrotalcites") [3,4]. La présence des anions X^{p-} est nécessaire afin de compenser l'excès de charge positive dû à la substitution partielle d'ions trivalents (L) aux ions divalents (M) au sein des feuillets. La structure est alors stabilisée par l'existence d'un réseau de liaisons hydrogène entre les molécules d'eau, les anions et les ions hydroxyle du feuillet ainsi que par des interactions électrostatiques s'exerçant entre les feuillets et les anions X^{p-}. Ces derniers jouent alors le rôle de piliers dans la structure.

Ces matériaux étant généralement préparés par précipitation à partir d'une solution appropriée contenant les ions M^{II} et L^{III}, ils présentent un état de cristallinité médiocre ainsi que des fluctuations de composition, dues essentiellement à l'écart existant entre les valeurs de pH de précipitation des hydroxydes $M(OH)_2$ et $L(OH)_3$. La formule chimique du matériau final est donc plutôt conditionnée par sa stabilité

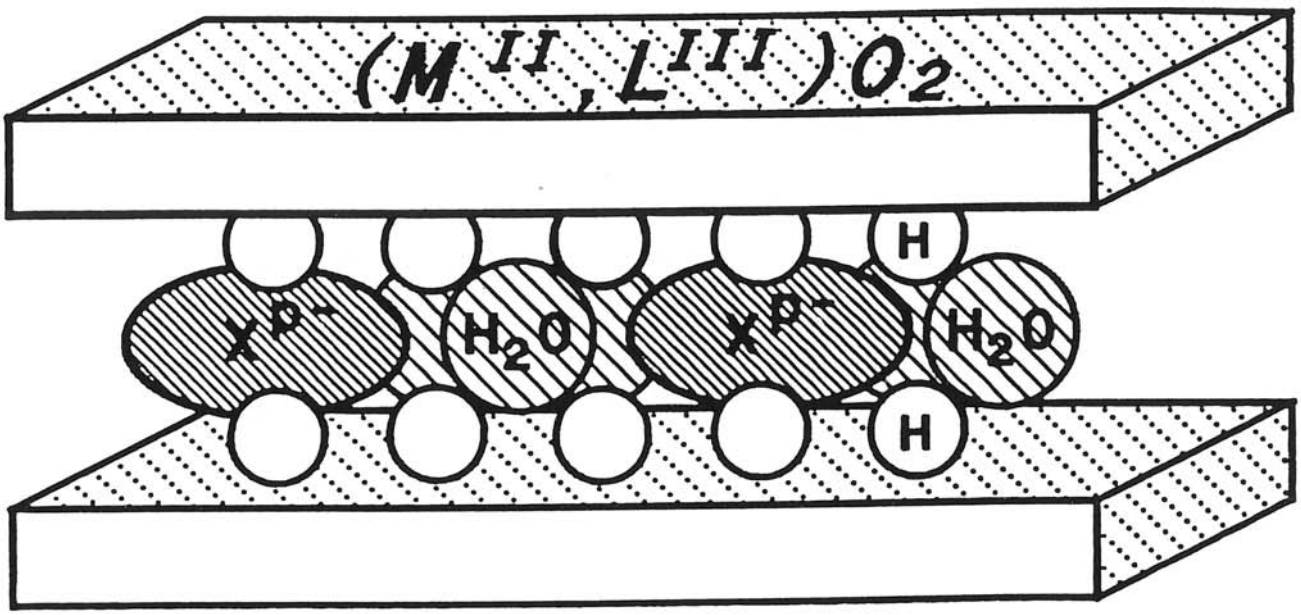

Fig. 1- Représentation schématique de la structure d'un hydroxyde double lamellaire.

intrinsèque que par la composition de la solution avant précipitation. Dans ces conditions, il s'avère difficile de contrôler la quantité d'anions insérés. Afin de contourner ces problèmes, nous avons développé au laboratoire une nouvelle voie de synthèse par chimie douce permettant de découpler la construction du feuillet $M_{1-y}L_yO_2$ de l'intercalation anionique proprement dite [5-8]. Cette méthode dérive de celle qui est utilisée dans notre laboratoire pour l'obtention d'hydroxydes de nickel hydratés substitués au cobalt ou au fer, utilisables en tant que matériaux d'électrode positive dans des batteries nickel-cadmium, nickel-hydrogène ou nickel-hydrure métallique [7-9]. Ainsi que le schématise la figure 2, la première étape consiste à préparer l'oxyde lamellaire $NaM_{1-y}L_yO_2$ par synthèse classique de chimie du solide à haute température. Dans une seconde étape, les LDHs désirés sont obtenus à partir de ces précurseurs par chimie douce (hydrolyse oxydante suivie d'une réduction). En supposant que le choix des éléments M et L soit approprié, lors de la réduction, M est réduit à l'état divalent alors que L reste dans un degré d'oxydation supérieur à 2. La quantité d'anions intercalés est directement liée au degré d'oxydation et à la concentration de l'élément L. Ainsi, un plus large domaine de composition peut être obtenu par chimie douce, presque indépendamment de la stabilité du produit final. Des travaux antérieurs ont montré que les LDHs mixtes de nickel et de cobalt ou de fer peuvent être obtenus par de telles réactions de chimie douce à partir des matériaux $NaNi_{1-y}Co_yO_2$ ($0.2 \leq y \leq 0.5$) [5] ou $NaNi_{1-y}Fe_yO_2$ ($0.2 \leq y \leq 0.7$) [9].

L'objectif de notre étude consiste à obtenir des LDHs similaires en insérant des espèces anioniques volumineuses susceptibles de générer dans l'espace interfeuillet de larges cavités adaptées aux réactions catalytiques. De ce point de vue, les espèces vanadates apparaissent comme de bons candidats pour l'intercalation dans les LDHs, ainsi que l'ont signalé Twu et al. [10]. De plus, il est bien connu que les oxydes de vanadium peuvent être utilisés pour l'oxydation sélective des hydrocarbures en vue de la préparation du butadiène, de l'anhydride maléique, etc. [10]. En conséquence, l'intercalation d'anions vanadate entre des feuillets $Ni_{0.70}Co_{0.30}(OH)_2$ a été entreprise. Le mécanisme d'intercalation des espèces vanadate a été étudié avec une attention particulière, ainsi que les propriétés d'échange et le comportement thermique.

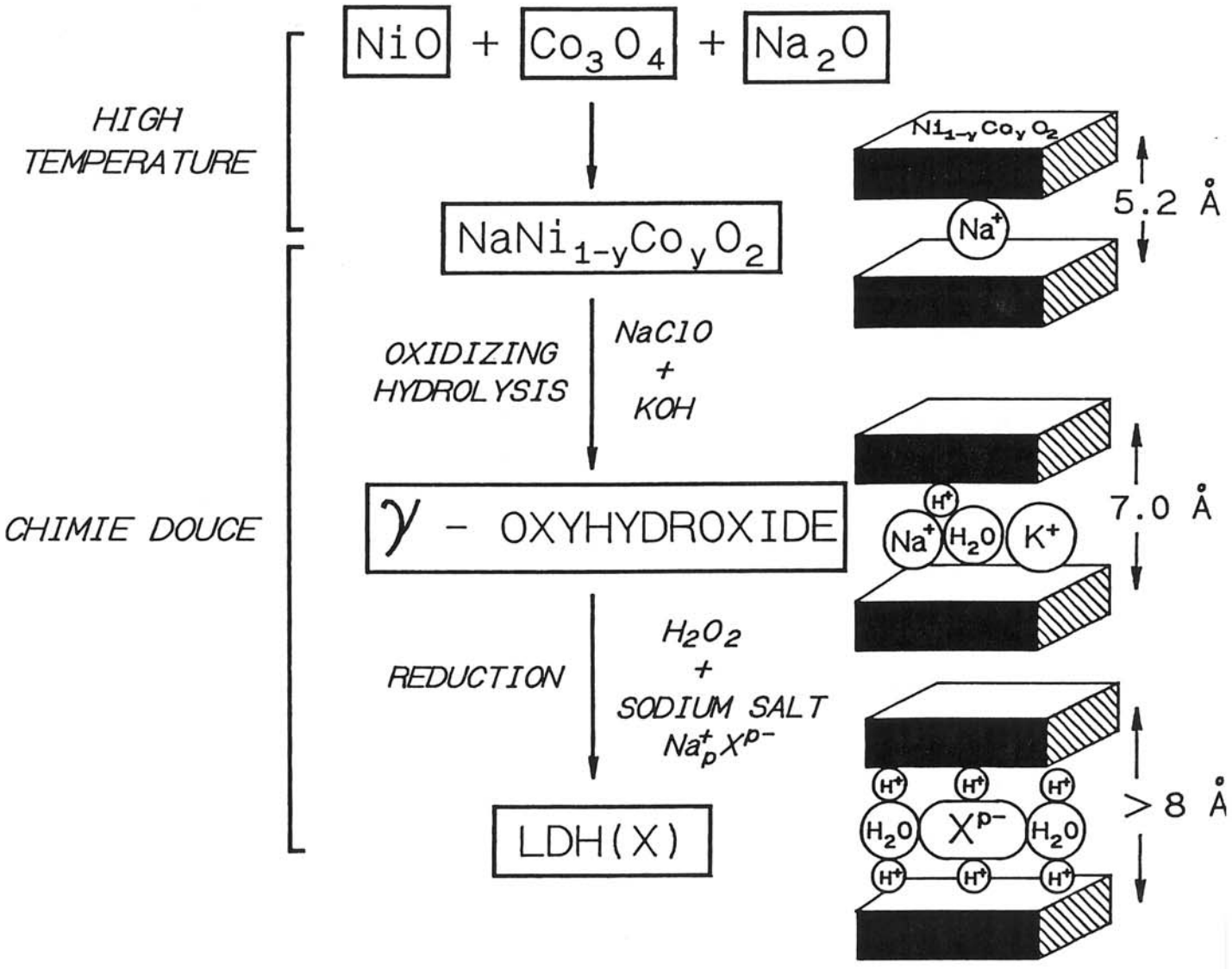

Fig. 2- Schéma représentant les différentes étapes intervenant lors de la préparation d'un hydroxyde double lamellaire par chimie douce.

II. 2. PREPARATION DES MATERIAUX

Les LDHs présentant des espèces vanadate intercalées sont préparés par réduction en milieu NH_4VO_3 / H_2O_2 d'un oxyhydroxyde de nickel substitué au cobalt noté γ dans la terminologie utilisée dans le domaine des hydroxydes de nickel [11,12]. Selon les conditions de préparation, deux familles de matériaux distincts ont été obtenues, ainsi que le schématise la figure 3. Le matériau de départ de la première famille, désigné par LDH(VO_3), est issu d'un séjour de 15 jours dans la solution réductrice [11]. Il a ensuite été traité soit thermiquement (à 100°C et 190°C) soit sous vide. En ce qui concerne la deuxième famille, le matériau de départ a été préparé par réduction et filtration simultanées ; il sera donc désigné par LDH fraîchement préparé. Ce matériau a ensuite été exposé à l'air et son évolution a été suivie en fonction du temps de vieillissement [12]. Notons que les conditions de préparation de LDH(VO_3) et du matériau obtenu après vieillissement à l'air de LDH fraîchement préparé sont différentes : le vieillissement s'effectue en effet dans le milieu liquide réactionnel dans le premier cas et dans l'air dans le second cas. Néanmoins, la caractérisation du LDH fraîchement préparé tout au long du vieillissement à l'air est susceptible de permettre une meilleure appréhension du mécanisme d'intercalation conduisant à LDH(VO_3).

II. 3. CARACTERISATION DE LDH(VO_3)

Ce matériau a été caractérisé par diffraction des rayons X, analyse chimique et spectroscopie infrarouge.

L' analyse chimique du matériau conduit à la formule : $Ni_{0.70}Co_{0.30}(OH)_2(VO_3)_{0.34}(H_2O)_{0.58}$. Cette formule implique la présence d'une charge négative par élément vanadium, ce qui suggère la présence d'espèces métavanadate intercalées. L'étude infrarouge permet alors de conclure qu'il s'agit de chaînes $(VO_3)_n^{n-}$ constituées de tétraèdres VO_4 liés par les sommets, similaires à celles présentes dans NH_4VO_3 solide. Ces résultats justifient l'appellation LDH(VO_3).

Le diffractogramme de rayons X présente de fortes analogies avec celui de phases homologues présentant des ions carbonate insérés et cristallisant dans le système rhomboédrique. Il révèle une distance interfeuillet de l'ordre de 9.15 Å ainsi que

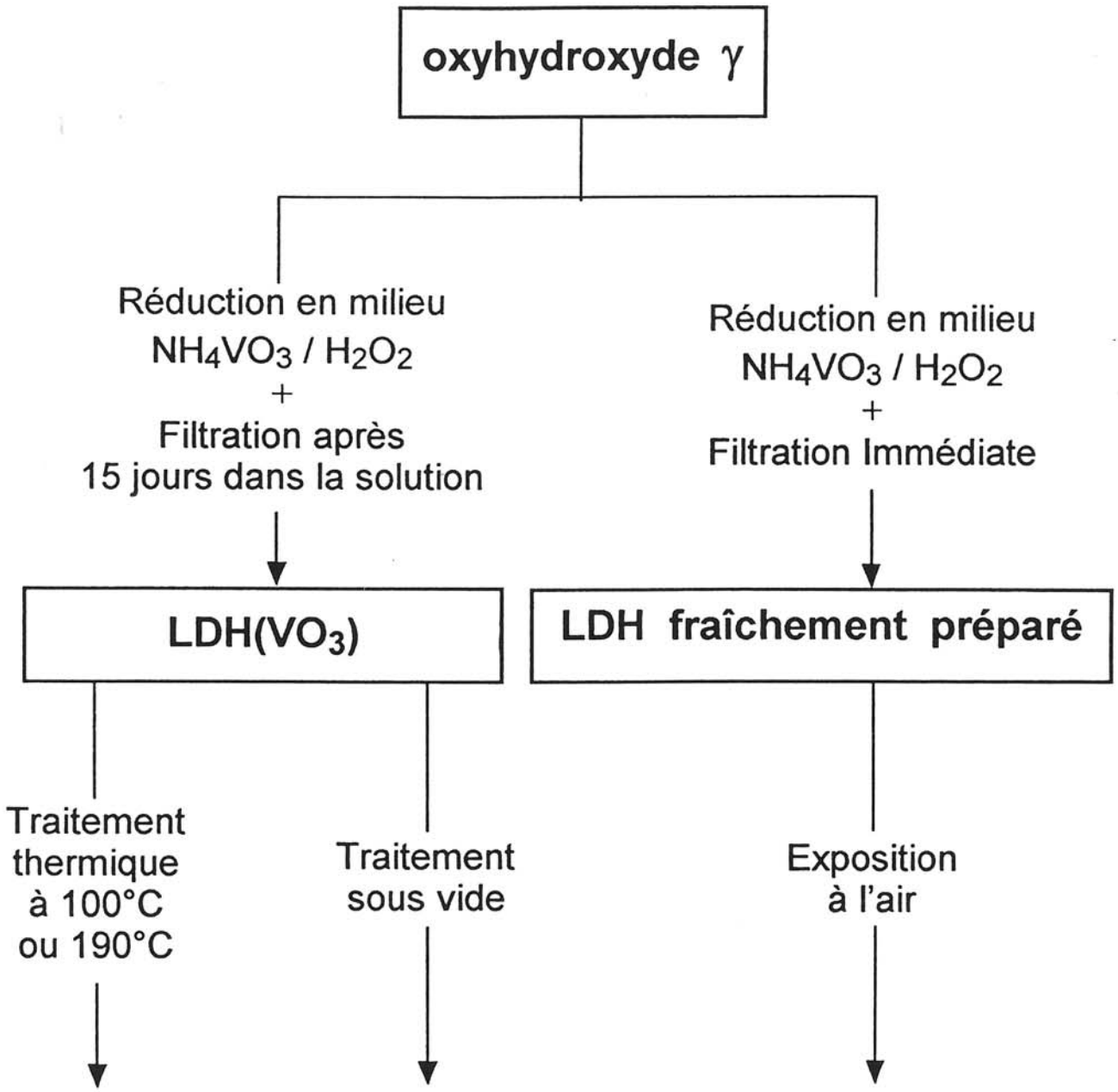

Fig. 3- Schéma de préparation des deux familles de matériaux étudiés.

l'existence de bandes (10ℓ) et (11ℓ) larges et dissymétriques (maille hexagonale), qui sont observées de manière usuelle dans les matériaux lamellaires présentant un caractère turbostratique marqué. Ce phénomène de turbostraticité correspond à une désorientation (rotation) les uns par rapport aux autres des plans régulièrement empilés le long de l'axe c_{hex}. Un cyclage chimique (oxydation et réduction successives) réalisé à partir du matériau LDH(VO_3) conduit à une résolution des raies (10ℓ) lors de l'oxydation suivie à nouveau d'un élargissement en bande lors de la réduction suivante. Ce comportement suggère dans le matériau LDH(VO_3) l'existence de distorsions locales au sein des feuillets plutôt qu'un caractère turbostratique effectif. Ces distorsions locales résultent vraisemblablement de contraintes intrafeuillets induites par les interactions électrostatiques entre les chaînes $(VO_3)_n^{n-}$ et les feuillets $Ni_{0.70}Co_{0.30}(OH)_2$.

Une étude du comportement thermique du matériau a été réalisée. L'ATG révèle entre 20°C et 190°C une première perte de masse, correspondant à un départ des molécules d'eau interfoliaires et à une déshydroxylation partielle des feuillets. Au delà de 190°C, la déshydroxylation se poursuit puis la structure s'effondre pour donner naissance aux oxydes NiO, V_2O_5 et Co_3O_4. L'évolution des diffractogrammes de rayons X lorsque la température augmente montre une diminution progressive de la distance interfeuillet de 9.15 Å (à 20°C) à 7.21 Å (à 190°C) ainsi qu'une structuration des bandes larges (10ℓ) et (11ℓ) en raies séparées, traduisant une diminution des distorsions locales au sein des feuillets. La diminution de la distance interfeuillet, observée par ailleurs dans des matériaux de type hydrotalcite [13], peut être interprété en terme de greffage des chaînes $(VO_3)_n^{n-}$ aux feuillets, c'est à dire le remplacement d'ions hydroxyles des feuillets par des ions oxygène des tétraèdres VO_4 constituant les chaînes. Les distances oxygène-oxygène au sein des feuillets $Ni_{0.70}Co_{0.30}(OH)_2$ (3.04 Å) et des chaînes $(VO_3)_n^{n-}$ insérées (2.91 Å) étant différentes, le greffage accroît les contraintes stériques au sein du matériau. Afin de relâcher ces contraintes, une fragmentation des chaînes se produit, se traduisant par la modification du profil des bandes de diffraction (10ℓ) et (11ℓ) précédemment évoquées. Ce comportement est en accord avec la formule chimique déduite de la courbe d'ATG à 190°C, $Ni_{0.70}Co_{0.30}(OH)_{1.66}(V_2O_7)_{0.17}$, qui

correspond à la présence d'entité V_2O_7 greffées via les deux ions oxygène apicaux des tétraèdres VO_4 à deux feuillets adjacents, ainsi que le montre la figure 4. Le greffage couplé à une fragmentation des chaînes conduit à la formation d'eau qui est éliminée lors du traitement thermique.

II. 4. EVOLUTION A L'AIR DU "LDH FRAICHEMENT PREPARE"

L'hydroxyde double lamellaire est obtenu par réduction d'un oxyhydroxyde en milieu NH_4VO_3 / H_2O_2 qui, dans les conditions expérimentales utilisées ici (0.5 M-H_2O_2, 0.14 M-NH_4VO_3 et pH = 4), contient des espèces peroxovanadate et non des chaînes métavanadate $(VO_3)_n^{n-}$. Sur la base de ces données issus de la littérature, l'évolution au cours du temps des entités vanadate insérées de prime abord dans l'hydroxyde double lamellaire a été étudiée par diffraction des rayons X, analyse chimique, spectroscopie infrarouge et RMN du ^{51}V.

La forte diminution de la distance interfeuillet (10.1 Å pour le LDH fraîchement préparé contre 8.6 Å après 4 jours à l'air) suggère que des ions diperoxovanadate, très volumineux, sont tout d'abord insérés puis se condensent pour donner des chaînes métavanadate $(VO_3)_n^{n-}$. La modification des espèces vanadate insérées s'accompagne ainsi d'une augmentation des distorsions locales au sein des feuillets qui se traduit par l'élargissement en larges bandes des raies (10ℓ) et (11ℓ). Ce phénomène est dû à la transformation des entités diperoxovanadate isolées en chaînes, qui tendent à créer des contraintes au sein du réseau. Cette évolution est pleinement confirmée par l'étude infrarouge et par l'analyse chimique, qui révèle une forte diminution du degré d'oxydation moyen (dosé par iodométrie) au sein du matériau. Signalons que les ions peroxovanadate insérés au sein du LDH fraîchement préparé sont facilement échangeables par les ions carbonate alors que les chaînes métavanadate présentes dans LDH(VO_3) ne le sont pas en raison de leur faible mobilité due à leur encombrement stérique. Ainsi que le suggère la figure 5, le processus de polycondensation des ions diperoxovanadate en chaînes peut être représenté par la réaction suivante :

$$n\ [V(OH)_2(OO)_2]^- \rightarrow (VO_3)_n^{n-} + n\ H_2O + n\ O_2.$$

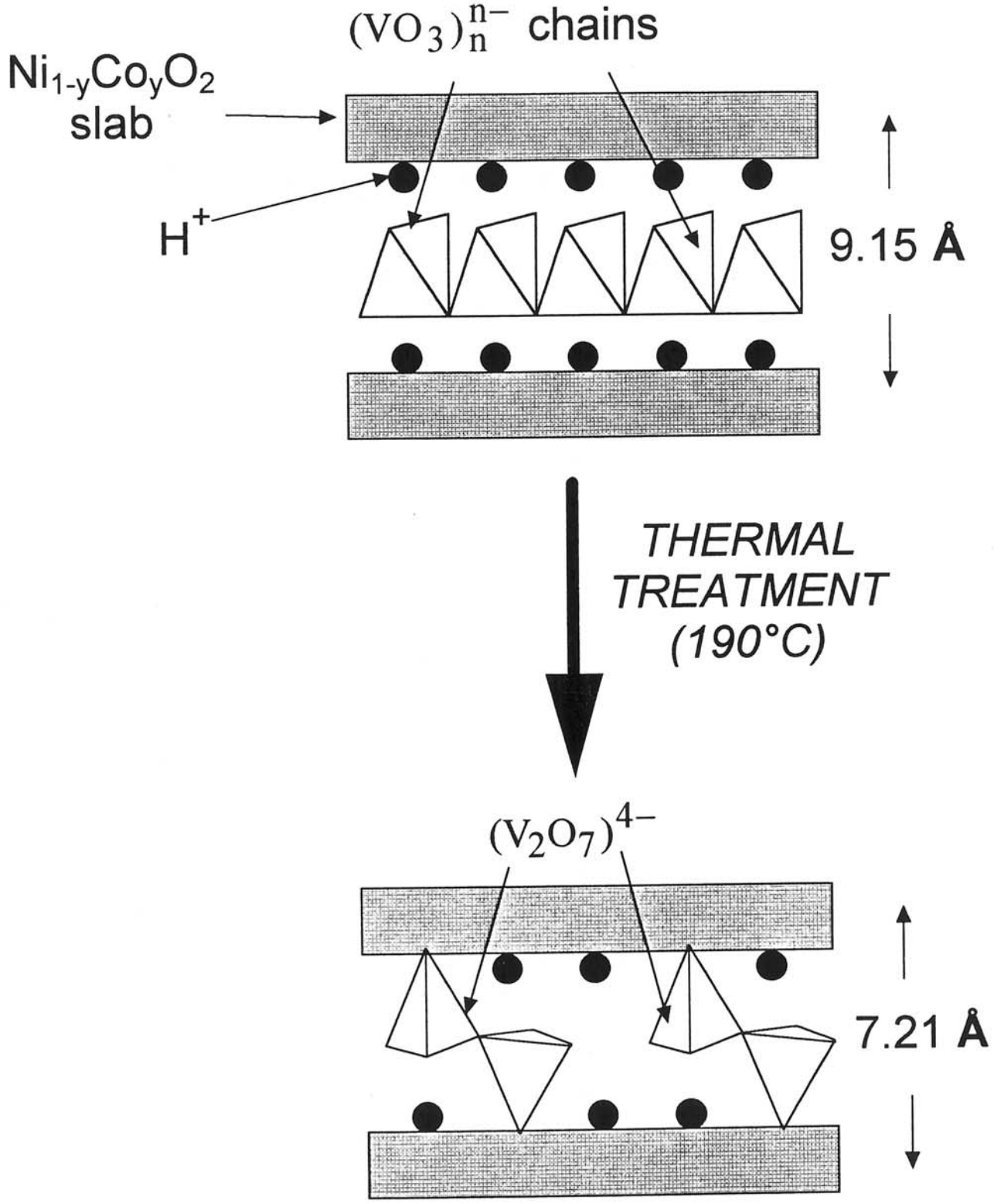

Fig. 4- Représentation schématique des modifications structurales intervenant lors du traitement thermique du matériau LDH(VO_3).

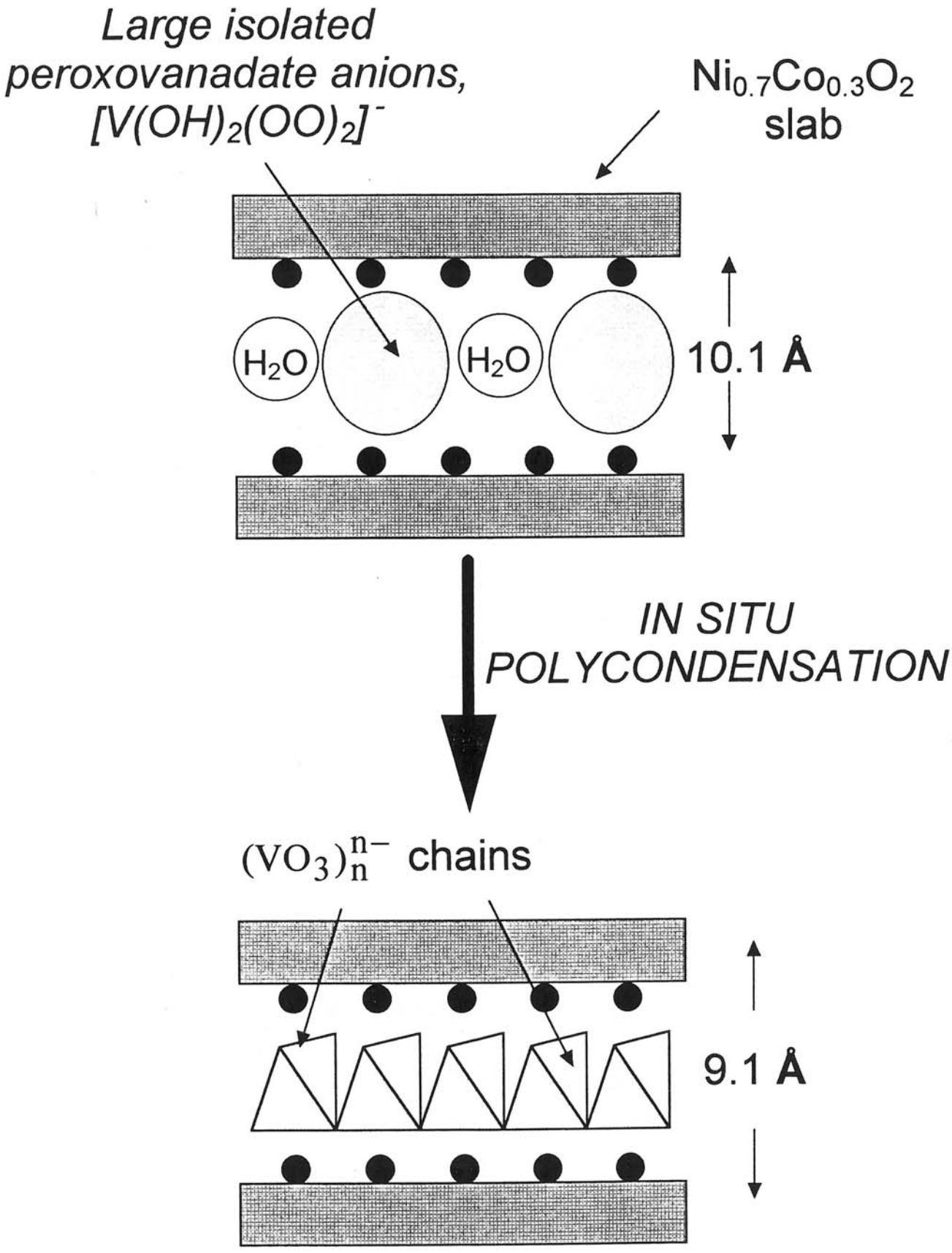

Fig. 5- Représentation schématique des modifications structurales intervenant lors du vieillissement à l'air de l'hydroxyde double lamellaire obtenu par réduction de l'oxyhydroxyde et filtration simultanées.

Ce dégagement d'oxygène résultant de cette réaction a pu être déterminé et corrélé à l'avancement de la réaction.

La RMN du ^{51}V s'est avérée une technique de choix pour caractériser les phénomènes couplés de polycondensation/greffage mis en jeu lors de l'obtention des hydroxydes doubles contenant des entités vanadate insérées. En effet, les ions Ni^{II} présents au sein des feuillets sont susceptibles d'exercer une interaction magnétique sur les noyaux vanadium si une liaison Ni-O-V existe, en d'autres termes si les ions vanadium sont greffés au feuillet. L'analyse des spectres RMN a révèlé que, sitôt insérés afin d'assurer la compensation de charges dans l'hydroxyde double, les ions diperoxovanadate isolés sont sujets à une compétition entre phénomènes de polycondensation et de greffage. Lorsque le matériau est maintenu dans la solution réductrice contenant les espèces peroxovanadate, un greffage partiel des espèces insérées se produit simultanément à la polycondensation, s'accompagnant d'un départ d'ions hydroxyle du feuillet vers la solution. Afin d'assurer la compensation de charges requise, des entités vanadate supplémentaires s'insérent et ce jusqu'à une occupation complète de l'espace interfeuillet. Ce phénomène entraîne que le taux de vanadium inséré est quasiment constant quel que soit le taux de cobalt dans le feuillet. Par contre, dès lors que le matériau est retiré très tôt de la solution réductrice, seuls les ions vanadate nécessaires à la compensation de charge initiale s'insérent. La polycondensation s'effectue alors à l'air et peut être suivie par la RMN du ^{51}V, qui met de surcroît en évidence un greffage spontané et simultané. Néanmoins, que le matériau soit maintenu dans la solution réductrice ou retiré très tôt de la solution, des chaînes métavanadate partiellement greffées sont présentes après l'étape de polycondensation. Puis le greffage se poursuit, s'accompagnant d'une fragmentation des chaînes, ces deux phénomènes mettant en jeu simultanément une déshydroxylation et une déprotonation des feuillets qui conduisent à la formation d'eau. Ce processus, très lent dans les conditions usuelles, est considérablement accéléré si le matériau est chauffé ou soumis à un traitement sous vide, qui permet de promouvoir le départ de l'eau.

BIBLIOGRAPHIE

[1] W. Jones and M. Chibwe, "Pillared Layered Structures", IV. Mitchell Ed., Elsevier, London, (1990) 67.

[2] F. Cavani, F. Trifiro and A. Vaccari, Catalysis Today, **11** (1991) 173.

[3] H. F. W. Taylor, Mineralogical Magazine, **39** (1973) 377.

[4] R. Allman, Acta Cryst., **B24** (1968) 972.

[5] C. Delmas and Y. Borthomieu, J. Solid State Chem., **104** (1993) 345.

[6] C. Delmas, J. J. Braconnier, Y. Borthomieu and M. Figlarz, Solid State Ionics, **28/30** (1988) 1132.

[7] C. Delmas, J. J. Braconnier, Y. Borthomieu and P. Hagenmuller, Mat. Res. Bull., **22** (1987) 741.

[8] J. J. Braconnier, C. Delmas, C. Fouassier, M. Figlarz, B. Beaudouin and P. Hagenmuller, Revue de Chimie Minérale, **21** (1984) 496.

[9] L. Guerlou-Demourgues, J. J. Braconnier and C. Delmas, J. Solid State Chem., **104** (1993) 359.

[10] J. Twu and P. K. Dutta, J. Phys. Chem., **93** (1989) 7863.

[11] K. S. Han, L. Guerlou-Demourgues and C. Delmas, Solid State Ionics, submitted.

[12] K. S. Han, L. Guerlou-Demourgues and C. Delmas, Solid State Ionics, submitted.

[13] K. El Malki, A. de Roy and J. P. Besse, Eur. J. Solid State Inorg. Chem., 26 (1989) 339.

PUBLICATIONS

Publication n°1

LITHIUM INTERCALATION IN $FeWO_4Cl$: A STRUCTURAL AND ELECTROCHEMICAL INVESTIGATION

K. S. HAN, P. GRAVEREAU, J. H. CHOY* and C. DELMAS**

Institut de Chimie de la Matière Condensée de Bordeaux
and Ecole Nationale Supérieure de Chimie et Physique de Bordeaux,
Av. Dr A. Schweitzer, 33608 Pessac Cedex, France.

* *Department of Chemistry, College of Natural Sciences,*
Seoul National University, Seoul 151-742, Korea.

ABSTRACT

Lithium has been chemically and electrochemically intercalated within the layered $FeWO_4Cl$ iron tungsten oxychloride. A very wide biphased domain is obtained for x in Li_xFeWO_4Cl ranging between 0 and 0.85. The structures of $FeWO_4Cl$ and $LiFeWO_4Cl$ were determined : from single crystal analysis and by Rietveld refinement of the powder X-ray diffraction pattern respectively. The modifications of the Fe-O bond lengths emphasize the iron reduction upon intercalation. Moreover, the strong change of Fe-Cl distance suggests a reversible framework modification.

** To whom correspondence should be addressed.

1. INTRODUCTION

The layered compound $FeWO_4Cl$ was recently reported by some of us [1]. Its structure is isotypic to that of $FeMoO_4Cl$ which had been extensively investigated by several research groups [2-5]. In the latter material, lithium can be reversibly chemically or electrochemically intercalated leading to the $LiFeMoO_4Cl$ phase. Only iron ions are reduced as shown by the magnetic and XPS studies [5,6]. Nevertheless, more than one lithium can be intercalated in $FeMoO_4Cl$; this reaction requires to reduce hexavalent molybdenum ions, in those conditions the reversibility is lost as shown by the very complicated behavior of this over-reduction. Lithium intercalation into $FeWO_4Cl$ has been undertaken. In this paper, the structural modifications induced by lithium intercalation are presented.

2. EXPERIMENTAL

$FeWO_4Cl$ was obtained, as previously reported, from WO_3, Fe_2O_3 and $FeCl_3$ in the molar ratio (3 : 1 : 1.05). Iron trichloride acts as a reactant but also as a transport agent. The reaction is performed in a sealed evacuated silica tube at 420°C for 30 days. In this chemical vapor transport technique, large single crystals of $FeWO_4Cl$, up to 4 x 4 x 1 mm in size, are obtained in the cold zone of the tube with a very low yield. It must be noted that all experiments realized to obtain $FeWO_4Cl$ by direct synthesis as a powder form failed. Therefore, only a very small amount of the starting material ($FeWO_4Cl$) was available for the chemical and electrochemical characterizations.

Single crystal structure determination was performed on an Enraf-Nonius CAD4 X-ray diffractometer after a preliminary study with the Weissenberg and Buerger techniques.

Chemical lithium intercalation was realized by action of an excess of LiI in CH_3CN.

Electrochemical lithium intercalation / deintercalation experiments were performed in small lithium batteries using a 1 M solution of $LiClO_4$ in propylene carbonate as electrolyte and a mixture of the studied material powder with ketjenblack (35 % in weight) as positive electrode. All electrochemical experiments were monitored by home made computerized system [7]. The thermodynamic electrochemical curves were obtained by alternating discharge (or charge) and relaxation periods. The relaxation was considered as finished when the slope of the $V = f(t)$ curve was smaller than 0.1 mV/hour.

For the intercalated material, the structure was determined from powder data using the Rietveld method (Fullprof program [8]).

3. STRUCTURAL STUDY OF THE $FeWO_4Cl$ STARTING PHASE

The X-ray diffraction pattern was indexed, as previously reported, in the tetragonal system with the following unit cell parameters : $a = 6.631(9)$ Å, $c = 5.223(9)$ Å. In order to improve the atomic positions previously reported from a powder analysis, but without using the Rietveld method, a single crystal structure determination was carried out.

A single crystal exhibiting a truncated rectangular habit $\{\bar{1}10\}$ with dimensions 150 x 200 x 30 µm was selected for collection of the intensities. A preliminary films study (Weissenberg, Buerger) confirmed the tetragonal symmetry with the Laue group 4/mmm. The systematic absences observed ($h + k = 2n + 1$ for (hk0)) are compatible with the P4/nmm space group. The experimental conditions used for the diffracted intensity collection are reported in Table I.

The observed intensities were treated for Lorentz polarization effects and an analytical correction for absorption using the shape and dimensions of the crystal was done. This absorption correction is important because of the platelet habit and the high value of the linear absorption coefficient (28.6 mm^{-1}). The transmission coefficient ranges from 0.073 to 0.444 : Table I indicates the evolution of the coherence factor (R_{int} : 0.083 before absorption correction ; 0.033 after absorption correction).

(1) The single crystal

Space group	P4/nmm (N°= 129)
a(Å)	6.677(5)
c(Å)	5.270(5)
$V(Å^3)$	234.95
$D_{cal}(g\ cm^{-1})$	4.79
$\mu(MoK_\alpha)\ (cm^{-1})$	285.6
F(000)	298

(2) Collection of intensities

Temperature	298 K
Crystal size (mm)	0.15 x 0.20 x 0.03
Automatic diffractometer	CAD4 Enraf-Nonius
Wave length (Å)	MoK_α (λ = 0.7107)
Monochromator	Graphite
Scan type	ω
Scan angle (°)	$(1.00 + 0.35 \tan\theta)$
Counter slit width (mm)	$(3.00 + 2.00 \tan\theta)$
Angular range	$\theta < 45°$
Miller index range	$-13 \leq h \leq 13$
	$-13 \leq k \leq 13$
	$-10 \leq l \leq 10$
Number of the measured intensities	7705
Number of the independent reflections ($I > 3\sigma(I)$)	507
R(INT) before the absorption correction	0.083
R(INT) after the absorption correction	0.033

(3) The refinement results of the structure

Number of refined variables	16
Parameter of the secondary extinction	$86(4) \times 10^{-4}$
Residuary electron density between W and O ($eÅ^{-3}$)	2.1
Reliability factor	R = 0.026
	$R_w(w = 1 / \sigma^2) = 0.032$

Table I : Experimental conditions for the $FeWO_4Cl$ single crystal structure determination and refinement results.

Atomic diffusion factors of W^0, Fe^{3+}, Cl^-, O^- have been corrected for anomalous dispersion. The correction terms $\Delta f'$ and $\Delta f''$ were taken in International Tables.

3. 1. Determination of the structure

The structure was solved using the SHELX 76 program, with the heavy atom method. The W coordinates obtained in the powder structural determination of $FeWO_4Cl$ by J. H. Choy and al. were utilized as a starting hypothesis [1]. The successive Fourier difference functions confirm the sites found for the Fe, Cl, O atoms. The refinement with individual isotropic thermal parameters for all of the atoms converged to a relatively high R value (R = 0.11) with a strong residue of electron density near the tungsten atom ($\cong 7$ eÅ^{-3}). An important improvement was obtained when anisotropic thermal parameters were authorized. Final calculation with the weighting scheme $w = 1 / \sigma^2(F_0)$, the x parameter of the secondary extinction correction $[F_c = F (1 - 10^{-4} x F^2 / \sin \theta)]$, and anisotropic thermal parameters for all atoms converged to R = 0.026 and $R_w = 0.032$ (Table I). The atomic coordinates are given in Table II. The main interatomic distance (Å) and angles (°) in $FeWO_4Cl$ are given in Table III.

3. 2. Structure description

Fig. 1 represents a perspective view of the structure of $FeWO_4Cl$ (CERIUS program). It consists of a packing of $FeWO_4Cl$ layers along the c axis. Iron is in an FeO_4Cl square pyramidal environment. The 4 oxygen atoms also belong to the WO_4 tetrahedra, leading to a puckered slab. The square pyramids alternately point their chlorine atoms up and down. The Fe-Cl distance within a square pyramid is equal to 2.18 Å ; this value is considerably smaller than the Fe-Cl′ distance which involves a chlorine atom of the next layer (3.03 Å). If the two distances were not so different, an octahedral environment for iron (FeO_4ClCl') would be considered and the layered character of this structure would be lost.

ATOMS	x / a	y / b	z / c	K	U_{11}	U_{22}	U_{33}	U_{23}	U_{13}	U_{12}
W	0.750(0)	0.250(0)	0.000(0)	0.125(0)	0.005(2)	0.005(2)	0.015(8)	0.000(0)	0.000(0)	0.000(0)
Fe	0.250(0)	0.250(0)	0.275(3)	0.125(0)	0.006(5)	0.006(5)	0.010(5)	0.000(0)	0.000(0)	0.000(0)
Cl	0.250(0)	0.250(0)	0.693(9)	0.125(0)	0.037(9)	0.037(9)	0.012(7)	0.000(0)	0.000(0)	0.000(0)
O	0.250(0)	0.964(4)	0.195(7)	0.500(0)	0.019(8)	0.008(2)	0.023(6)	-0.001(8)	0.000(0)	0.000(0)

Table II : Positional and thermal parameters for the atoms of $FeWO_4Cl$.

	Distances (Å)	
	$FeWO_4Cl$	**$LiFeWO_4Cl$**
Fe-Cl	2.18(6)	2.62(2)
Fe-Cl′	3.03(6)	2.44(3)
$Fe-O_1$, $Fe-O_3$	1.93(9)	1.97(4)
$Fe-O_2$	1.93(9)	2.18(2)
$Fe-O_4$	1.93(9)	1.94(8)
$W-O_1$, $W-O_3$	1.75(1)	1.77(8)
$W-O_2$	1.75(1)	1.84(4)
$W-O_4$	1.75(1)	1.80(6)
$Li-O_1$	-	2.18(8)
$Li-O_2$	-	2.21(7)
Li-Cl	-	2.63(6)

Table III (a) : Main interatomic distances in $FeWO_4Cl$ and $LiFeWO_4Cl$.

	Angles (°)	
	$FeWO_4Cl$	**$LiFeWO_4Cl$**
Cl-Fe-Cl′	180.0(0)	175.0(4)
Cl-Fe-O_1	102.3(8)	89.1(7)
Cl-Fe-O_2	102.3(8)	80.0(1)
Cl-Fe-O_4	102.3(8)	95.8(2)
O_2-W-O_5	109.9(0)	109.2(5)
O_4-W-O_5	109.9(0)	105.0(3)
O_2-W-O_4	108.5(5)	111.7(0)
O_1-Fe-O_2	87.3(5)	83.6(6)
O_1-Fe-O_3	155.2(6)	167.3(0)
Fe-O_2-W	156.6(7)	127.3(6)
Fe-O_4-W	156.6(7)	160.1(8)

Table III (b) : Main interatomic angles in $FeWO_4Cl$ and $LiFeWO_4Cl$.

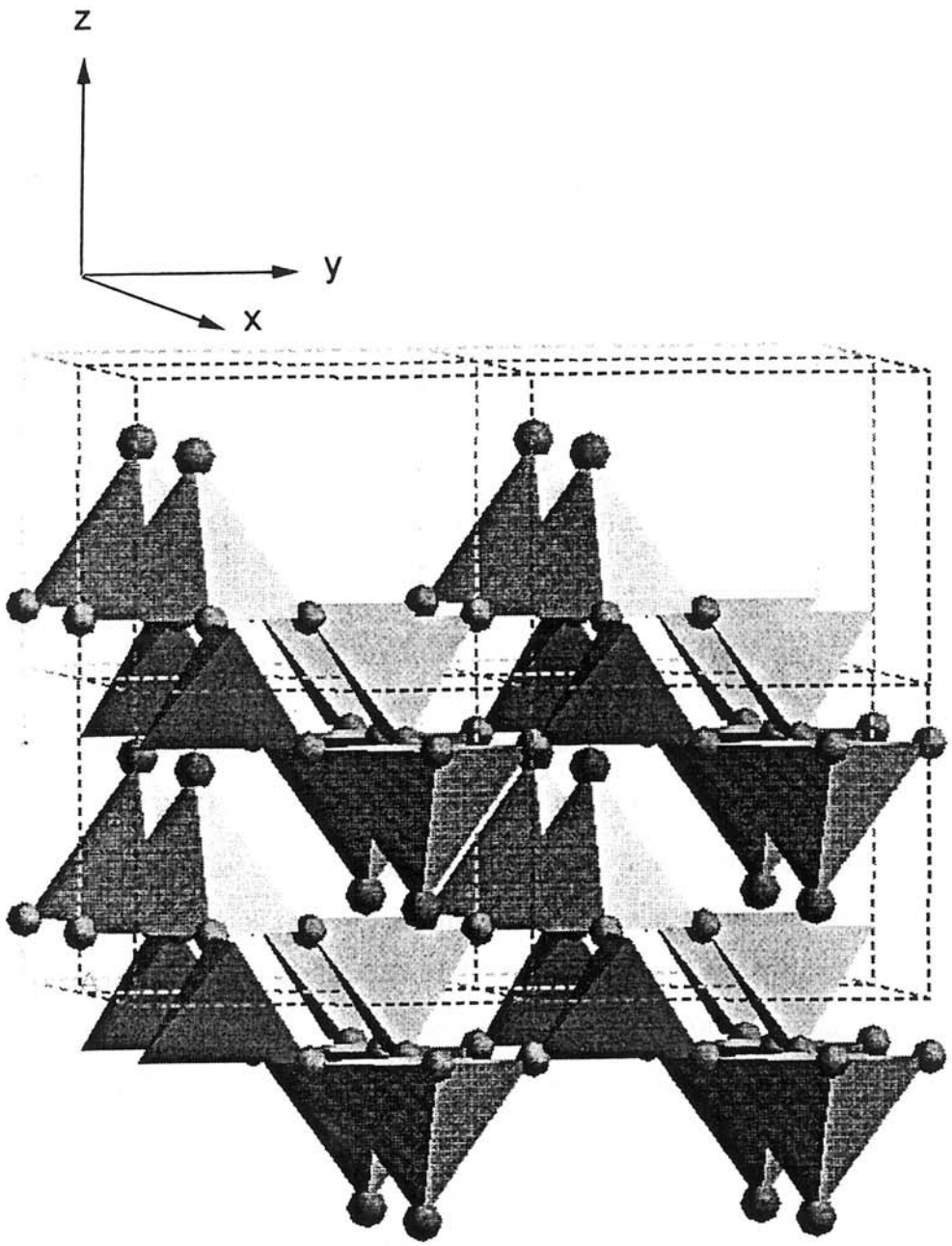

Fig. 1 : A perspective view of the structure of $FeWO_4Cl$ showing the arrangement of two stacked layers.

4. LITHIUM INTERCALATION

All experiments was realized on ground powders of $FeWO_4Cl$. All trials to intercalate directly on the single crystals have failed.

4. 1. Chemical intercalation

The reaction of an excess of LiI in CH_3CN on $FeWO_4Cl$ leads to $LiFeWO_4Cl$. This material was characterized by X-ray diffraction. The results are discussed further. This material has been used as the positive electrode of lithium batteries in order to compare the electrochemical behavior of $FeWO_4Cl$ and of $LiFeWO_4Cl$ obtained chemically.

4. 2. Electrochemical intercalation

As only a small amount of starting material was available, only OCV experiments were realized in order to obtain directly the Li-$FeWO_4Cl$ phase diagram. Fig. 2 gives the variation of the cell voltage vs the amount of intercalated lithium. The discharge curve is constituted by three potential plateaux and two domains where the cell voltage decreases rapidly upon intercalation. A close examination of this curve shows that only the first plateau ($0.00 < x < 0.85$) corresponds to a true biphased domain between two well identified materials : the OCV is absolutely constant in all the involved composition domain. On the contrary for the other two plateaux, the OCV values vary slightly from one composition to the next one indicating the occurrence of some irreversible process. For the last plateau, this point is confirmed by the X-ray diffraction study of the material obtained after intercalation of two lithium atoms which indicates a mixture of $LiFeWO_4Cl$ with an amorphous phase. As a result, in the following of this study, our attention has been specially focused on the intercalation of the first lithium atom.

As shown in Fig. 3, the first lithium atom can be deintercalated with a relatively small hysteresis effect. The wide potential plateau is characteristic of a biphased domain between the $FeWO_4Cl$ composition and a composition close to $Li_{0.85}FeWO_4Cl$ (Fig. 2). The latter can be considered as the lower limit of a solid solution which extends in the

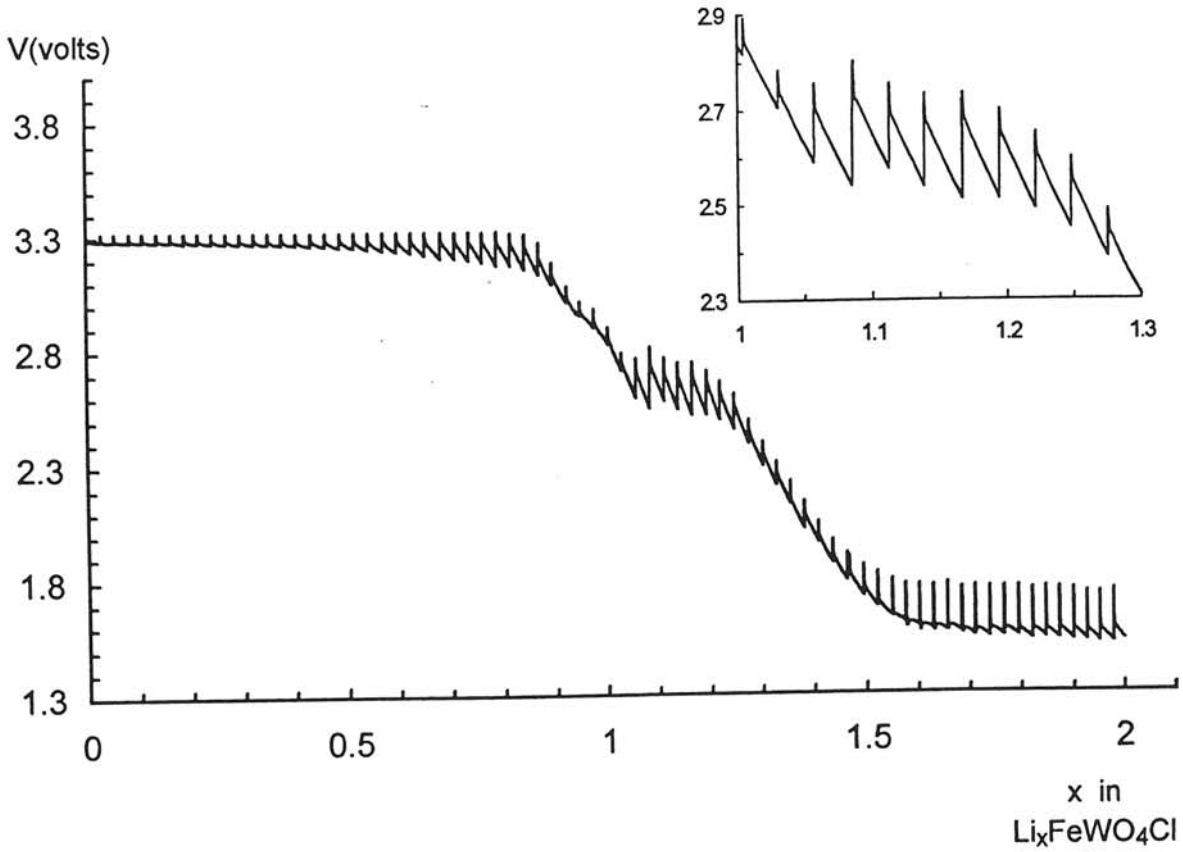

Fig. 2 : Variation of the open circuit voltage vs the amount of intercalated lithium (x) during a first discharge to x = 2 for a Li//$FeWO_4Cl$ cell.

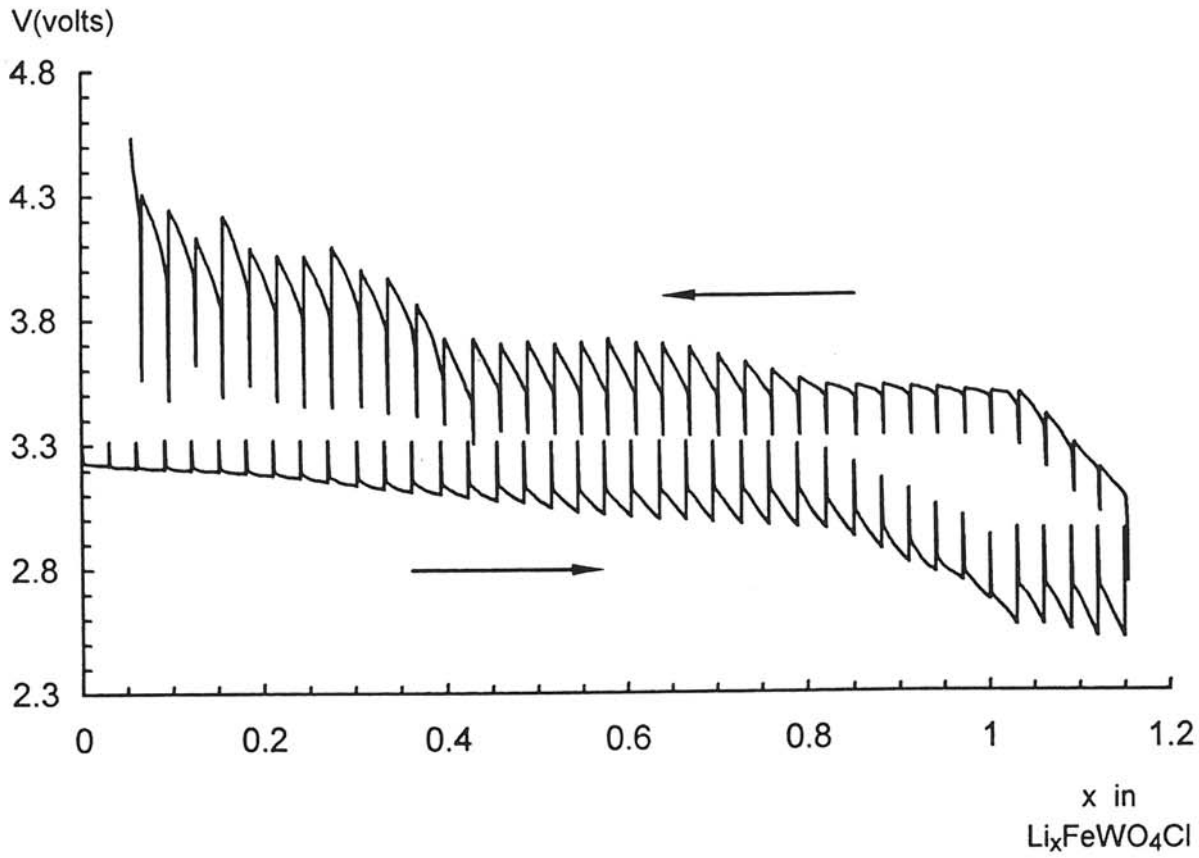

Fig. 3 : Variation of the open circuit voltage vs the x in Li_xFeWO_4Cl during a discharge/charge cycle starting from $FeWO_4Cl$.

vicinity of the $LiFeWO_4Cl$ composition. In order to have a better characterization of the extent of this solid solution, two cells, using the $LiFeWO_4Cl$ phase obtained chemically by action of LiI on $FeWO_4Cl$, were built. Both of them have been cycled in OCV conditions around the starting composition. The cycling curves are shown in Fig. 4. In order to suppress the irreversible processes shown in discharge when the cell voltage becomes smaller than 2.55 V, the end of discharge has been limited to 2.60 V. Under these conditions the reversibilty is very good. The solid solution around the $LiFeWO_4Cl$ composition extends in the range $0.90 < x < 1.07$. These values must be compared to those found during the lithium intercalation into $FeWO_4Cl$ (Fig. 2) ($0.85 < x < 1.05$). The very small discrepancy between the two limits can result from a slight inaccuracy in the weight of the $FeWO_4Cl$ phase within the cell and/or the starting composition considered for the material obtained by chemical intercalation with LiI. There is no reason why this composition should be exactly $LiFeWO_4Cl$. As a solid solution exits, the true composition is fixed by the equilibrium in potential between the I° / I^- redox couple and Li_xFeWO_4Cl.

The electrochemical behavior of this system is very close to the one we have previously reported for the $Li\text{-}FeMoO_4Cl$ system : a large two phase domain and a narrow solid solution around the $LiFeMoO_4Cl$ composition [2]. The OCV values of the equilibrium plateau are very close to 3.32 V in the iron-tungsten material against 3.40 V in the iron-molybdenum material. This very small difference shows that the electronic transfer from molybdate and tungstate ions are very similar. A similar result was found for the lithium intercalation in tridimensional $Fe_2(MoO_4)_3$and $Fe_2(WO_4)_3$. On the contrary, in the case of the lithium intercalation in $Fe_2(SO_4)_3$, as reported by Goodenough, the cell voltage is 600 mV higher than for homologous molybdenum and tungsten phases due to the decrease of the Fe-O bond covalency resulting from the presence of SO_4^{2-} anions [9-11].

As we have discussed in the case of the $Li\text{-}FeMoO_4Cl$ system, the existence of a large biphased system between the two end members may result from the important

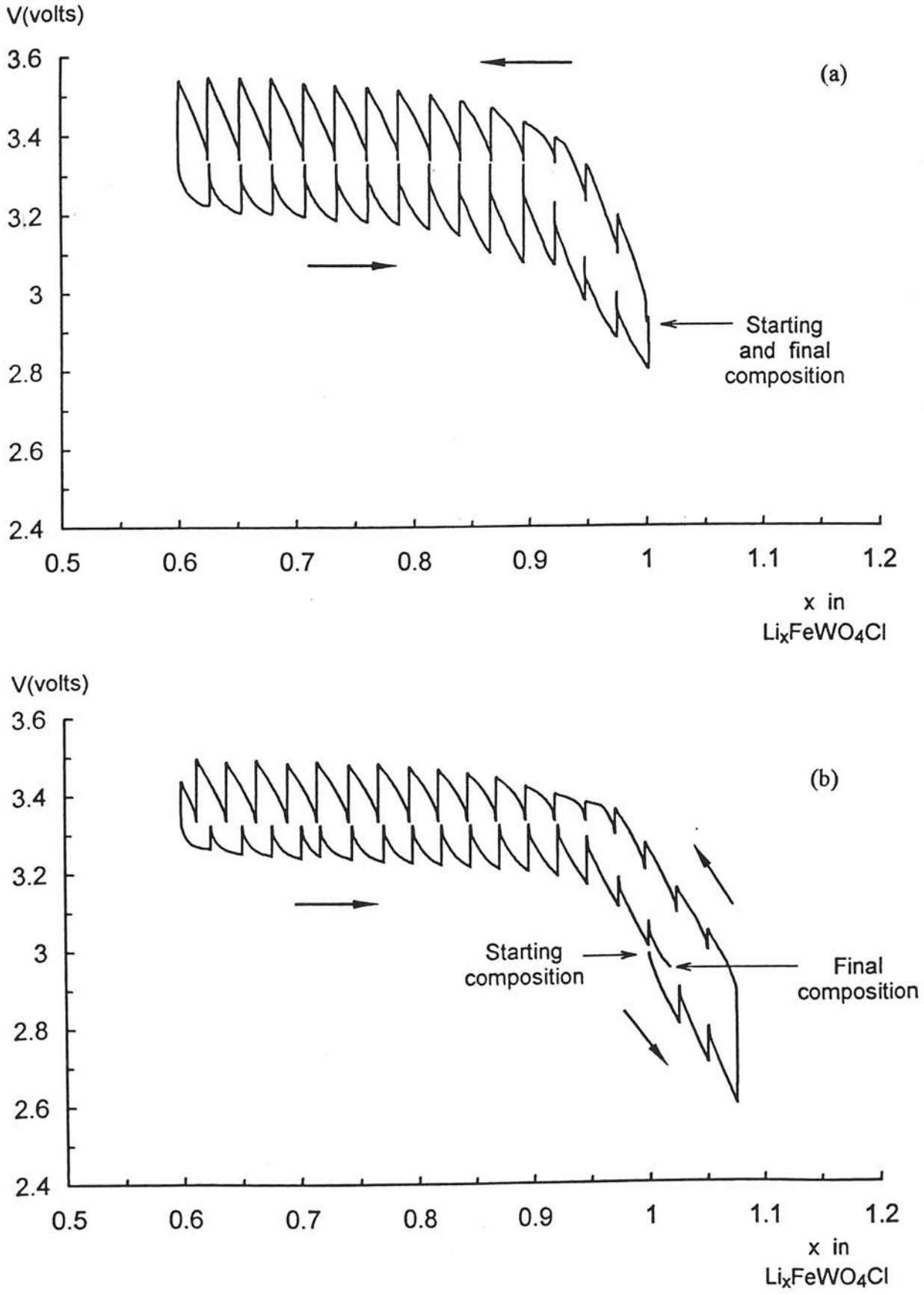

Fig. 4 : Variation of the open circuit voltage vs the x in Li_xFeWO_4Cl during a cycle starting from $LiFeWO_4Cl$ obtained chemically :

(a) charge, discharge (b) discharge, charge, discharge.

structural modifications imposed by the lithium intercalation. It must be noticed that any solid solution in the vicinity of the $FeW(Mo)O_4Cl$ composition cannot be detected. This result shows that the iron reduction leads immediately to the nucleation of the $Li_xFeW(Mo)O_4Cl$ phase ($x \cong 1$). As the structure of the unintercalated material was known precisely from a single crystal study, a structural study using the Rietveld refinement method was carried out on the $LiFeWO_4Cl$ phase obtained after the electrochemical cycle represented in Fig. 4 (a).

4. 3. Structural characterization of $LiFeWO_4Cl$

Like the homologous molybdenum phase, $LiFeWO_4Cl$ crystallizes in the monoclinic system. Its unit cell parameters are reported in Table IV in comparison with those of the pristine material and those relative to the molybdenum system [3,12]. Both unintercalated phases crystallize in the tetragonal system. This lowering in symmetry may indicate an ordered occupancy by lithium of part of the available sites within the structure.

An X-ray diffraction pattern of the electrode material corresponding to the $LiFeWO_4Cl$ composition was carefully recorded (step of 0.02°(2θ) / 40 s counting time). As the material amount was quite small, the lines of the aluminum sample holder appear on the diffraction pattern. Regions of the scan which include these diffraction peaks were excluded for the refinement. The starting atomic positions were those of $LiFeMoO_4Cl$ [12]. The background was determined by using a polynomial function. The reliability factors obtained after the fits were $R_I = 0.056$, $R_{wp} = 0.171$. Fig. 5 gives the observed and calculated X-ray diffraction patterns and the difference between them. The R values, although not very good due to the difficult experimental conditions imposed by the study of an electrode material, can be considered with interest for the structure discussion. The atomic positions are reported in Table V, while the main interatomic distances and angles are reported in Table III in comparison with those of the starting material. The Rietveld refinement does not allow to fit the lithium positions, therefore those determined by Torardi et al. for $LiFeMoO_4Cl$ in the neutron diffraction study have been used [12]. A

Unit cell parameters	a (Å)	b (Å)	c (Å)	β (°)
$FeWO_4Cl$	6.631(9)	6.631(9)	5.223(9)	90.00
$LiFeWO_4Cl$	7.071(3)	6.947(1)	5.060(0)	91.5(2)
$FeMoO_4Cl$	6.672(3)	6.672(3)	5.223(3)	90.00
$LiFeMoO_4Cl$	6.994(4)	6.871(2)	5.014(6)	91.2(7)

Table IV : Lattice parameters for $FeWO_4Cl$, $LiFeWO_4Cl$, $FeMoO_4Cl$ and $LiFeMoO_4Cl$.

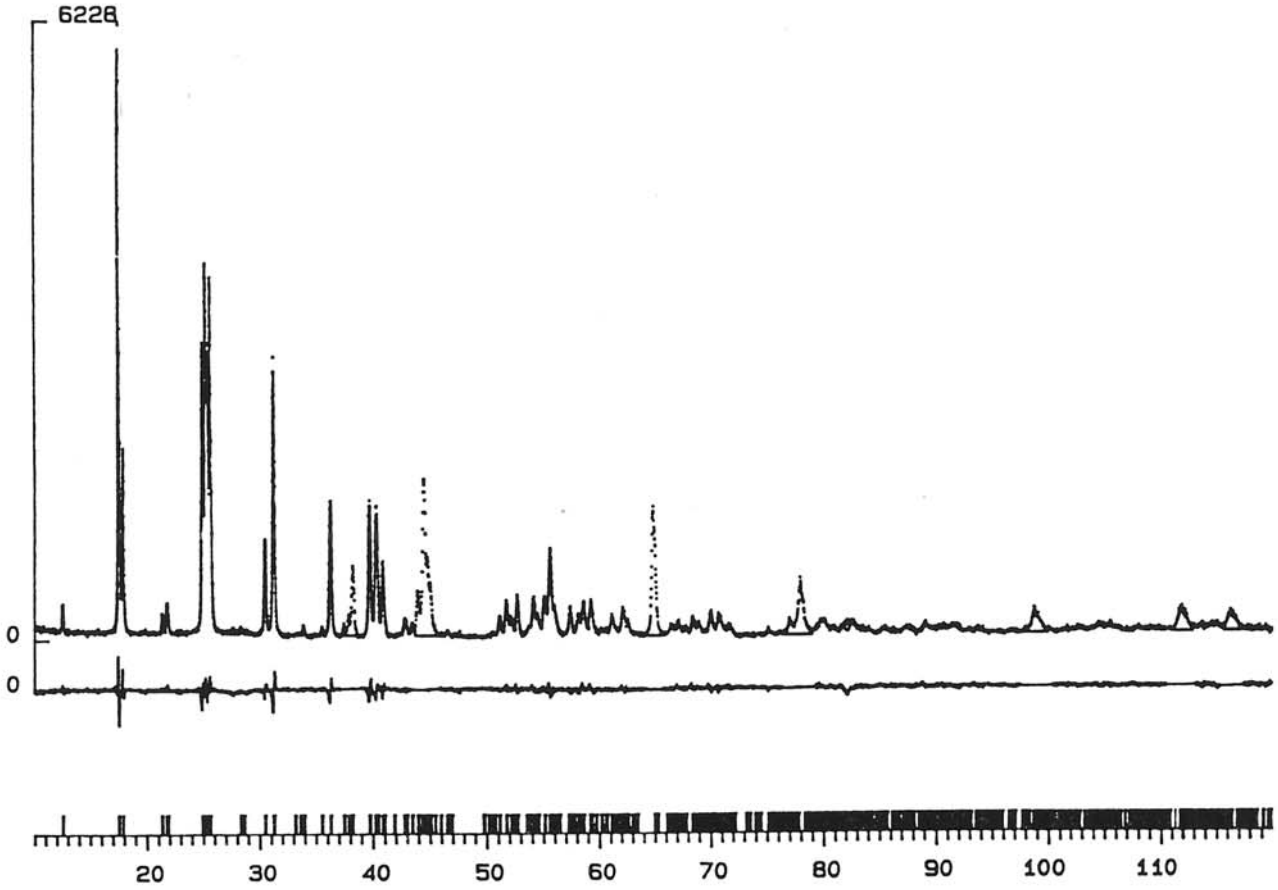

Fig. 5 : X-ray powder diffraction profile and difference between observed and calculated intensities for $LiFeWO_4Cl$.

ATOMS	x / a	y / b	z / c	K	B(Å^2)
W	0.736(9)	0.250(0)	0.998(3)	1.000(0)	1.1
Fe	0.246(7)	0.250(0)	0.181(0)	1.000(0)	0.7
Cl	0.262(2)	0.250(0)	0.699(3)	1.000(0)	1.8
O_1	0.277(5)	0.967(6)	0.186(0)	2.000(0)	2.2
O_2	0.552(7)	0.250(0)	0.249(3)	1.000(0)	1.0
O_4	0.971(6)	0.250(0)	0.147(8)	1.000(0)	1.3
Li	0.500(0)	0.000(0)	0.500(0)	1.000(0)	1.9

Table V : Positional and isotropic thermal parameters for the atoms of $LiFeWO_4Cl$.

perspective representation of the overall structure is given in Fig. 6. A view of one slab is represented (in Fig. 7) perpendicularly to the previous figure. A comparison of this structure with that of the pristine phase (Fig. 1) suggests that the polyhedra around iron atoms are strongly modified. In fact, during the reduction, the Fe-Cl distance within the FeO_4Cl square pyramid increases considerably. It follows that the structural representation privileges an FeO_4Cl' square pyramidal environement instead of an FeO_4ClCl' distorted octahedral one. These structural modifications upon lithium intercalation are schematically represented in Fig. 8 in comparison with those of $FeMoO_4Cl$. In the case of $LiFeMoO_4Cl$ Torardi et al. have shown that the iron ion was in octahedral site ; therefore, the structure could be considered as being three dimensional after intercalation. In the case of the tungsten derivative, the distortion of the octahedra is quite strong and the structure of $LiFeWO_4Cl$ can rather be considered as being bidimensional. This behavior is illustrated by the larger value of the c parameter : the larger the 2 D character, the weaker the interslab bonds and the larger the interslab distance.

The increase of the Fe-O distances (Table III) shows that iron is reduced to the divalent state upon intercalation, this reduction leads to an increase of the basal distances ($a_{mon.}$ and $b_{mon.}$) as shown on Table IV. A similar result was demonstrated by XPS in the case of the $LiFeMoO_4Cl$ phase [6]. On the contrary, the lithium intercalation entails a contraction of the interslab space as illustrated by the strong decrease of the c parameter.

ACKNOWLEDGEMENT

The authors would like to thank L. Guerlou-Demourgues, J. P. Pérès and M. Ménétrier for fruitful discussions.

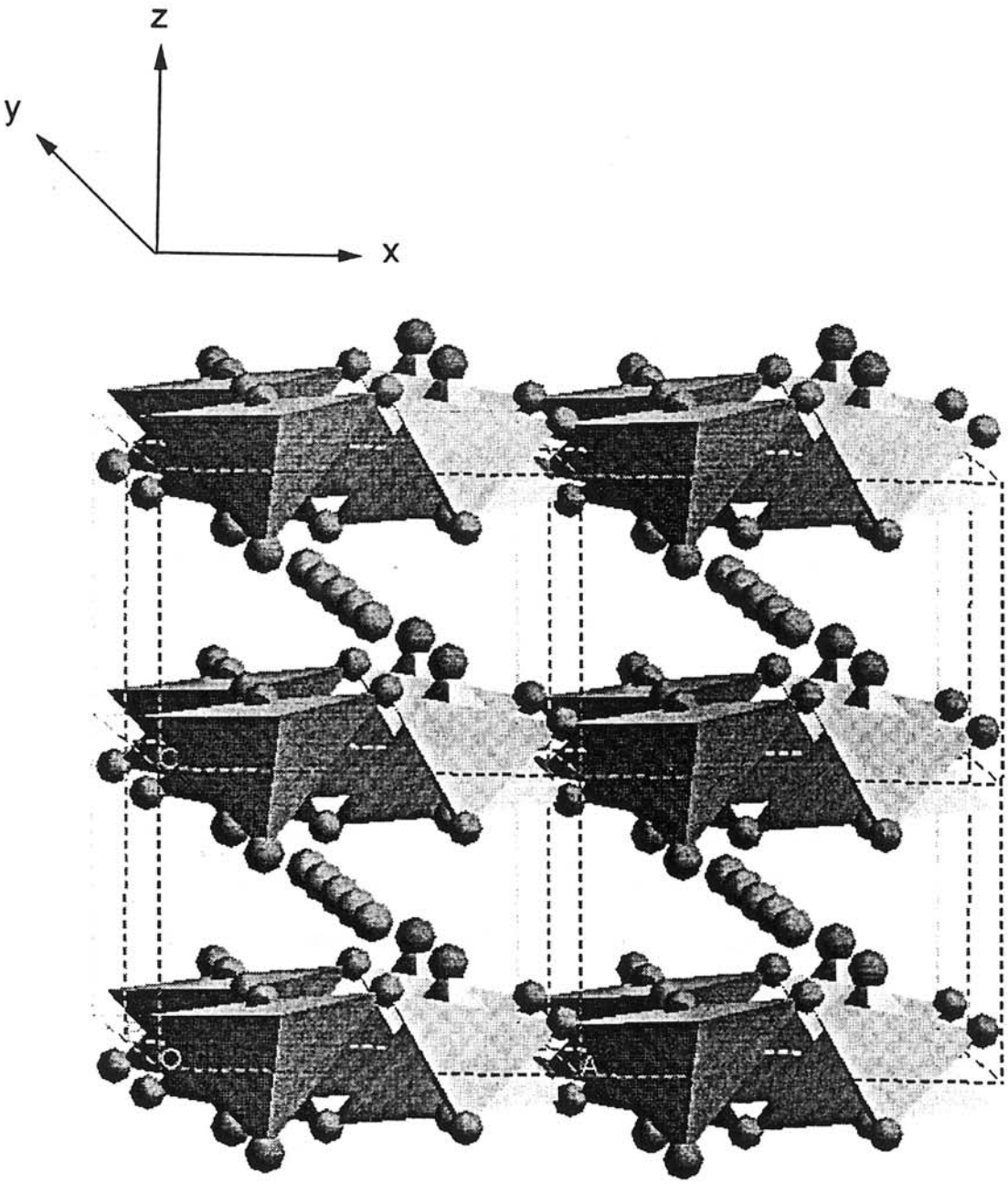

Fig. 6 : A perspective view of the structure of $LiFeWO_4Cl$ showing the actual intercalated Li atom positions and the arrangement of three stacked layers.

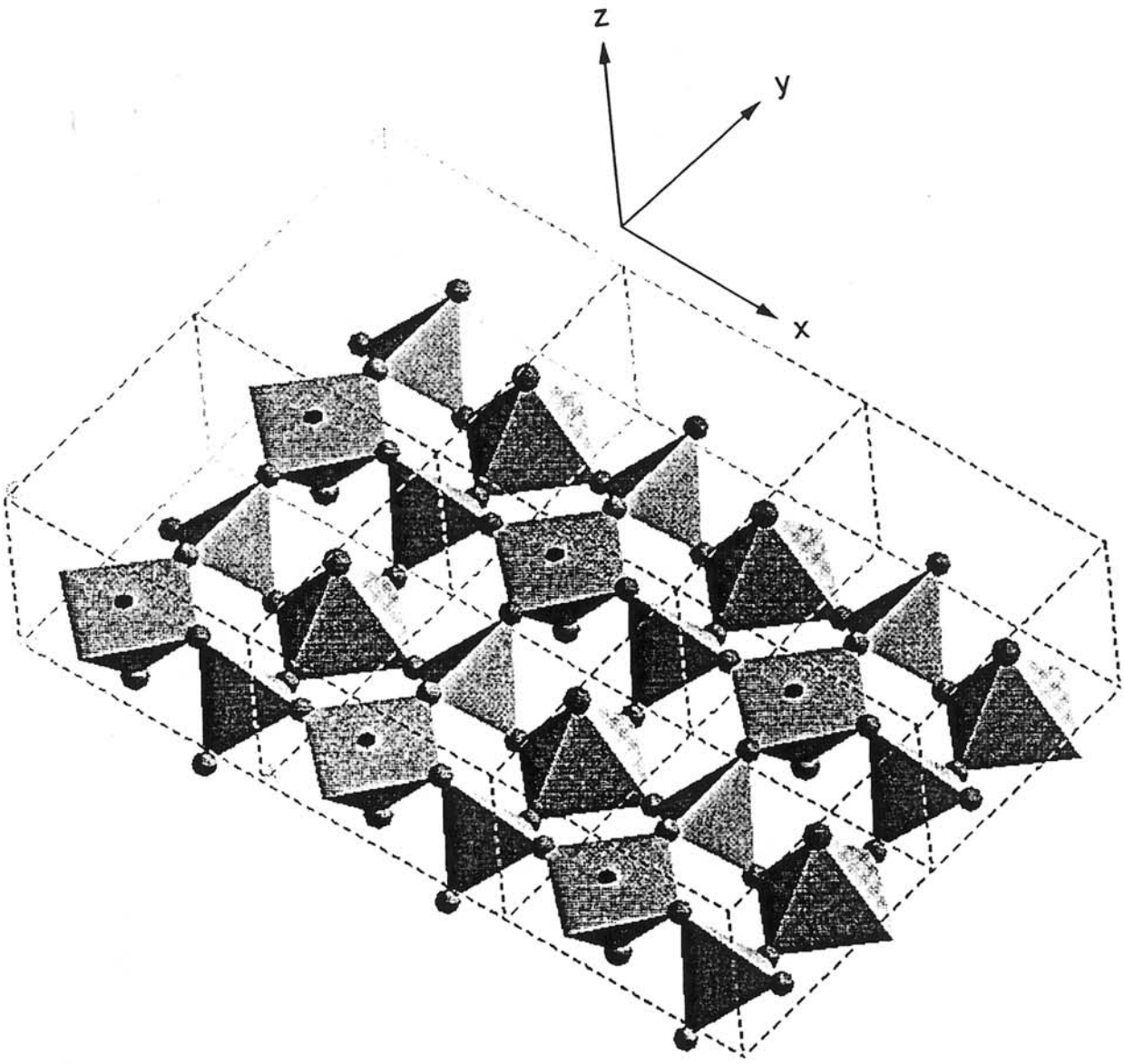

Fig. 7 : A perspective view of one layer of $LiFeWO_4Cl$.

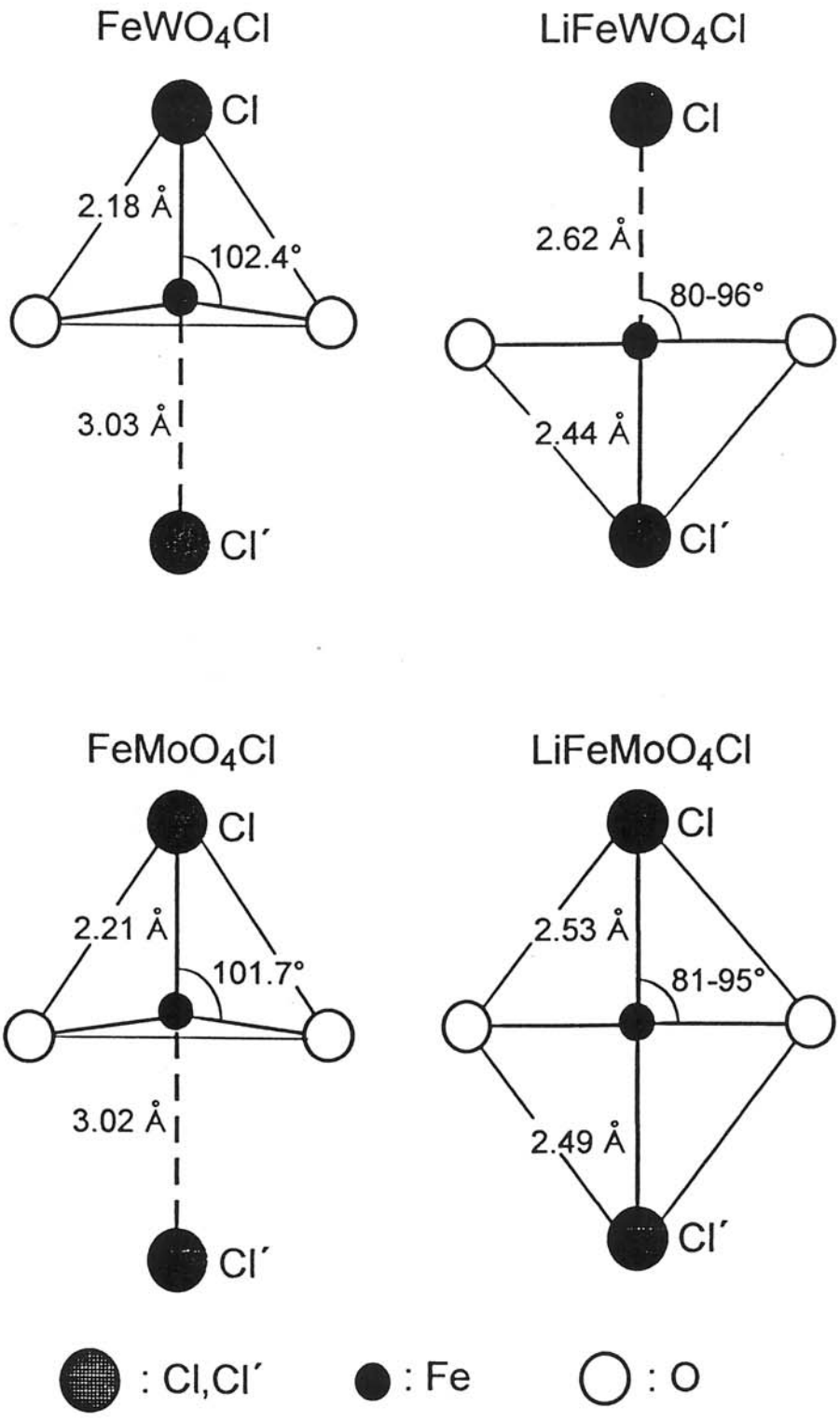

Fig. 8 : Schematic representations of the main structural modifications upon lithium intercalation in $FeWO_4Cl$ and $FeMoO_4Cl$.

REFERENCES

[1] J. H. Choy, D. Y. Noh, H. H. Park and J. C. Park, J. Chem. Soc. Dalton Trans., (1991) 1647.

[2] C. Delmas, S. H. Chang, D. Y. Dnoh and J. H. Choy, Solid State Ionics, 40/41 (1990) 563.

[3] C. C. Torardi, W. M. Reiff, K. Lazar, J. H. Zhang and D. E. Cox, J. Solid State Chem., 66 (1987) 105.

[4] C. C. Torardi, J. C. Calabrese, K. Lazar and W. M. Reiff, J. Solid State Chem., 51 (1984) 376.

[5] J. H. Choy, D. Y. Noh, J. C. Park, S. H. Chang, C. Delmas and P. Hagenmuller, Mat. Res. Bull., 23 (1988) 73.

[6] J. H. Choy, D. Y. Noh, S. H. Chang and C. Delmas, Eur. J. Solid State Inorg. Chem., 27 (1990) 391.

[7] A. Mendiboure and C. Delmas, Computer and Chemistry, 11(3) (1987) 153.

[8] J. Rodriguez-Carvajal, Collected Abstracts of Powder Diffraction Meeting, Toulouse (France) (1990) 127.

[9] C. Delmas and P. Hagenmuller, Recent Advances in Fast Ion Conducting Materials and Devices, B. V. R. Chowdari, Q. G. Liu and L. Q. Chen Ed., (1990) 23.

[10] A. Manthiram and J. B. Goodenough, J. Solid State Chem., 71 (1987) 349.

[11] A. Manthiram and J. B. Goodenough, J. Power Sources, 26 (1989) 403.

[12] C. C. Torardi, W. M. Reiff, K. Lazar and E. Prince, J. Phys. Chem. Solids, 47(8) (1986) 741.

Publication n°2

A NEW METAVANADATE INSERTED LAYERED DOUBLE HYDROXIDE PREPARED BY CHIMIE DOUCE

K. S. HAN, L. GUERLOU-DEMOURGUES and C. DELMAS

Institut de Chimie de la Matière Condensée de Bordeaux - C.N.R.S. and Ecole Nationale Supérieure de Chimie et Physique de Bordeaux, Av. Dr A. Schweitzer, 33608 Pessac Cedex, France.

ABSTRACT

A new metavanadate inserted layered double hydroxide was prepared by a chimie douce method. This material was characterized by X-ray diffraction, infrared spectroscopy, chemical analysis and thermogravimetry. Its structure consists of a packing of $Ni_{0.70}Co_{0.30}(OH)_2$ slabs, with $(VO_3)_n^{n-}$ metavanadate anionic chains intercalated within the interslab space. The influence of the presence of such chains on the structural features and the exchange properties of the material was investigated. The thermal treatment of this material at 190°C leads to a grafting of the VO_4 tetrahedra to the slabs coupled with a partial chain fragmentation.

1. INTRODUCTION

Layered double hydroxides (LDHs) are of great interest as a result of their well-known anionic exchange properties and of their possible use as precursors for new catalytic materials [1,2]. As suggested by the general formula : $[M^{II}_{1-y}\ L^{III}_{y}\ (OH)_2\ ]^{y+}\ X^{p-}_{y/p}\ [H_2O]_z$ ($X^{p-} = CO_3^{2-}$, NO_3^-, Cl^-, OH^-, SO_4^{2-}, etc.), the structure of these lamellar materials consists of stacked brucite-type $\left[M^{II}_{1-y}\ L^{III}_{y}\ (OH)_2\right]$ slabs, with water molecules and X^{p-} anions intercalated in the interslab spaces [2]. The presence of X^{p-} anions is required in order to compensate for the excess positive charge due to the partial substitution of trivalent cations (L) for the divalent cations (M) within the slabs. The structure is stabilized by a hydrogen bond network between the water molecules, the anions and the slab hydroxyls as well as by electrostatic interactions between the slabs and the X^{p-} anions, which indeed act as pillars within the structure.

Since these materials are generally prepared by precipitation from a suitable mixture of solutions, they are often poorly crystallized and exhibit compositional fluctuations, which are mainly due to the difference in the values of the precipitation pH of the $M(OH)_2$ and $L(OH)_3$ hydroxides. Consequently, the chemical formula of the final material tends to be determined by its own intrinsic stability rather than by the composition of the solution before the precipitation. Therefore, adjusting the amount of inserted anions in such conditions is very difficult.

In order to overcome these problems, a new chimie douce preparation method, where the building of the $M_{1-y}L_yO_2$ slab and the anionic intercalation are decoupled, was proposed in our laboratory. LDHs with the typical formula : $Ni_{1-y}\ Co_y\ (OH)_2\ X_{y/p}\ (H_2O)_z$ ($X^{p-} = CO_3^{2-}$, SO_4^{2-}, NO_3^-, OH^-) were obtained [3]. The amount of inserted anions is directly related to its own negative charge (p) and to the concentration of the L trivalent cation within the slabs. This method is derived from that previously designed in our laboratory for the preparation of cobalt or iron substituted hydrated nickel hydroxides, which were intended to be used in positive electrodes of nickel-cadmium, nickel-hydrogen or nickel-metal hydride batteries [4-6].

The main goal of our work consists in inserting large ionic species which may create large cavities suitable for catalytic reactions within the interslab space. From this point of view, the vanadate species appear as good candidates for the intercalation in LDH-type materials, as reported by Twu et al. [7]. It is well-known that vanadium oxides can be used for selective oxidation of hydrocarbons to manufacture butadiene, maleic anhydride, etc.[7]. Pillaring of various LDHs with $V_{10}O_{28}^{6-}$ decavanadate anions has already been reported by several authors [8-13]. These materials were prepared by ion exchange from organic-anion pillared (terephtalate as an example) magnesium-aluminum LDHs [8,11] or zinc-aluminum, zinc-chromium, nickel-aluminum and magnesium-chromium precursors, which were primarily pillared with carbonate or chloride ions [9,10,12,13]. The exchange of the initially inserted anion was achieved in polyvanadate aqueous solutions at pH = 4.5.

The intercalation of vanadate anions between $Ni_{0.70}Co_{0.30}(OH)_2$ slabs is reported in the present paper, which deals with the characterization of the obtained material and, especially, of the intercalated vanadate species. Special attention is devoted to the exchange properties as well as to the thermal behavior.

2. MATERIAL PREPARATION

The preparation procedure, as schematized in the preparation flow chart of Fig. 1, consists of three steps : classical solid state reaction at high temperature, oxidizing hydrolysis and reduction.

The cobalt substituted sodium nickelate, $NaNi_{0.70}Co_{0.30}O_2$, prepared at high temperature (700-800°C), was used as the starting material for the chimie douce reactions. The γ-oxyhydroxide was prepared by an oxidizing hydrolysis of the $NaNi_{0.70}Co_{0.30}O_2$ phase in an oxidizing medium (4 M-KOH, 0.8 M-NaClO). These two reactions have been previously described in detail [5,14].

Preparation of the LDH by reduction from the γ-oxyhydroxide in the presence of NH_4VO_3.

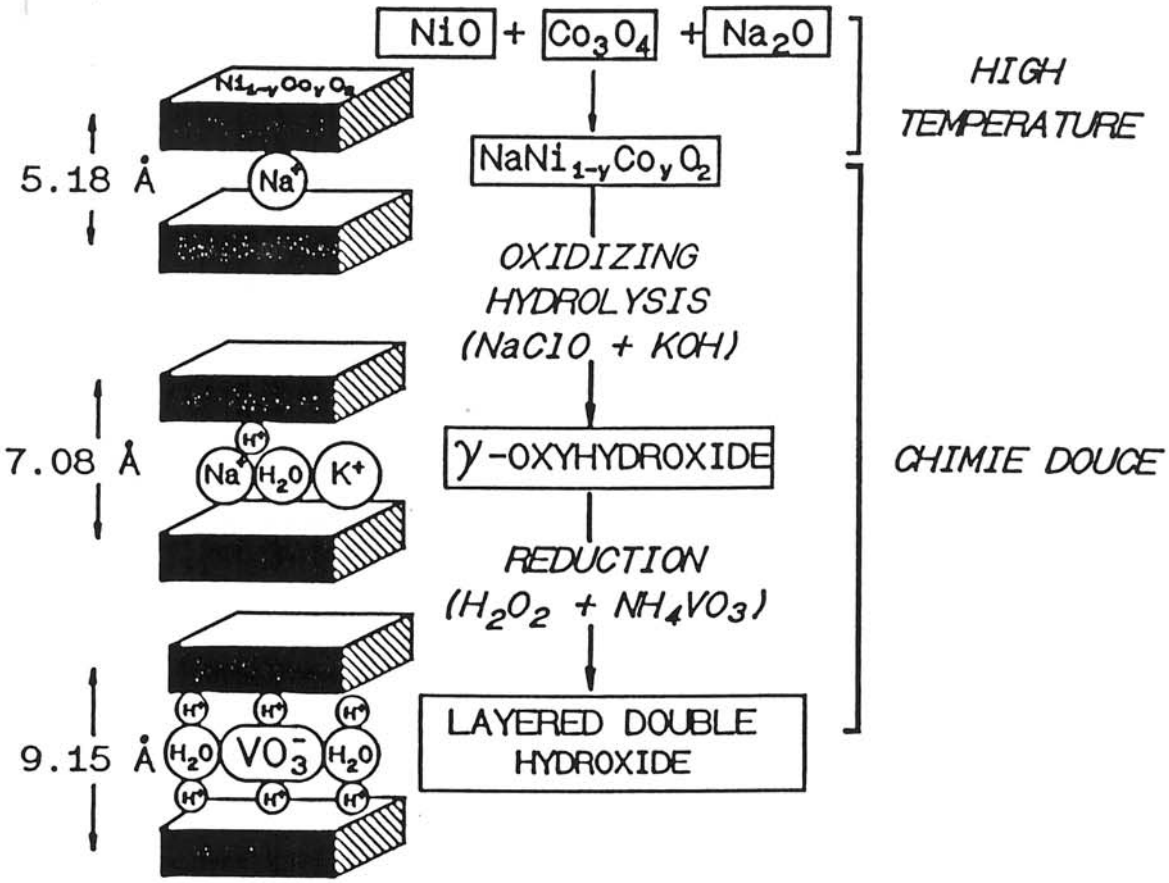

Fig. 1 : Schematization of the successive reaction steps involved in the preparation of the LDH by chimie douce.

100 ml of a mixture of 0.5 M-H_2O_2 and 0.14 M-NH_4VO_3 (pH = 4) were added dropwise into an other solution containing 1 g of γ-oxyhydroxide in suspension in 100 ml of deionised water. After stirring for 15 days, the obtained material was filtered, washed with deionised water and dried under vacuum.

The use of H_2O_2 as the reducing agent allows the selective reduction of nickel to the divalent state and of cobalt to the trivalent state [15], thus giving rise to the cationic oxidation states that are characteristic of an LDH. The role of NH_4VO_3 is to supply vanadate species, which are the candidates to be intercalated, into the reaction medium. All the preparative steps were performed in an air-free atmosphere so as to prevent the possible formation of any parasitic carbonate inserted LDH. Indeed, previous works have reported the higher stability of these carbonated materials in comparison with similar ones inserted with SO_4^{2-}, NO_3^-, Cl^-, ClO_4^-, CH_3COO^- anions [3,16].

3. RESULTS AND DISCUSSION

It should be noted that, in an H_2O_2 medium, a complex equilibrium involving various vanadate ionic species takes place, which depends on the concentrations of H_2O_2 and of the vanadate ions as well as on the pH of the solution [17,18]. As a consequence, in order to investigate the intercalation process, an accurate study of the evolutional changes in the vanadate species inserted within the LDH is required to be carried out during the reaction period. The results of such investigations will be published elsewhere. The present paper deals exclusively with the characterization of the final LDH, obtained after 15 days in the reaction medium. The results of X-ray diffraction, chemical analysis, infrared spectroscopy, thermal treatment and anionic exchange studies are reported and discussed hereafter.

3. 1. Crystal chemistry

The compositional and structural modifications of the materials involved during the chimie douce preparation, schematized in Fig. 1, have been intensively discussed from a general point of view in previous papers [3,5]. Nevertheless, some peculiar points worthy of note remain. Fig. 2 gathers the X-ray diffraction patterns of the precursor sodium nickelate, the γ-oxyhydroxide and the final LDH. The chimie douce reactions, in particular the reduction step, entail a material grinding which shows itself on the diffraction patterns as a line broadening.

3. 1. 1. Sodium nickelate

The $NaNi_{0.70}Co_{0.30}O_2$ precursor crystallizes in the rhombohedral system (SG : $R\bar{3}m$) with an O3 type structure [19]. The indexation with a hexagonal cell, reported in Fig. 2, yields the following parameters : $a = 2.933 \pm 0.005$ Å, $c = 15.51 \pm 0.03$ Å.

3. 1. 2. γ-oxyhydroxide

Obtaining of the γ-oxyhydroxide from the $NaNi_{0.70}Co_{0.30}O_2$ precursor proceeds with a partial exchange of Na^+ ions for protons and K^+ ions and an intercalation of water molecules [5,20]. The general formula of the γ-phase has been previously determined [5,20]. The following one, $H_{0.20}Na_{0.12}K_{0.21}(H_2O)_{0.47}\,Ni_{0.70}Co_{0.30}O_2$, given as an example, must be considered as one member of a more general set of materials in which the amount of intercalated species can slightly vary.

The γ-phase crystallizes in the rhombohedral system, but unlike sodium nickelate, does so in the R3m space group with a P3 type structure [5,19]. The O3 → P3 structural change that occurs during the oxidizing hydrolysis proceeds by a slab gliding [14,20]. As shown in Fig. 2, the metal-metal intraslab distance (which is equal to twice the d_{110} distance) decreases as expected during the oxidation while the interslab distance (which is equal to the d_{003} distance) increases as a result of the intercalation of water molecules.

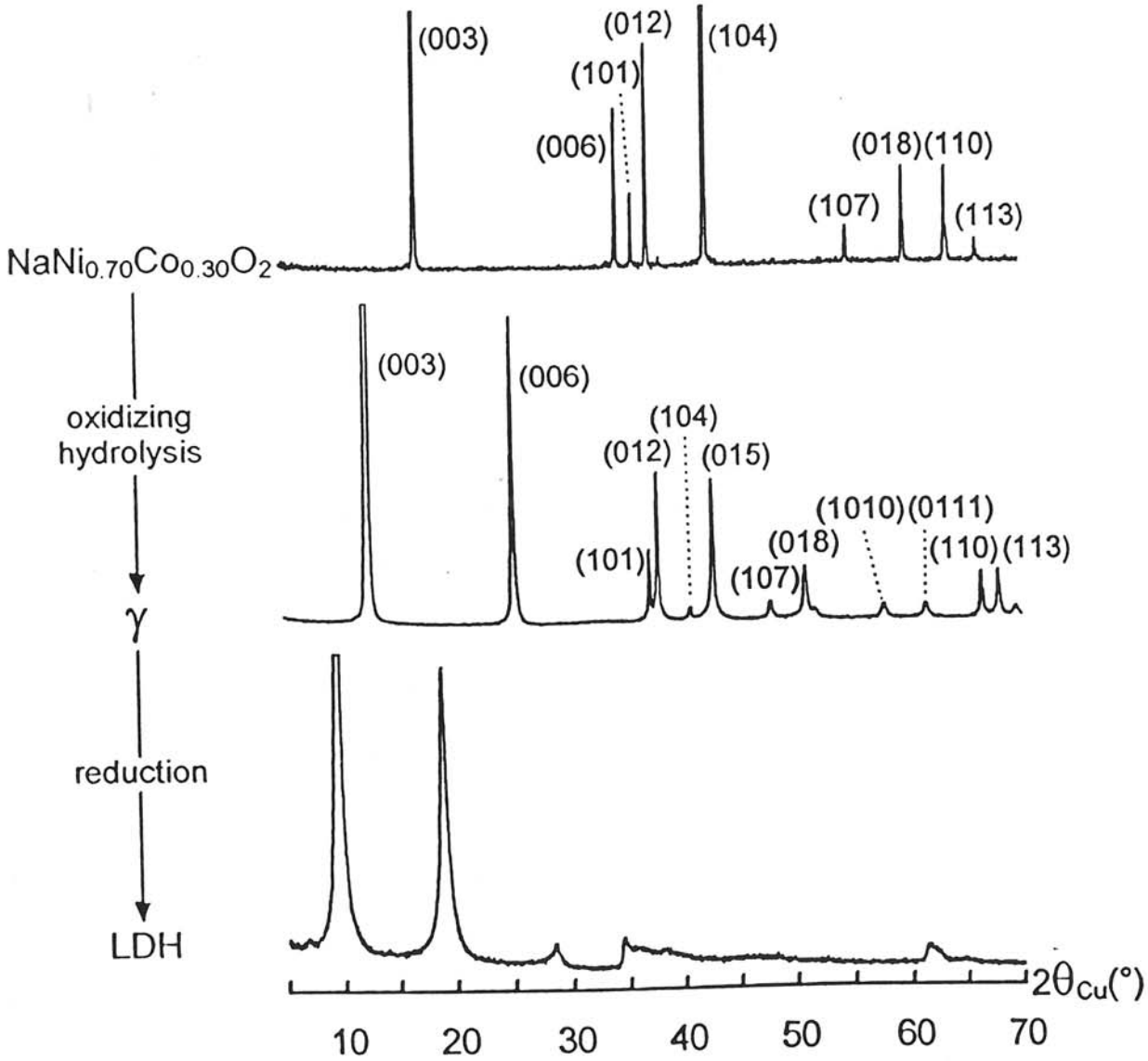

Fig. 2 : Evolution of the X-ray diffraction patterns of the materials involved during the preparation of the LDH.

3. 1. 3. The LDH

The LDH obtained after reduction of the γ-phase in the presence of NH_4VO_3 has to be systematically compared to the carbonate inserted cobalt substituted nickel hydroxide ($LDH(CO_3)$), which was prepared under identical conditions in our laboratory (reduction in H_2O_2 medium in the presence of carbonate ions) [5]. This phase used to be denoted as $\alpha^*(CO_3)$. This current notation is found for nickel hydroxides, intended to be used as positive electrode materials of nickel-cadmium batteries. However, in this paper, this phase will be denoted as $LDH(CO_3)$ rather than $\alpha^*(CO_3)$ in order to emphasize the concept of the layered double hydroxide. In addition, as a result of the structural similarity between the $LDH(CO_3)$ phase and the LDH phase obtained in the presence of NH_4VO_3 and in accordance with the results of chemical analysis and infrared spectroscopy, which will be presented in the subsequent section, the LDH phase obtained in the presence of NH_4VO_3 will be denoted hereafter as $LDH(VO_3)$.

The X-ray diffraction patterns of the two materials are represented in Fig. 3. The $LDH(CO_3)$ phase crystallizes in the rhombohedral system [3]. Indexation of the diffraction lines can be done with a hexagonal cell with three $Ni(OH)_2$ slabs per cell, as indicated in Fig. 3, and yields the following cell parameters : $a = 3.04 \pm 0.02$ Å and $c = 23.0 \pm 0.3$ Å. The (10ℓ) and (11ℓ) diffraction line series present in the X-ray diffraction pattern of the $LDH(CO_3)$ phase are replaced, for the $LDH(VO_3)$ phase, by two large asymmetric « bands » in the 30-60° and 60-70° ($2\theta_{Cu}$) ranges, respectively. Such a behavior is characteristic of a disorder in the periodicity of both the (10ℓ) and (11ℓ) planes and does not allow any indexation of the X-ray diffraction pattern. That shape of the X-ray diffraction pattern suggests actually a turbostratic-like character. The similarity of the X-ray diffraction patterns between the $LDH(CO_3)$ and the $LDH(VO_3)$ phases shows that the interslab distance is 9.15 Å for the $LDH(VO_3)$ phase, while the metal-metal distance within the slabs is close to 3.04 Å. As emphasized in Fig. 2, the large increase in the interslab distance from 7.08 Å in the γ-phase up to 9.15 Å in the

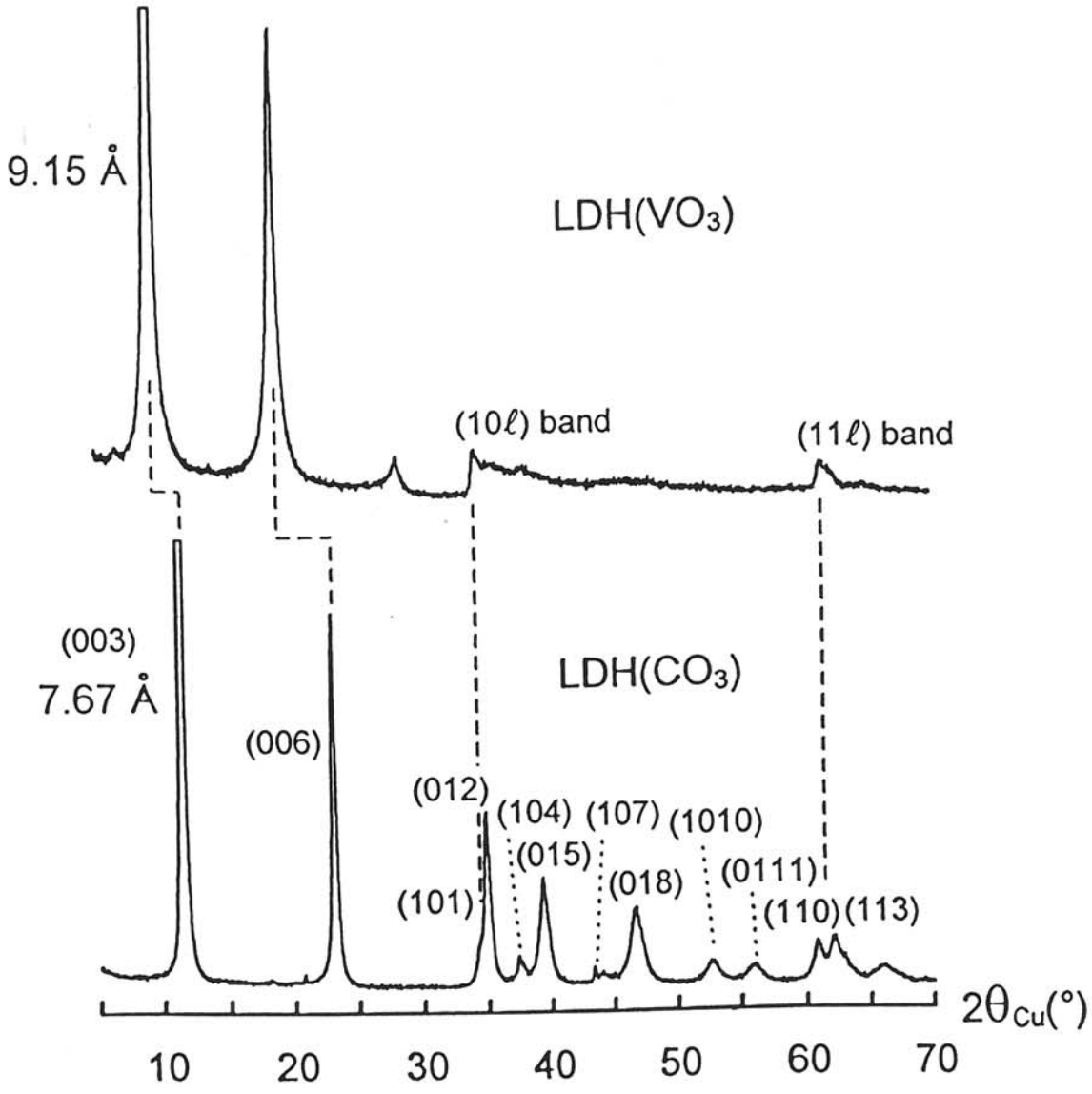

Fig. 3 : Comparison of the X-ray diffraction patterns of the homologous LDH(VO_3) and LDH(CO_3) phases.

$LDH(VO_3)$ phase results from the insertion of anionic species into the interslab space during the reduction step.

The existence of large asymmetric diffraction bands, characteristic of a disorder in the periodicity of the (10ℓ) and (11ℓ) planes, was already observed in α-type nickel hydroxides or cobalt substituted derivatives [21,22]. Such behavior is classically assigned to a turbostratic character of the material, which consists of parallel and equidistant slabs disoriented with regard to one another along the c axis. However, the existence of those large asymmetric bands in the X-ray diffraction pattern of the $LDH(VO_3)$ phase may also be attributed to local distortions within each slab, due to microstrains arising from the distribution of the electrostatic charges within the material. The X-ray diffraction pattern of the precursor γ-phase (Fig. 2) does not exhibit large asymmetric bands as the $LDH(VO_3)$ phase but reveals distinct (10ℓ) lines. The hypothesis of turbostraticity for the $LDH(VO_3)$ phase would suggest a rotation of the slabs with regard to one another during the step of reduction from the γ-phase. Since the energy involved in the chimie douce reactions is not sufficient to achieve such a rotation of the slabs, one can assume that the $LDH(VO_3)$ phase exhibits probably local distortions within each slab rather than a turbostratic character. In order to further confirm the hypothesis of local distortions within the slab, a chemical cycling (oxidation reaction followed by reduction) was attempted starting from the the $LDH(VO_3)$ phase. The X-ray diffraction patterns of the various obtained materials are gathered in Fig. 4. For the aforementioned reasons, the obtention of a well-ordered γ-phase, denoted as $\gamma_{oxid.}$ in Fig. 4, arising from oxidation of the $LDH(VO_3)$ phase confirms the hypothesis of local distortions within the slabs. In addition, if we assume a rotation of the slabs during the successive steps of oxidation and reduction, strong strains would occur and generate a grain grinding. This would be expected to appear in the X-ray diffraction pattern of the $\gamma_{oxid.}$-phase and of the $LDH(VO_3)_{rcd.}$ phase as a line broadening more important than the observed one. This behavior leads to reject again the hypothesis of turbostratic character in favor of local distortions within the slabs.

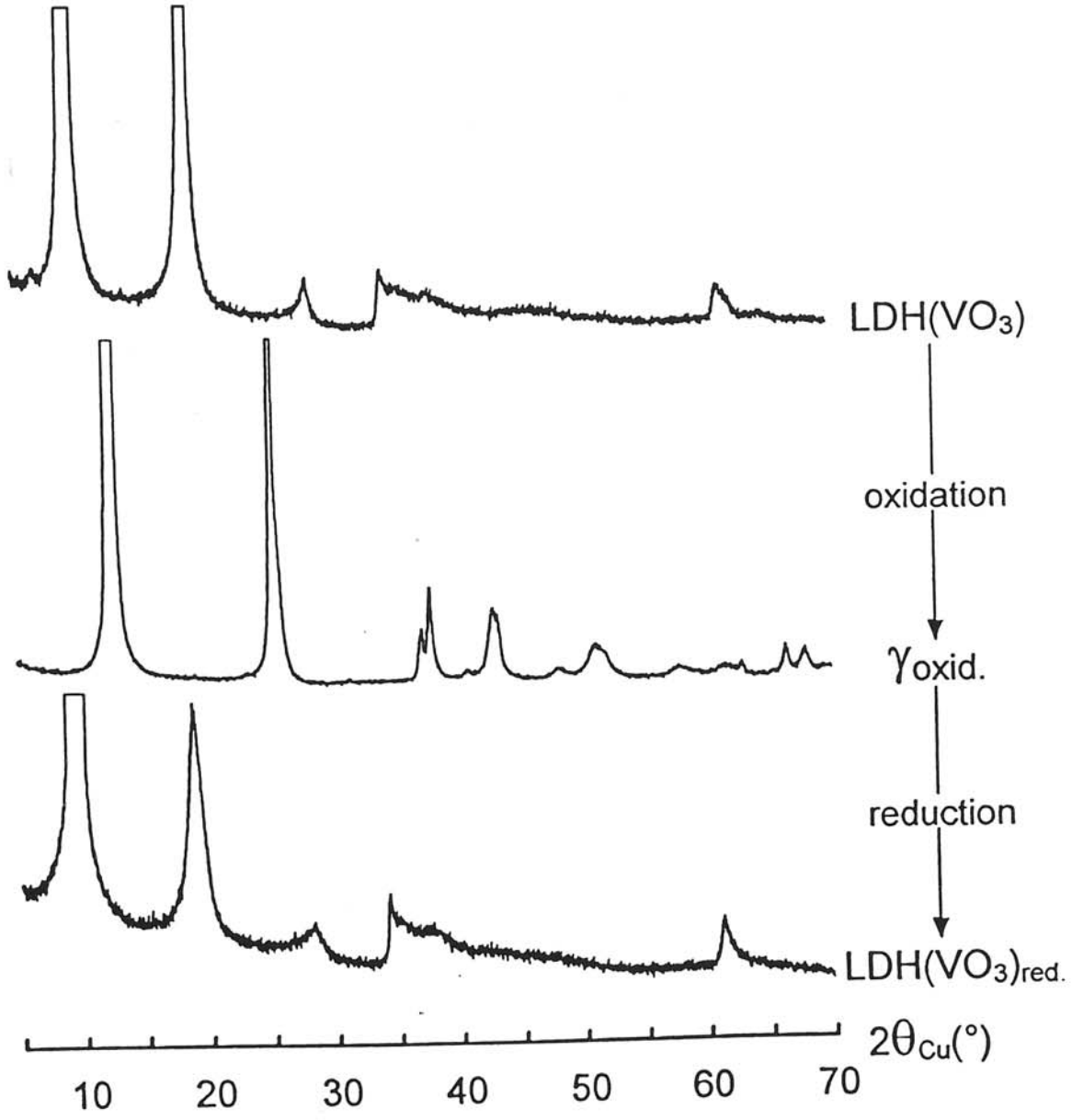

Fig. 4 : Evolution of the X-ray diffraction patterns of the materials involved during the chemical cycling of the LDH(VO_3) phase.

3. 2. Chemical analysis

The weight percentages of the various elements present in the LDH(VO_3) phase were determined at the CNRS Analysis Facility in Vernaison (France). The atomic ratios, A / (Ni + Co) (where A designates a given element), calculated on the basis of the weight percentage values, are reported in Table I for the LDH(VO_3) phase and for the material obtained after a thermal treatment of LDH(VO_3). In order to establish more precisely the chemical formula of the material, the average oxidation state of the metal cations within the slabs and of the interlamellar vanadium ions were determined by iodometric titration. Experiments showed that nickel and cobalt ions are reduced to the divalent state by iodide ions while vanadium ions are reduced to the tetravalent state under the same conditions. The iodometric titration of LDH(VO_3) yields therefore the difference in average cationic oxidation state of the nickel, cobalt and vanadium ions before and after the reduction by iodide ions. The value obtained, 0.69 ± 0.05, suggests the presence of 0.70 Ni^{2+} and 0.30 Co^{3+} ions within the slabs plus 0.39 ± 0.05 V^{5+} ions corresponding to the inserted vanadate species. These cationic oxidation state values and the overall values reported in Table I suggest the following average formula : $Ni_{0.70}Co_{0.30}(OH)_2\ (VO_3)_{0.34}(H_2O)_{0.58}$, which is very similar to that previously obtained for carbonated LDH phases [5,6] and for hydrotalcite-type materials [2].

The above formula shows the presence of approximately one negative charge per vanadium ion, which indicates the existence of metavanadate type species inserted within the interslab space. As several types of metavanadate anion have been reported in the literature, an infrared study of the material has been performed.

	$\frac{A}{(Ni + Co)}$ molar ratio	
A	**LDH(VO_3)**	**After thermal treatment at 190°C**
Ni	0.70	0.70
Co	0.30	0.30
V	0.34	0.34
II	3.17	1.95

Table I : Values of the A / (Ni + Co) molar ratios for various elements in the LDH(VO_3) phase and in the material obtained after a thermal treatment at 190°C.

3. 3. Infrared study

The powder samples were dispersed in acetone, placed on a CsI plate and analyzed after evaporation of acetone using a PERKIN-ELMER 983 spectrometer in the 4000-200 cm^{-1} range. The infrared spectrum of the LDH(VO_3) phase is reported in Fig. 5 in comparison with the spectra of the LDH(CO_3) one and of NH_4VO_3. It is clear that the first spectrum exhibits strong similarities with the other two.

The general shape of the spectrum of the LDH(VO_3) phase is similar to that of the LDH(CO_3) phase, which has already been extensively discussed in previous papers [23,24]. The wide bands around 3400 cm^{-1} and 1650 cm^{-1} correspond to the ν (H_2O) and δ (H_2O) vibration modes of the water molecules, mainly intercalated within the interslab space. In the spectrum of the LDH(VO_3) phase, the absence of a band at 1360 cm^{-1}, characteristic of the presence of carbonate ions (in D_{3h} symmetry), indicates that no parasitic carbonate ion has been inserted, confirming the results of the chemical analysis.

The comparison of the top two spectra in the 1000-200 cm^{-1} range in Fig. 5 shows the insertion, in the LDH(VO_3) phase, of vanadate species that exhibit similarities with those present in NH_4VO_3. It is well known that the metavanadate anions, either in solution or in crystals such as NH_4VO_3 or KVO_3, exhibit a $(VO_3)_n^{n-}$-type infinite-chain structure, made of corner-sharing VO_4 tetrahedra [25]. Since the conformation of the chain within the LDH(VO_3) material is probably different from that in the NH_4VO_3 or KVO_3 crystal, the values of the vibrational frequencies observed for the $(VO_3)_n^{n-}$ chains (consisting of VO_4 groups with the C_{2v} symmetry) in aqueous solution as well as in solid materials were examined. The corresponding data are reported in Table II [26,27]. The existence of « cyclic polymer » metavanadate anions such as $V_3O_9^{3-}$ or $V_4O_{12}^{4-}$, studied by Griffith [26], was also envisaged. Examination of the frequency values reported in Table II shows that the presence of cyclic metavanadate anions would result in the

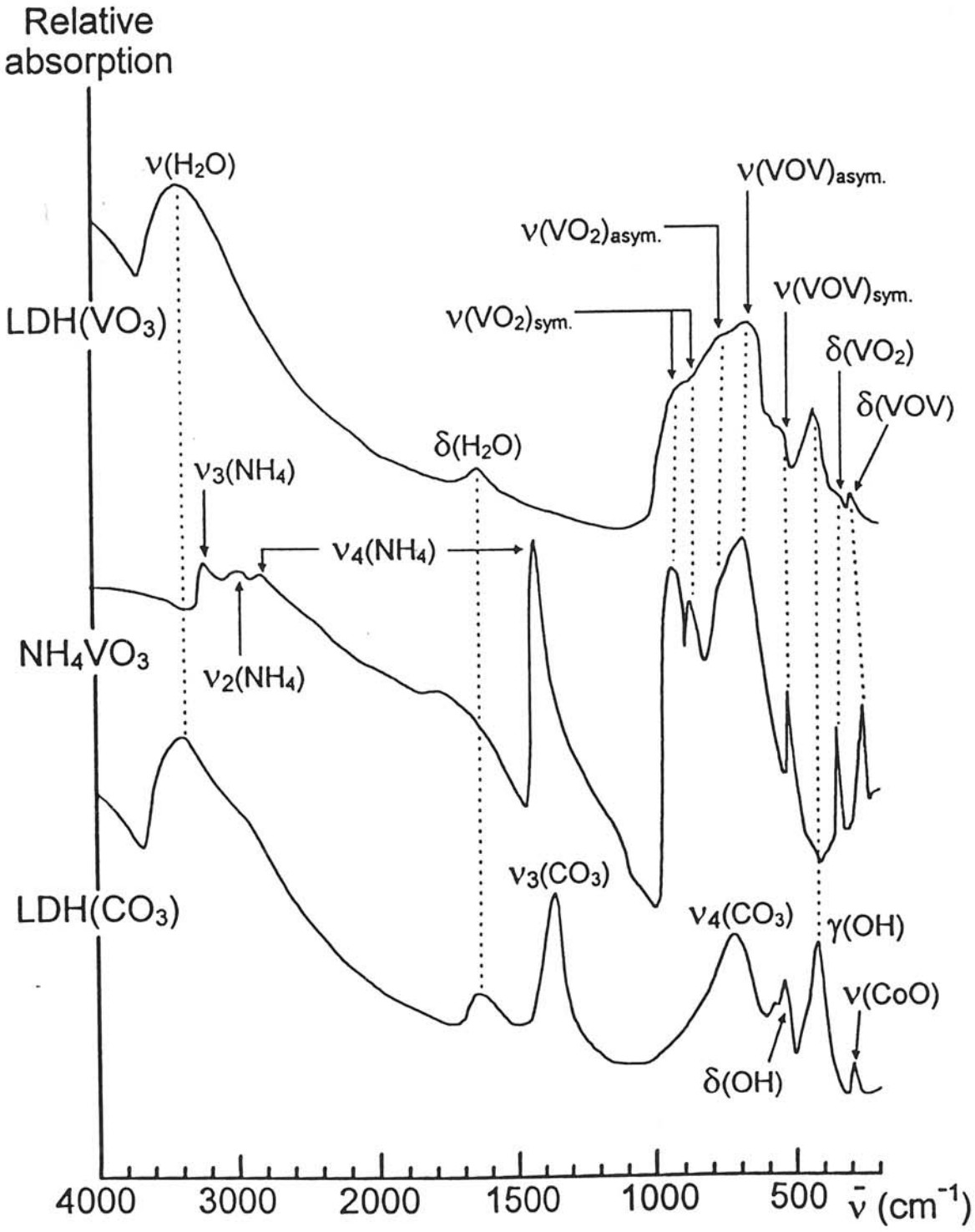

Fig. 5 : Comparison of the infrared spectra of the LDH(VO_3), NH_4VO_3 and LDH(CO_3) phases.

Vibrational wave numbers (cm^{-1})						
LDH(VO_3) (this work)	$(VO_3)_n^{n-}$ chain in solid NH_4VO_3 (this work)	$(VO_3)_n^{n-}$ chain in solution (27)	Cyclic tetramer $V_4O_{12}^{4-}$ in solution (26)	$(VO_3)_n^{n-}$ chain in solid NH_4VO_3 (27)	$(VO_3)_n^{n-}$ chain in solid KVO_3 (27)	Vibrational modes
900	915 880	920	952	935 895	960 935 890	$\nu(VO_2)_{sym.}$
800	800	820	905	850	850	$\nu(VO_2)_{asym.}$
670	660	640		690	693	$\nu(VOV)_{asym.}$
550	505	530		495	495	$\nu(VOV)_{sym.}$
350	330	326		333	385 352 318	$\delta(VO_2)$
220	235	223		223	262 231 219	$\delta(VOV)$

Table II : Comparison of the vibrational frequency values experimentally observed in the infrared spectrum of the LDH(VO_3) phase to the values reported for metavanadate chains (consisting of VO_4 groups in C_{2v} symmetry) in aqueous solution or in solid materials.

absence of several vibrations in the 700-200 cm^{-1} range. Since those vibrations (ν $(VOV)_{asym.}$, ν $(VOV)_{sym.}$, δ (VO_2) and δ (VOV)) are in fact present in the spectrum of the LDH(VO_3) phase, the hypothesis of cyclic metavanadate entities can be excluded in this material. Further, good agreement is obtained between the vibrational frequencies observed for the LDH(VO_3) phase and those gathered in Table II for $(VO_3)_n^{n-}$ chains in solution or in solid materials. This behavior confirms the presence of such chains within the interslab space of the LDH(VO_3) phase.

3. 4. Discussion about the structure

The difference between the nickel-nickel interslab distance of the LDH(VO_3) phase (9.15 Å) and that of a β(II) nickel hydroxide (4.6 Å) shows that the interslab space of the LDH(VO_3) phase contains two oxygen layers, therefore two ideal chain conformations can be envisaged [25,27,28]. One (a), illustrated in Fig. 6 (a), is similar to that observed in NH_4VO_3. A calculation based on the available crystallographic data [25], taking the ionic radius of oxygen into account (1.34 Å) [29], leads to a value for the thickness of the chain close to 5.0 Å. The other possible conformation of the chain (b), illustrated in Fig. 6 (b), leads to a value of the thickness close to 4.7 Å. The interslab distance can be very simply considered as the sum of the thicknesses of the metavanadate chain and of the $Ni_{0.70}Co_{0.30}(OH)_2$ slab, which is approximately equal to 4.6 Å. Consequently, the previously calculated values of the chain thicknesses lead to interslab distances equal to 9.6 Å and 9.3 Å respectively, which are both in good agreement with the experimental value (9.15 Å, as indicated in Fig. 3). Even if the 9.3 Å value seems to be the most suitable one (chain conformation b), it is not reasonable to propose, from this consideration only, any precise chain conformation because the atomic positions within the interslab space are not known.

The presence of interlamellar $(VO_3)_n^{n-}$ chains may account for the local distortions within the slab, deduced from the presence of the (10ℓ) and (11ℓ) X-ray asymmetric diffraction bands, as previously discussed. Indeed, the oxygen-oxygen distance (3.04 Å) within the $Ni_{0.70}Co_{0.30}(OH)_2$ slabs is significantly different from that

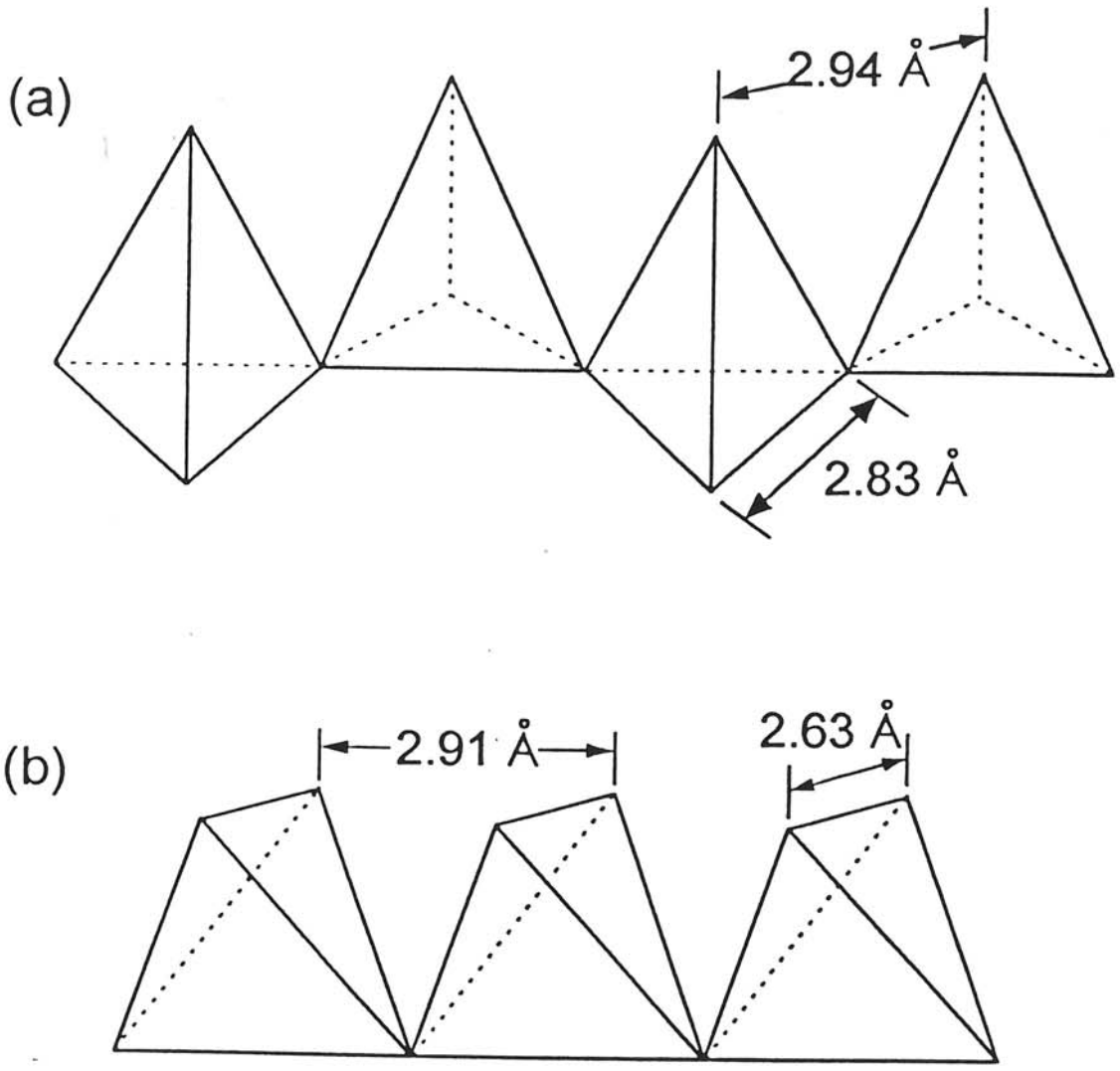

Fig. 6 : Two possible conformations of the metavanadate chains within the interslab spaces of the LDH(VO_3) phase.

observed within the inserted $(VO_3)_n^{n-}$-type chains (2.91 Å) [28,29], so that the various oxygen layers cannot fit in a convenient way, which leads to microstrains and therefore to local distortions within the slabs. This hypothesis is supported by the fact that, in the case of isolated inserted anions (CO_3^{2-}, NO_3^-, SO_4^{2-}), such behavior is not observed due to an easier accommodation of the successive oxygen layers.

3. 5. Study of the anionic exchange

The strong selectivity of the layered double hydroxides for the intercalation of carbonate anions has been reported by several authors [3,16,30]. This generally results in a high facility for any intercalated anion (Cl^-, NO_3^-, SO_4^{2-}, ClO_4^-, etc.) to be exchanged by carbonate ions. An exchange reaction of the metavanadate chains by carbonate ions within the LDH(VO_3) phase was attempted. For this purpose, 500 mg of material were added to 250 ml of a 0.11 M-K_2CO_3 solution (corresponding to a carbonate / vanadate ratio equal to 22). After stirring for two days, the material was filtered, washed with deionised water and dried. No significant change in the X-ray diffraction pattern, nor in the infrared spectrum, nor in the chemical composition was detected, showing that no exchange reaction has occured. Such a behavior may be attributed to a very weak mobility of the metavanadate chains within the interslab space as a result of their steric hindrance.

3. 6. Study of the thermal behavior

3. 6. 1. Thermogravimetric analysis

The thermogravimetric analysis of the LDH(VO_3) phase was performed at a rate of +1°C/min, from room temperature to 800°C, under an oxygen flow. The weight loss curve obtained under these conditions is given in Fig. 7. It shows two stages leading finally to a mixture of NiO, Co_3O_4 and V_2O_5 oxides, identified by X-ray diffraction. The first stage of weight loss, which ranges from room temperature to 190°C, is in accordance with the removal of 0.75 water molecules. As further discussed, a layered structure is obtained in these conditions. Beyond 190°C, the weight loss, corresponding

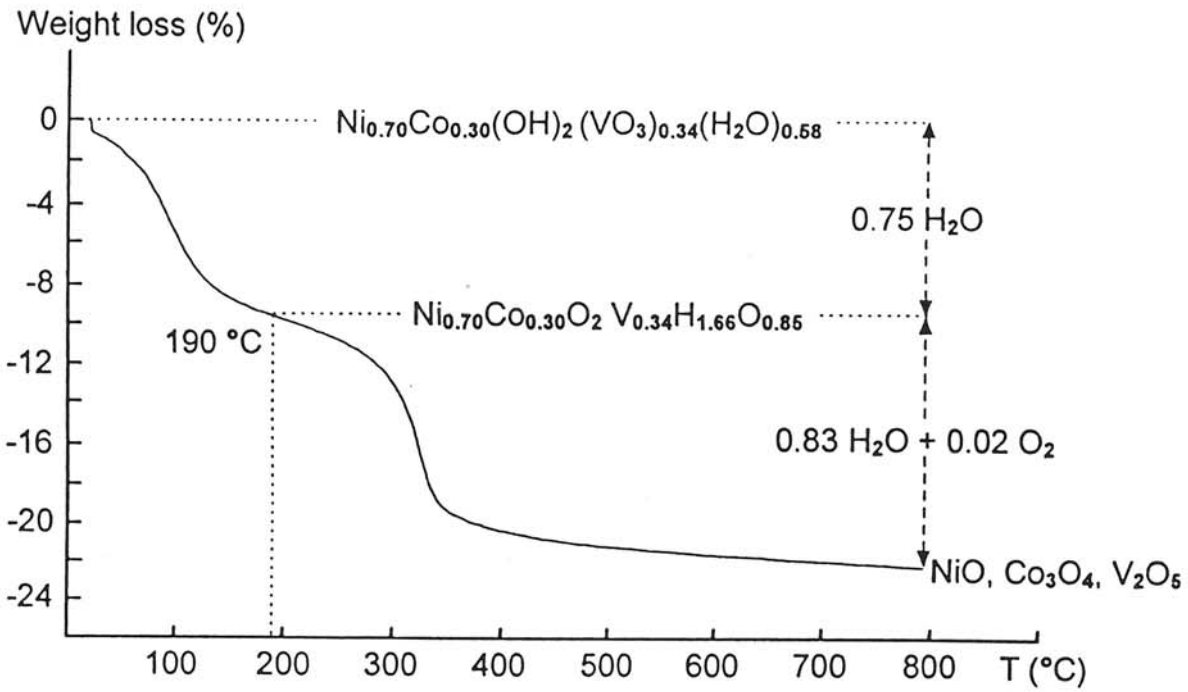

Fig. 7 : Thermogravimetric analysis curve of the LDH(VO_3) phase.

to 0.83 water molecules and 0.02 oxygen molecules, continues and the destruction of sheets occurs. This oxygen release results from the formation of Co_3O_4 from the trivalent cobalt ions of the LDH(VO_3) phase. These weight losses will be discussed in the subsequent section.

3. 6. 2. Characterization of the material obtained after a thermal treatment of the LDH(VO_3) phase at 190°C

The 190°C temperature was chosen for the thermal treatment because it corresponds approximately to the end of the first stage of the TGA curve. The treatment was performed under an oxygen flow in three steps : +1°C/min from room temperature to 190°C, 3 hours at 190°C and finally -1°C/min from 190°C to room temperature. The material obtained after this thermal treatment was characterized by X-ray diffraction, elemental analysis and infrared spectroscopy.

The X-ray diffraction pattern after the thermal treatment is reported in Fig. 8 in comparison with that of the LDH(VO_3) starting material. The large asymmetric diffraction bands observed for the LDH(VO_3) phase are replaced by separate diffraction lines after the thermal treatment, which indicates a disappearance of the microdistortions and therefore a decrease in the slab / interslab strains. Indexation of the X-ray diffraction pattern of the thermally treated material shows that it cristallizes in the hexagonal system with the following cell parameters : $a = 3.04 \pm 0.01$ Å and $c = 7.21 \pm 0.03$ Å. The interslab distance decreases significantly from 9.15 Å in the LDH(VO_3) phase to 7.21 Å in the material after the thermal treatment. This value, which lies in the same range as that observed for LDH(CO_3) (7.67 Å) (Fig. 3), suggests that only one oxygen layer belonging to the vanadate anions is located between the slabs. A similar behavior has already been observed in our laboratory for homologous materials with the typical formula $Ni_{0.70}Co_{0.30}(OH)_2(SO_4)_{0.15}(H_2O)_z$ [3] and by El Malki et al. in a chromium copper hydroxide : $[Cu_{0.67}Cr_{0.33}(OH)_2](SO_4)_{0.17}(H_2O)_z$ [31], which belong to the layered double hydroxide group of materials. This behavior has been attributed to a grafting of the intercalated sulphate anions to the slab upon heating : a bond is

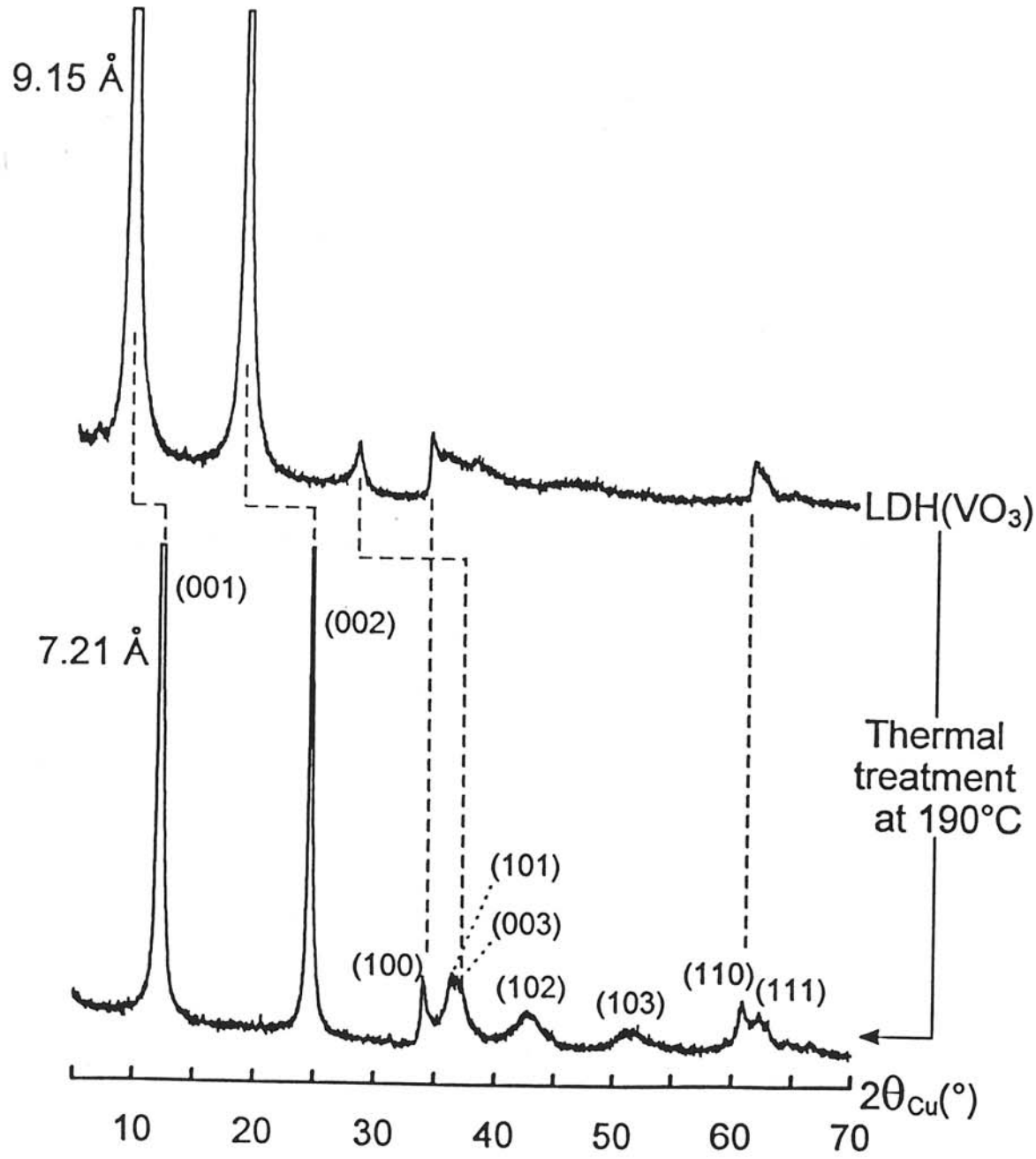

Fig. 8 : Comparison of the X-ray diffraction patterns of the LDH(VO_3) phase and of the material obtained after thermal treatment at 190°C under an oxygen flow.

established between one oxygen ion of the intercalated anion and one metal cation of the slab, which proceeds through the replacement of one hydroxyl ion of the slabs by the apical oxygen ion of the sulfate anions [3]. As a result of the significant difference in the oxygen-oxygen distance within the $Ni_{0.70}Co_{0.30}(OH)_2$ slabs and within the inserted $(VO_3)_n^{n-}$-type chains, previously stated, the grafting of the chains to the slabs should enhance the steric strains. On the contrary, the opposite effect occurs : the local distortions within the slab (characterized by large asymmetric diffraction bands) disappear. Such a behavior can be assigned to a partial fragmentation of the chains when the grafting processes, in order to better accommodate the steric and electrostatic interactions. A mechanism for the grafting / fragmentation phenomenon of the metavanadate chains is schematically proposed in Fig. 9. The more the chain fragmentation occurs, the more the structural strains decrease, therefore the more the structural microdistortions disappear. The linking of an oxygen ion of one $(VO_3)_n^{n-}$-type chain to a metal cation of the slab in replacement of one slab hydroxyl ion entails a breaking of the chain into two parts. The terminal vanadium ion of the first part is, as expected, tetrahedrally coordinated while the termination of the second part can be achieved via the linking of the terminal vanadium ion to one oxygen ion of a slab hydroxyl group, which is therefore deprotonated.

The infrared spectra of the materials before and after the thermal treatment, which are reported in Fig. 10, show a decrease in the intensity of the $\nu\,(VO_2)_{asym.}$, $\nu\,(VO_2)_{sym.}$ and $\delta\,(VO_2)$ bands upon heating. Such a change can be attributed to a blocking of the vibrations of one part of the VO_2 groups due to the linking of some oxygen ions to the metal cations of the slabs. In addition, the intensity of the vibrations corresponding to the VOV groups is maintained upon heating, which implies that small metavanadate entities consisting of at least two corner-sharing VO_4 tetrahedra must remain within the interslab space after the thermal treatment. Such a hypothesis is in agreement with the chemical formula deduced from the TGA curve at 190°C, $Ni_{0.70}\,Co_{0.30}\,(OH)_{1.66}\,(V_2O_7)_{0.17}$, which corresponds to the presence of interlamellar V_2O_7 entities grafted via the two apical oxygen ions of the VO_4 tetrahedra to two adjacent slabs, as schematized in Fig. 11. This model is in accordance with the existence,

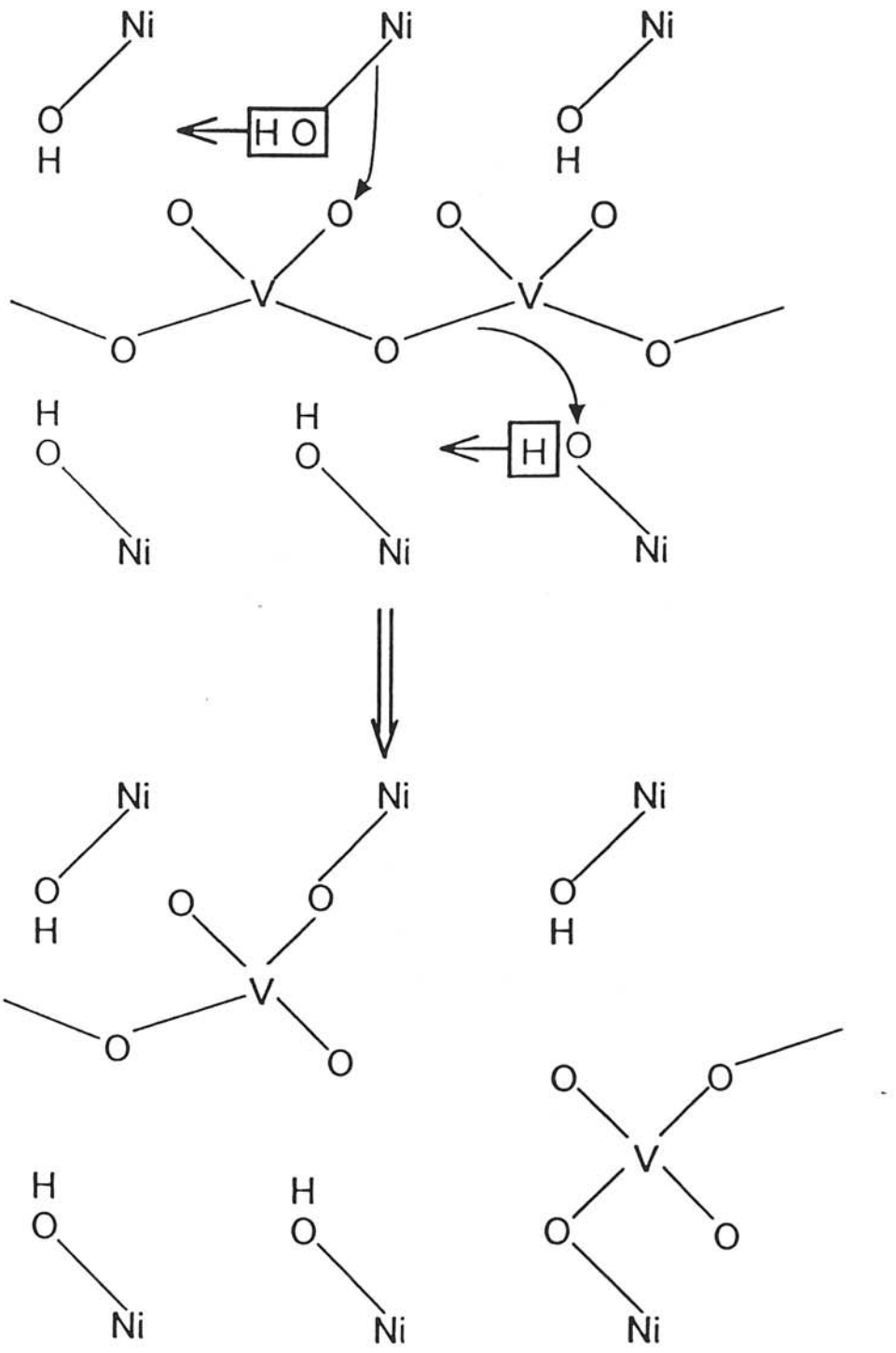

Fig. 9 : Schematic representation of the grafting / fragmentation mechanism of the metavanadate chains.

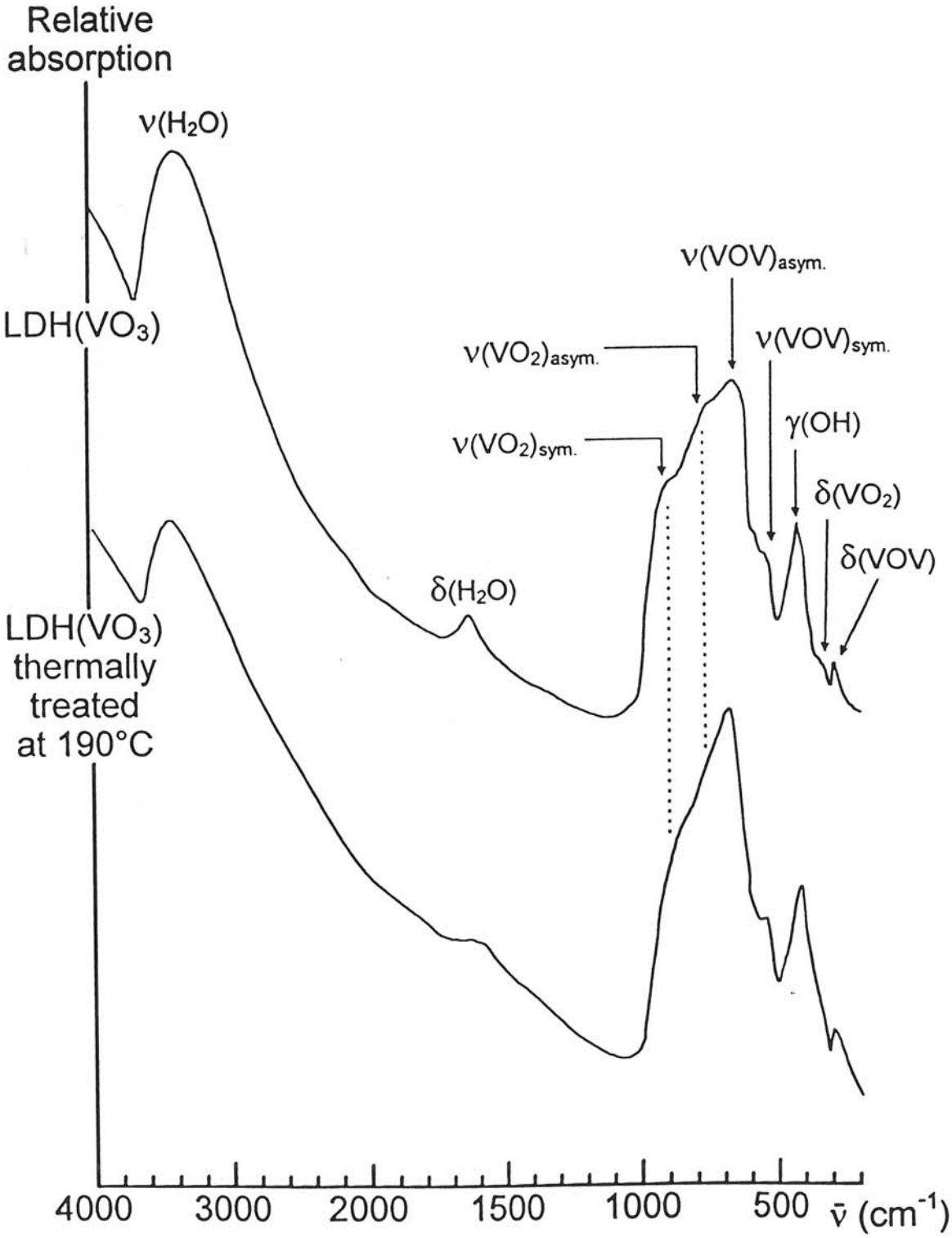

Fig. 10 : Comparison of the infrared spectra of the LDH(VO_3) phase and of the material obtained after thermal treatment at 190°C.

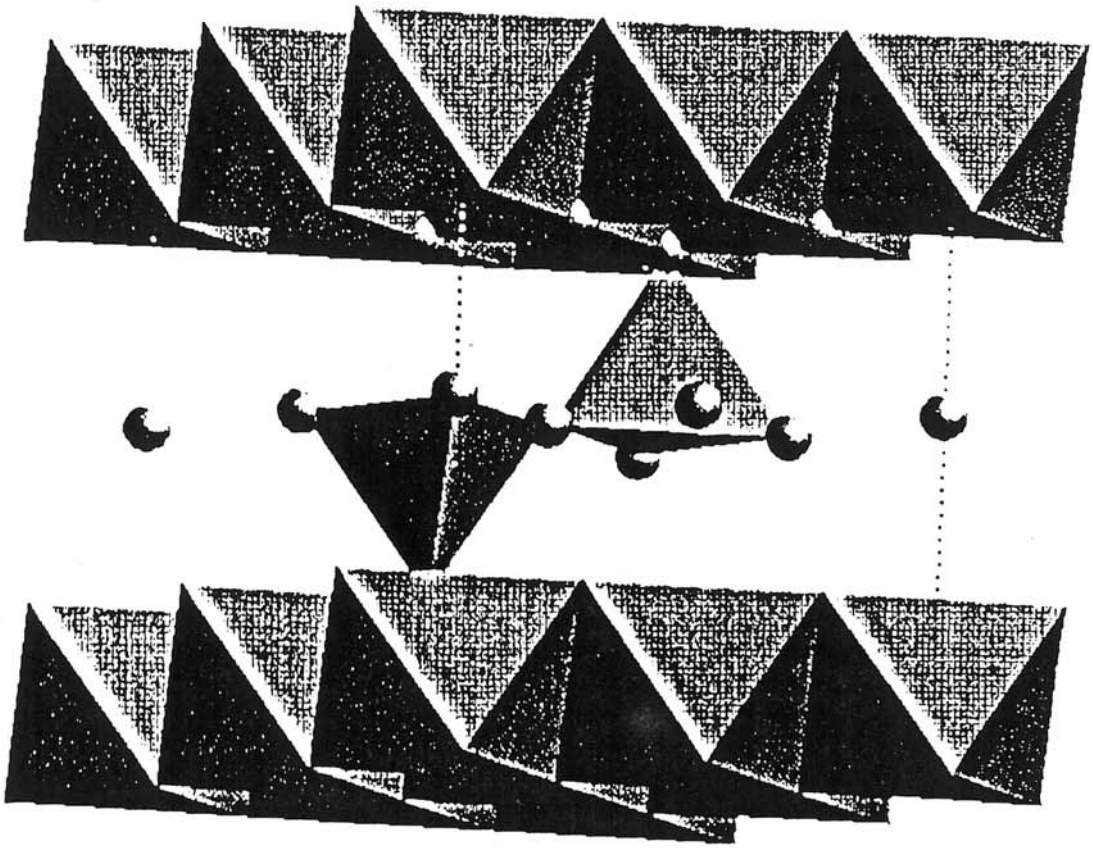

Fig. 11 : Schematic representation of the structure of the LDH thermally treated at 190°C.

previously stated, of one oxygen layer between the $Ni_{0.70}Co_{0.30}(OH)_2$ slabs. In addition, the general shape of the X-ray diffraction pattern simulated on the basis of that structural model is in good agreement with that of the experimental one, but the broadening of the diffraction lines prevents any structural refinement.

The preparation of metavanadate chains pillared LDHs by reconstruction in polyvanadate solutions at pH higher than 4.5 from precalcined nickel-aluminum and magnesium-chromium carbonate pillared precursors has already been reported by Kooli et al. [10,12]. Nevertheless, the data presented in Section 3.4. show that the interslab distances obtained by these authors (7.3 Å) are too short to allow the presence of free-$(VO_3)_n^{n-}$ chains within the interslab space. Such value of the interslab distance is indeed characteristic of one oxygen layer between the slabs, which rather suggests the presence of interlamellar vanadate entities grafted to the slabs, in a similar fashion to the material containing V_2O_7 grafted species that we obtained by thermal treatment of the free-$(VO_3)_n^{n-}$ chains inserted LDH(VO_3) material.

Examination of the infrared spectra shows also a decrease in the intensity of the ν (H_2O) and δ (H_2O) bands, which accounts for a decrease upon heating in the amount of water molecules, which are mainly intercalated within the interslab space. This behavior is confirmed by the change in the chemical composition, reported in Table I, which shows a noticeable decrease in the H / (Ni + Co) molar ratio : 1.22 hydrogen atoms per (Ni + Co) atom are lost during the thermal treatment. These hydrogen atoms can arise either from inserted and adsorbed water molecules or from water molecules which can be produced by the combination of the OH^- ions released from the slabs during the grafting and the protons arising from the simultaneous fragmentation and grafting of the chains, above mentioned. The loss of hydrogen atoms calculated on the basis of the thermogravimetric analysis performed up to 190°C (1.50 per metal cation), is different from the value determined by chemical analysis for the material recovered after a cooling following the thermal treatment (1.22 per metal cation). This behavior probably results from an adsorption or a slight reinsertion of water molecules when the temperature decreases. It should be noticed that the formula deduced from the TGA weight loss at 190°C shows that all water molecules have been removed in these conditions. Anyhow, provided that the dehydroxylation and the deprotonation of the

slabs are complete, 1.58 water molecules and 0.02 oxygen molecules expected from the chemical formula are in full agreement with the total weight loss observed by TGA upon heating to 800°C.

Note that all the attempted rehydrations of the heated material have been unsuccessful : the interslab distance is not modified by such a treatment, which further evidences the linking of the VO_4 tetrahedra to the slab.

In all cases, the VO_3 / Co molecular ratio has been found to be slightly larger than 1. In a first step, this result was attributed to some inaccuracy of the analytical study. Nevertheless, such a departure could also result from an initial spontaneous grafting of a small amount of VO_4 tetrahedra to the slabs.

Further studies are required in order to determine whether the metavanadate chains are directly inserted into the interslab space during the preparation or arise from an in situ condensation of intercalated vanadate species within the interslab space. The investigation of such a process will be reported in forthcoming papers.

4. CONCLUSION

A new layered double hydroxide with the chemical formula : $Ni_{0.70}Co_{0.30}(OH)_2\ (VO_3)_{0.34}(H_2O)_{0.58}$ was prepared by a chimie douce method. The studies by X-ray diffraction and infrared spectroscopy and the chemical analysis show that $(VO_3)_n^{n-}$ metavanadate anionic chains are actually intercalated between the hydroxide slabs. The strains due to the electrostatic interactions between the chains and the $Ni_{0.70}Co_{0.30}(OH)_2$ slabs lead to local distortions within the slab. All attempted exchanges of the chains by other anions have failed as a result of the poor mobility of the chains. The thermal treatment leads to a grafting / fragmentation of the metavanadate anionic chains coupled with a removal of water.

REFERENCES

[1] W. Jones and M. Chibwe, Pillared Layered Structures, IV. Mitchell Ed., Elsevier, London, (1990) 67.

[2] F. Cavani, F. Trifiro and A. Vaccari, Catalysis Today, 11 (1991) 173.

[3] C. Delmas and Y. Borthomieu, J. Solid State Chem., 104 (1993) 345.

[4] J. J. Braconnier, C. Delmas, C. Fouassier, M. Figlarz, B. Beaudouin and P. Hagenmuller, Revue de Chimie Minérale, 21 (1984) 496.

[5] C. Delmas, J. J. Braconnier, Y. Borthomieu and P. Hagenmuller, Mat. Res. Bull., 22 (1987) 741.

[6] L. Guerlou-Demourgues, J. J. Braconnier and C. Delmas, J. Solid State Chem., 104 (1993) 359.

[7] J. Twu and P. K. Dutta, J. Phys. Chem., 93 (1989) 7863.

[8] M. A. Drezdzon, Inorg. Chem., 27 (1988) 4628.

[9] T. Kwon, G. A. Tsigdinos and T. J . Pinnavaia, J. Am. Chem. Soc., 110 (1988) 3653.

[10] F. Kooli, V. Rives and M. A. Ulibarri, Materials Science Forum, Trans Tech Publications, Switzerland, 152-153 (1994) 375.

[11] M. A. Ulibarri, F. M. Labajos, V. Rives, R. Trujillano, W. Kagunya and W. Jones, Inorg. Chem., 33 (1994) 2592.

[12] F. Kooli, V. Rives and M. A. Ulibarri, Inorg. Chem., 34 (1995) 5114.

[13] F. Kooli, V. Rives and M. A. Ulibarri, Inorg. Chem., 34 (1995) 5122.

[14] C. Delmas, J. J. Braconnier, Y. Borthomieu and M. Figlarz, Solid State Ionics, 28/30 (1988) 1132.

[15] S. Veil, C. R. Acad. Sc., (Paris) (1925) 932.

[16] A. Mendiboure and R. Schöllhorn, Revue de Chimie Minérale, 23 (1986) 819.

[17] O. W. Howarth and J. R. Hunt, J. Chem. Soc., Dalton Trans., (1979) 1388.

[18] J. S. Jaswal and A. S. Tracey, Inorg. Chem., 30 (1991) 3718.

[19] C. Delmas, C. Fouassier and P. Hagenmuller, Physica, 99B (1980) 81.

[20] C. Delmas, Y. Borthomieu, C. Faure, A. Delahaye and M. Figlarz, Solid State Ionics, 32/33 (1989) 104.

[21] C. Faure, C. Delmas and P. Willman, J. Power Sources, 35 (1991) 263.

[22] S. Le Bihan and M. Figlarz, J. Cryst. Growth, 13/14 (1972) 458.

[23] C. Faure, C. Delmas, M. Fouassier and P. Willmann, J. Power Sources, 35 (1991) 249.

[24] C. Faure, Y. Borthomieu, C. Delmas and M. Fouassier, J. Power Sources, 36 (1991) 113.

[25] H. T. Evans Jr, Z. Krist., 114(s) (1960) 257.

[26] W. P. Griffith, J. Chem. Soc., A (1967) 905.

[27] S. Onodera and Y. Ikegami, Inorg. Chem., 19 (1980) 615.

[28] A. F. Wells, Structural Inorganic Chemistry, 4th Ed., Clarendon Press, Oxford, (1975) 470.

[29] R. D. Shannon, Acta. Cryst., A32 (1976) 751.

[30] W. T. Reichle, Solid State Ionics, 22 (1986) 135.

[31] K. El Malki, A. de Roy and J. P. Besse, Eur. J. Solid State Inorg. Chem., 26 (1989) 339.

Publication n°3

INTERCALATION PROCESS OF METAVANADATE CHAINS INTO A NICKEL-COBALT LAYERED DOUBLE HYDROXIDE

K. S. HAN, L. GUERLOU-DEMOURGUES and C. DELMAS

Institut de Chimie de la Matière Condensée de Bordeaux - CNRS
and Ecole Nationale Supérieure de Chimie et Physique de Bordeaux,
Av. Dr A. Schweitzer, 33608 Pessac Cedex, France.

ABSTRACT

A Layered Double Hydroxide (LDH) built up of a packing of $Ni_{0.70}Co_{0.30}(OH)_2$ slabs with interlamellar $(VO_3)_n^{n-}$ metavanadate chains was prepared by a chimie douce method. In order to investigate the process of intercalation yielding this material, the structural changes of the vanadate species primarily inserted into the LDH during the preparation step were followed by X-ray diffraction, infrared spectroscopy and chemical analysis. The results show that diperoxovanadate ions are first inserted, then polycondense to give rise to $(VO_3)_n^{n-}$ metavanadate chains in the final LDH.

1. INTRODUCTION

Layered Double Hydroxides (LDHs) are well-known for their anionic exchange properties and for their use as precursors of new catalytic materials [1,2]. Their structure consists of a stacking of brucite type slabs, $\left[M^{II}_{1-y}\ L^{III}_{y}\ (OH)_2\right]$, made of edge-sharing $(M,L)O_6$ octahedra, with water molecules and X^{p-} anions intercalated within the interslab space, which leads to the general formula : $[M^{II}_{1-y}\ L^{III}_{y}\ (OH)_2]^{y+}\ X^{p-}_{y/p}\ [H_2O]_z$ [2]. The anions are inserted in order to compensate for the excess positive charge due to the partial substitution of trivalent cations (L) for divalent cations (M) within the hydroxide slab. The structure is stabilized by a hydrogen bond network between the water molecules, the anions and the slab hydroxyls as well as by electrostatic interactions between the slab and the X^{p-} anions, which act as pillars within the structure.

A new chimie douce method for the preparation of the LDHs has been performed in our laboratory, as reported in previous papers [3,4]. This method is similar to that we have already used for obtaining cobalt or iron substituted nickel hydroxides, which were intended to be used as positive electrode materials in nickel-cadmium, nickel-hydrogen or nickel-metal hydride batteries [5-7]. In comparison with the classical precipitation, the main advantage of the chimie douce method arises from the fact that the building of the hydroxide slab and the intercalation of the anionic species (X^{p-}) into the interslab space are decoupled. This allows one to better control the amount of inserted anions : the anionic amount is indeed directly related to its negative charge (p) and to the concentration of the L cation (y) within the slab, which is choosen and fixed during the step of the slab building.

We recently reported the preparation by a chimie douce method and the characterization of a new metavanadate inserted LDH, which exhibits the following general formula : $Ni_{0.70}Co_{0.30}(OH)_2\ (VO_3)_{0.34}(H_2O)_{0.58}$ [4]. This material was designated by LDH(VO_3) [4].

X-ray diffraction, infrared spectroscopy, chemical analysis as well as anionic exchange properties of this material have shown that $(VO_3)^{n-}_{n}$ metavanadate chains

consisting of corner-sharing VO_4 tetrahedra are actually intercalated between the hydroxide slabs of the LDH(VO_3) phase [4]. As expected from the poor mobility of the chains between the slabs, every attempted exchange by other anions such as carbonate was unsuccessful. Besides, a difficult accommodation of the electrostatic interactions between the chains and the $[Ni_{0.70}Co_{0.30}(OH)_2]$ slabs leads to local structural distortions within the slabs [4].

The presence of $(VO_3)_n^{n-}$ metavanadate chains within the interslab space raises the problem of the intercalation process : either the metavanadate chains are directly inserted into the interslab space during the preparation or they result from an in situ condensation, within the interslab space, of some primarily intercalated vanadate species. In order to try to answer this question, an investigation of the structural changes of the vanadate species primarily inserted into the LDH during the last step of the chimie douce preparation procedure was carried out. Therefore, studies by X-ray diffraction, chemical analysis and infrared spectroscopy of the evolution vs time of the material exposed to air were undertaken immediately after the reduction reaction. The results are reported and discussed in the present paper.

2. EXPERIMENTAL

As described in a previous paper [4], the preparation procedure of the LDH by chimie douce consists of three successive steps : (i) building of the $Ni_{0.70}Co_{0.30}O_2$ slab via the preparation of the $NaNi_{0.70}Co_{0.30}O_2$ sodium nickelate, (ii) oxidizing hydrolysis of the sodium nickelate leading to the γ-oxyhydroxide, (iii) reduction starting from the oxyhydroxide in the presence of vanadate ions, which are supplied by an NH_4VO_3/H_2O_2 medium (pH = 4).

A layered double hydroxide, which can be designated as freshly obtained LDH, was prepared by simultaneous reduction in the NH_4VO_3/H_2O_2 medium and filtration. This material was dried under vacuum, then exposed to air without any special care and characterized vs ageing time. It should be noted that the preparation conditions of LDH(VO_3), previously reported [4], are different from those of the material obtained

after an ageing in air of the freshly obtained LDH : in the former case, the ageing was performed in the liquid reaction medium during 15 days, while in the latter case, it was performed directly in air for easier experiment. Nevertheless, following the evolution of the freshly obtained LDH vs ageing time (in air) may allow to improve the knowledge of the intercalation process leading to LDH(VO_3). Several authors have reported that there are no $(VO_3)_n^{n-}$ metavanadate chains in the NH_4VO_3/H_2O_2 solution but instead complex equilibria of various peroxovanadate species, depending on pH, temperature as well as vanadium and H_2O_2 concentrations [8-14]. On the basis of these data, the evolution of the vanadate species primarily inserted into the LDH then exposed to air for increasing periods of time, was followed by X-ray diffraction, chemical analysis and infrared spectroscopy.

It should be noticed that the predominant vanadate species in the aqueous solution without H_2O_2 (pH = 4 adjusted by HCl solution) is the decavanadate anion [15-17]. Various LDHs pillared with decavanadate anions were therefore obtained by anionic exchange starting from organic-anion pillared (terephtalate as an example), chloride or carbonate inserted LDHs [18-22].

3. RESULTS AND DISCUSSION

3. 1. X-ray diffraction study

The changes with time of the X-ray diffraction patterns of the LDH exposed to air are shown in Fig. 1. The X-ray diffraction pattern of the freshly obtained LDH can be indexed with a hexagonal cell with the parameters : a = 3.03 Å and c = 10.1 Å. In such a layered material, the d_{001} and d_{110} distances correspond to the interslab distance and to half the metal-metal intraslab distance respectively. During the ageing in air, the separated (10ℓ) diffraction lines, observed in the 30-50° angular range for the freshly obtained LDH, give rise to one broad asymmetric band, which is usually observed in the case of materials exhibiting a turbostratic-like character. Therefore, no indexation can be proposed for the X-ray diffraction patterns obtained during the ageing. However, the similarity observed between all X-ray diffraction patterns shows that the distances

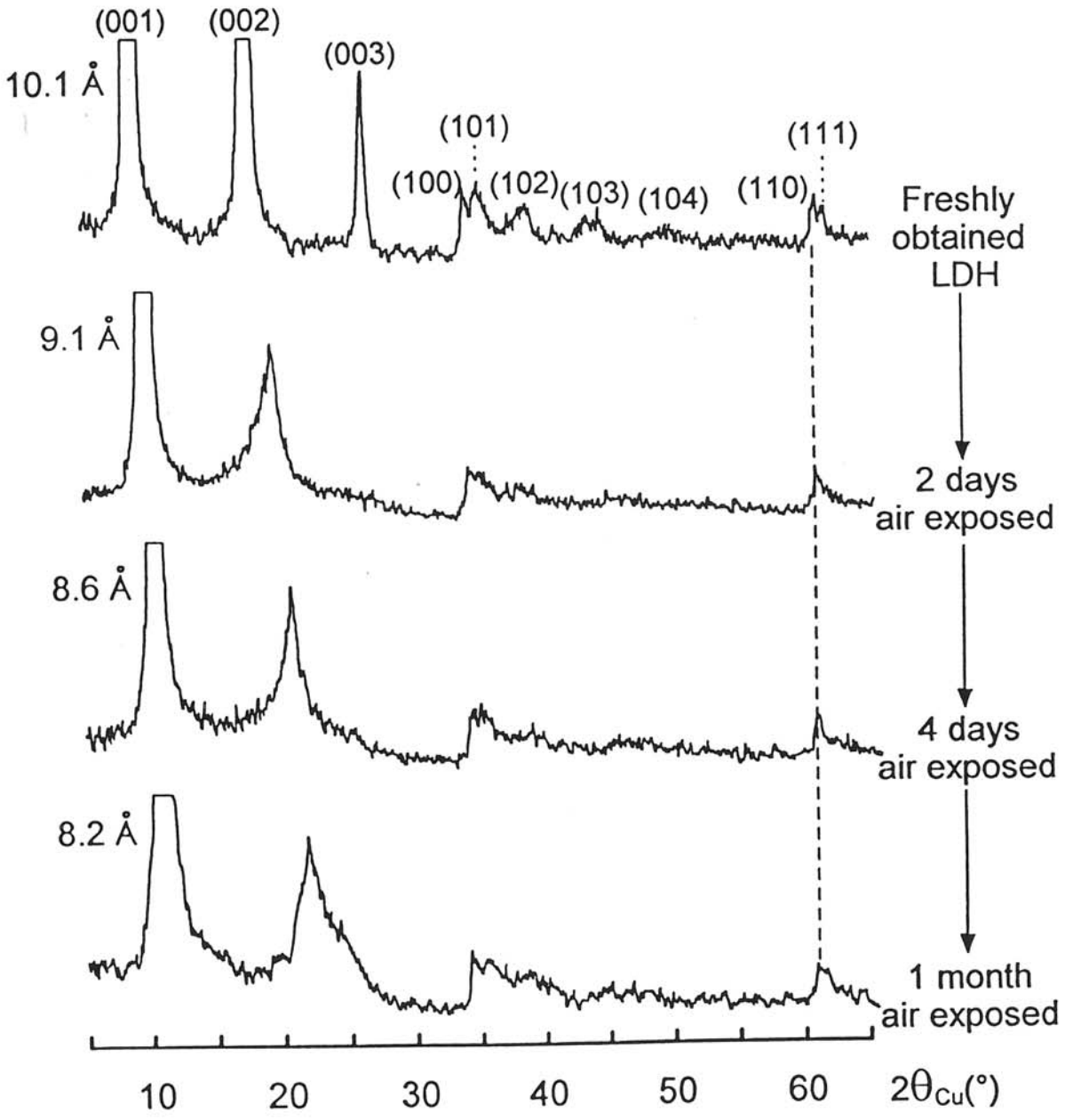

Fig. 1 : Evolution of the X-ray diffraction patterns during the exposure to air of the freshly obtained LDH.

corresponding to the lines present in the 5-15° range and in the 60-65° range reflect in all cases the interslab and the metal-metal intraslab distances respectively.

The evolution of the interslab distance, deduced from successive X-ray diffraction patterns, is represented in Fig. 2 as a function of the ageing time. The interslab distance decreases from 10.1 Å for the freshly obtained LDH to 8.2 Å for the material exposed to air for one month. Such a behavior indicates a decrease in the size of the intercalated vanadate species. However, the metal-metal intraslab distance is maintained during the ageing, which shows that the cationic oxidation states within the $Ni_{0.70}Co_{0.30}(OH)_2$ slab maintain, as expected.

The presence of a broad asymmetric band in the 30-50° range was previously reported for the LDH(VO_3) phase which contains $(VO_3)_n^{n-}$ metavanadate chains within the interslab space [4]. This behavior results from local distortions within the slabs, due to microstrains arising from the difficult accommodation of the electrostatic interactions between the interlamellar chains and the slabs [4]. Consequently, the change in the shape of the (10ℓ) and (11ℓ) bands for the air exposed LDHs may be attributed to a modification of the intercalated vanadate species which may exhibit the $(VO_3)_n^{n-}$-type chain structure like in LDH(VO_3). The vanadate species primarily inserted into the freshly obtained LDH can be reasonably assumed to be isolated entities immediately after the preparation of the LDH and to polycondensate into chains later on. In order to further investigate this hypothesis, an infrared spectroscopy study was first performed.

3. 2. Infrared study

The series of materials was studied using a Perkin-Elmer 983 spectrometer in the 4000-200 cm^{-1} range. For this purpose, the powder samples were dispersed in a few drops of acetone, placed onto a CsI plate and analyzed after evaporation of acetone.

The infrared spectra of the LDH, recorded immediately after the reduction step and then after increasing ageing times, are compared in Fig. 3 with that of LDH(VO_3) as reference. The general shapes of the spectra exhibit similarities ; in particular, the wide bands around 3400 cm^{-1} and 1650 cm^{-1} have to be attributed to the $\nu(H_2O)$ and $\delta(H_2O)$ vibration modes of water molecules intercalated within the interslab space, as

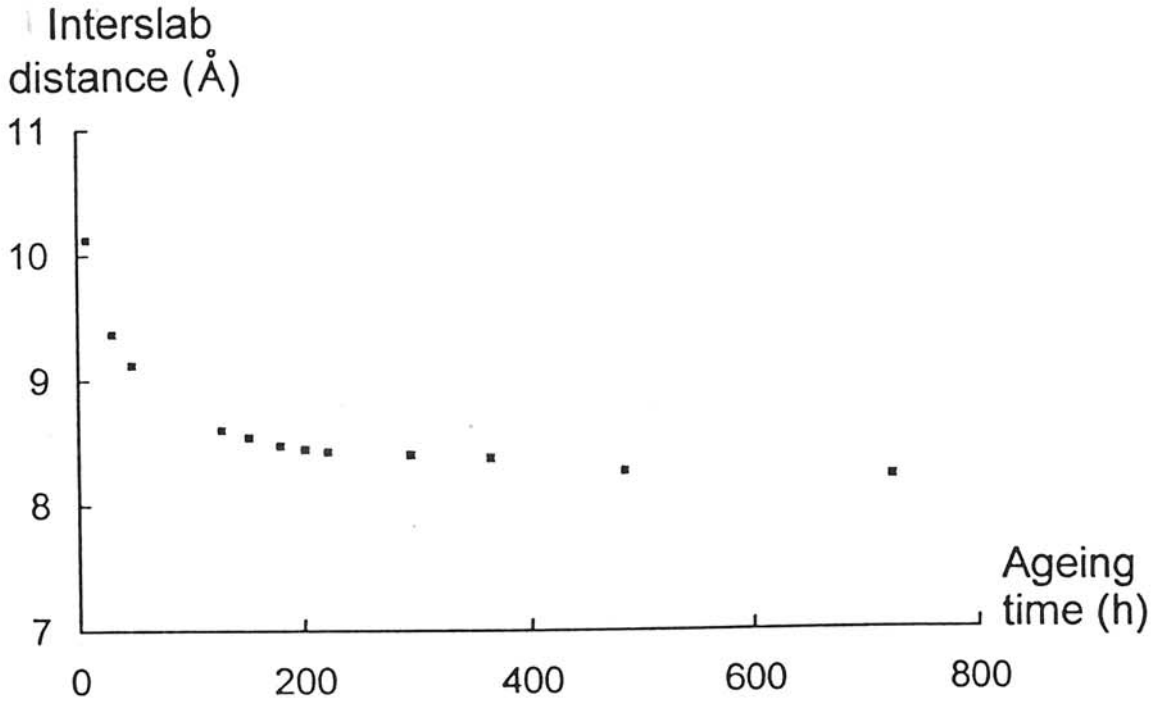

Fig. 2 : Variation of the interslab distance during the exposure to air of the freshly obtained LDH.

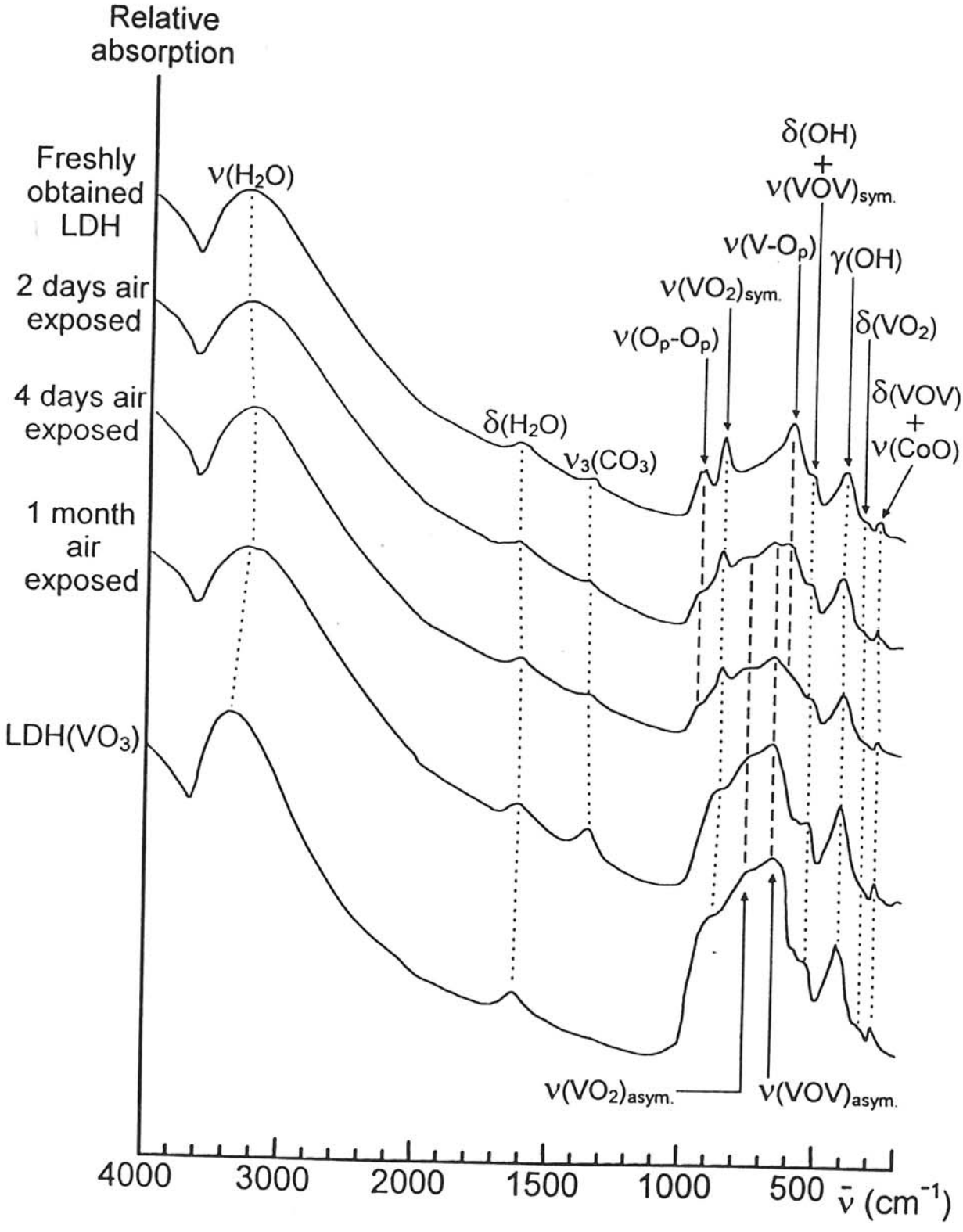

Fig. 3 : Evolution of the infrared spectra during the exposure to air of the freshly obtained LDH. The infrared spectrum of $LDH(VO_3)$ is also given for comparison.

previously reported for the homologous LDH(CO_3) material [6]. The bands at 540 cm^{-1} and 420 cm^{-1}, already observed in the infrared spectrum of the well-known β(II) phase, are characteristic of the δ (OH) and γ (OH) vibration modes of the slab hydroxyls [23-25]. These results confirm that the general structure of the material, consisting of packed (Ni,Co)$(OH)_2$ slabs with interlamellar water, is maintained during ageing.

However, the appearance of the large complex band in the 1000-200 cm^{-1} range, characteristic of inserted vanadate species, undergoes noticeable changes throughout the ageing. This behavior obviously results from modifications of the primarily inserted vanadate species, which has already been suggested by the X-ray diffraction study reported above. The values of the vibrational wave numbers observed in the 1000-200 cm^{-1} range throughout the ageing time are reported in Table I. They have been systematically compared to those corresponding to $(VO_3)_n^{n-}$ chains, present in NH_4VO_3 or in the previously reported LDH(VO_3) phase [4,26], and to the literature data reported for peroxovanadate species [27], which, as previously stated at the beginning of this paper, are predominant in the H_2O_2 reaction medium used for preparing the LDH.

Examination of Table I and Fig. 3 reveals similarities between the vibrational wave numbers observed in the 1000-200 cm^{-1} range for the material exposed for one month to air, for $(VO_3)_n^{n-}$ chains in NH_4VO_3 and for the LDH(VO_3) phase. These results suggest that the LDH after one month in air contains interlamellar $(VO_3)_n^{n-}$ metavanadate chains, as the LDH(VO_3) phase. The infrared spectrum of the freshly obtained LDH exhibits two bands at 949 cm^{-1} and 615 cm^{-1}, which, in agreement with several authors, can be attributed to the ν (O_p-O_p) and ν (V-O_p) vibration modes of peroxovanadate species [27]. Fig. 3 shows a gradual decrease in the intensity of these two bands and an increase in the intensity of the $\nu\,(VOV)_{asym.}$ and $\nu\,(VO_2)_{asym.}$ bands. These coupled evolutions show a gradual transformation of the peroxovanadate species into $(VO_3)_n^{n-}$ metavanadate chains.

Vibrational wave numbers (cm^{-1})						
Freshly obtained LDH	**2 days air exposed**	**4 days air exposed**	**1 month air exposed**	**Vanadium(V) peroxocomplex (27)**	**$(VO_3)_n^{n-}$ in NH_4VO_3 (26)**	**Vibrational modes (26,27)**
949	945	949		910		$\nu(O_p\text{-}O_p)$
874	870	874	874		935 895	$\nu(VO_2)_{sym.}$
	770	776	770		850	$\nu(VO_2)_{asym.}$
	674	678	678		690	$\nu(VOV)_{asym.}$
615	623			625		$\nu(V\text{-}O_p)$
532	538	538	538		495	$\nu(VOV)_{sym.}$ + $\delta(OH)$
337	337	338	336		333	$\delta(VO_2)$
280	280	280	280		223	$\delta(VOV)$ + $\nu(CoO)$

Table I : Evolution of the vibrational frequency values experimentally observed during the ageing in air of the freshly obtained LDH. Comparison with the values reported for vanadium peroxocomplexes and metavanadate chains in NH_4VO_3.

The presence of a vibration band at 1360 cm^{-1}, attributed to carbonate ions, must be noticed. This additional band suggests the parasitic insertion during the ageing in air of carbonate ions arising from CO_2 present in air. This phenomenon was not observed in the case of LDH(VO_3) because the preparation of this phase was performed in an air-free atmosphere.

3. 3. Chemical analysis

The elemental analysis of the LDH obtained after one month in air was carried out at the CNRS Analysis Facility in Vernaison (France). The atomic ratios, A / (Ni + Co) (where A designates a given element), deduced from the weight percentages are gathered in Table II. The values of the V / (Ni + Co) and C / (Ni + Co) atomic ratios (0.23 and 0.03 respectively) suggests the coinsertion of vanadate and carbonate ions into the interslab space. This feature is in agreement with the infrared spectrum, presented in the previous section.

In order to determine more precisely the changes in the chemical formula of the material upon ageing, the percentages of nickel and cobalt ions as well as the average oxidation state of cobalt, nickel and vanadium ions were followed throughout the ageing by classical complexometric titration with EDTA and by iodometric titration respectively. The results are gathered in Table III. A continuous increase with the ageing time of the relative amounts of nickel and cobalt within the material is observed. This is particularly obvious in Fig. 4. This evolution shows, conversely, a decrease in the weight percentage of the inserted species, which supports the hypothesis of polycondensation of the peroxovanadate species to metavanadate chains upon ageing. Interpreting the results of iodometric titration is not a simple matter because, as revealed by experiments, several species within the solution are reduced by iodide under the same conditions : nickel and cobalt ions to the divalent state, vanadium ions to the tetravalent state while $(O - O)^{2-}$ peroxide ions are reduced to O^{2-} oxide ions [4]. Therefore the iodometric titration yields the total number of electrons involved in the reduction for the sample, which can then easily be evaluated per (Ni + Co) ion. This value will be denoted as $\Delta_{titrated}$. Since the nickel, cobalt and vanadium ions have previously been shown to be at the divalent,

A	$\frac{A}{(Ni+Co)}$ molar ratio
Ni	0.70
Co	0.30
V	0.23
C	0.03
H	2.82

Table II : Values of the A / (Ni + Co) molar ratios for various elements in the LDH after one month in air.

Time exposed to air	(Ni + Co) weight %	Δ titrated	$\frac{(O-O)^{2-}}{Ni+Co}$ molar ratio
Freshly obtained LDH	39.7	1.46	0.46
1 day	39.7	1.29	0.38
2 days	41.7	1.09	0.28
4 days	44.2	0.76	0.12
6 days	44.6	0.74	0.11
7 days	44.6	0.73	0.10
8 days	44.6	0.73	0.10
10 days	44.6	0.73	0.10
1 month	45.1	0.61	0.04

Table III : Evolution of the amounts of metal cations and of peroxide ions within the LDH after various ageing times in air.

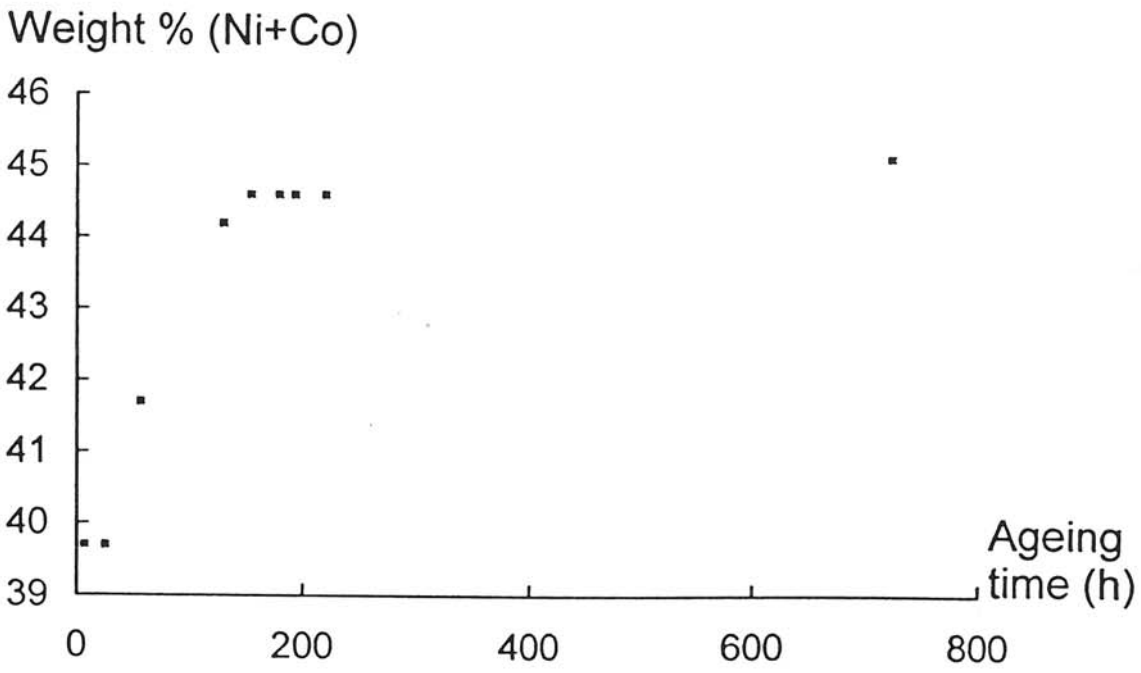

Fig. 4 : Variation of the overall weight % of nickel and cobalt (titrated by EDTA) in the LDH during its ageing in air.

trivalent and pentavalent oxidation states respectively [4], calculating the contribution to $\Delta_{titrated}$ of these ions, which will be denoted as $\Delta_{Ni+Co+V}$, is quite easy : the value of $\Delta_{Ni+Co+V}$ is the difference in average oxidation state of the nickel, cobalt and vanadium ions before and after the reduction by iodide. The calculation leads to : $\Delta_{Ni+Co+V} = 0.53$. The $\frac{(O-O)^{2-}}{Ni+Co}$ molar ratio can then be deduced as half the difference between $\Delta_{titrated}$ and $\Delta_{Ni+Co+V}$. The evolutions with the ageing time of the values of $\Delta_{titrated}$ and of the $\frac{(O-O)^{2-}}{Ni+Co}$ molar ratio are presented in Table III. The variation of the peroxide ion concentration vs ageing time is also presented in Fig. 5. A continuous decrease in the amount of peroxide ions within the LDH is observed, which validates again the hypothesis of polycondensation of the peroxovanadate species upon ageing. Provided that very few $(VO_3)_n^{n-}$ metavanadate chains are present within the freshly obtained LDH, which is consistent with the shape of the (10ℓ) set of diffraction lines in the X-ray diffraction pattern, the values of the $\frac{(O-O)^{2-}}{Ni+Co}$ and $\frac{V}{Ni+Co}$ molar ratios, 0.46 and 0.23 respectively (Table II and Table III), suggest the presence of 2 peroxide ions per vanadium ion in this material. This ratio is in accordance with the chemical formula of the diperoxovanadate ion $[V(OH)_2(OO)_2]^-$, which has been stated by several authors to be the predominant vanadate species in the reaction conditions (H_2O_2 medium, pH = 4) [8-12].

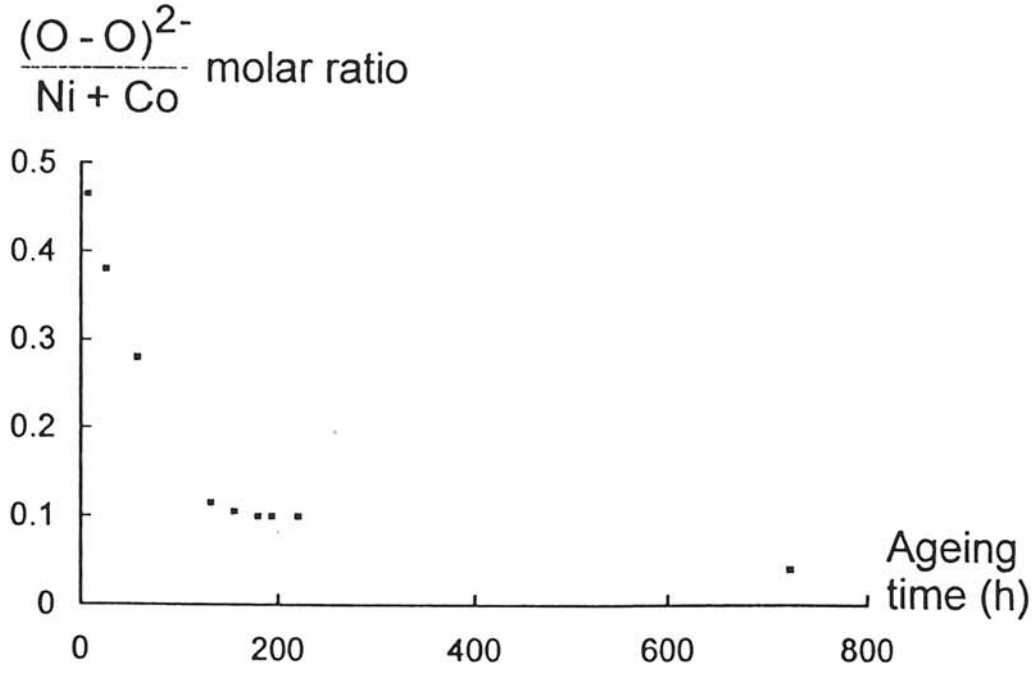

Fig. 5 : Variation of the peroxide to overall nickel and cobalt molar ratio in the LDH during its ageing in air.

3. 4. Anionic exchange reactions

Three independent exchange reactions were attempted :

❶ exchanging $(VO_3)_n^{n-}$ chains for carbonate ions, starting from the LDH(VO_3) phase. 1 g of LDH(VO_3) was added to 500 ml of a 0.11 M-K_2CO_3 solution. The material was stirred for 2 days in air, filtered, washed with deionised water and dried [4].

❷ exchanging CO_3^{2-} ions for $(VO_3)_n^{n-}$ chains, starting from the previously reported LDH(CO_3) phase. 1 g of LDH(CO_3) was added to 200 ml of a 0.5 M-$NaVO_3$ solution (pH = 7). It should be noted that the $NaVO_3$ solution (pH = 7) contains $(VO_3)_n^{n-}$ metavanadate chains. The material was stirred for 2 days, filtered, washed with decarbonated water and dried in an air-free atmosphere.

❸ exchanging CO_3^{2-} ions for peroxovanadate ions, starting from the LDH(CO_3) phase. 1 g of LDH(CO_3) was added to 200 ml of a 0.5 M-NH_4VO_3, 0.5 M-H_2O_2 solution (pH = 4). The material was obtained under the same conditions as in experiment ❷.

In all cases, five successive treatments were performed.

The first two exchange reactions failed while the third one was successful. As shown by the evolution of the infrared spectra presented in Fig. 6, in the case of experiment ❸, the disappearance of the ν_3 (CO_3) vibration band and the appearance of the ν (O_p-O_p), ν (VO_2), ν (V-O_p) and δ (VO_2) ones show the shift of an LDH(CO_3) phase to a peroxovanadate-inserted LDH. This behavior is confirmed by the evolution of the X-ray diffraction patterns which reveals that this evolution proceeds via a two-phase mixture.

The fact that experiments ❶ and ❷ were unsuccessful may be attributed to the very poor mobility of the metavanadate chains within the interslab space of the LDH. Conversely, diperoxovanadate ions are isolated and smaller than $(VO_3)_n^{n-}$ metavanadate chains so that their mobility is less affected by their steric hindrance. However, this cannot totally account for the successful exchange between the peroxovanadate ions and the carbonate ions, the well known high stability of which is

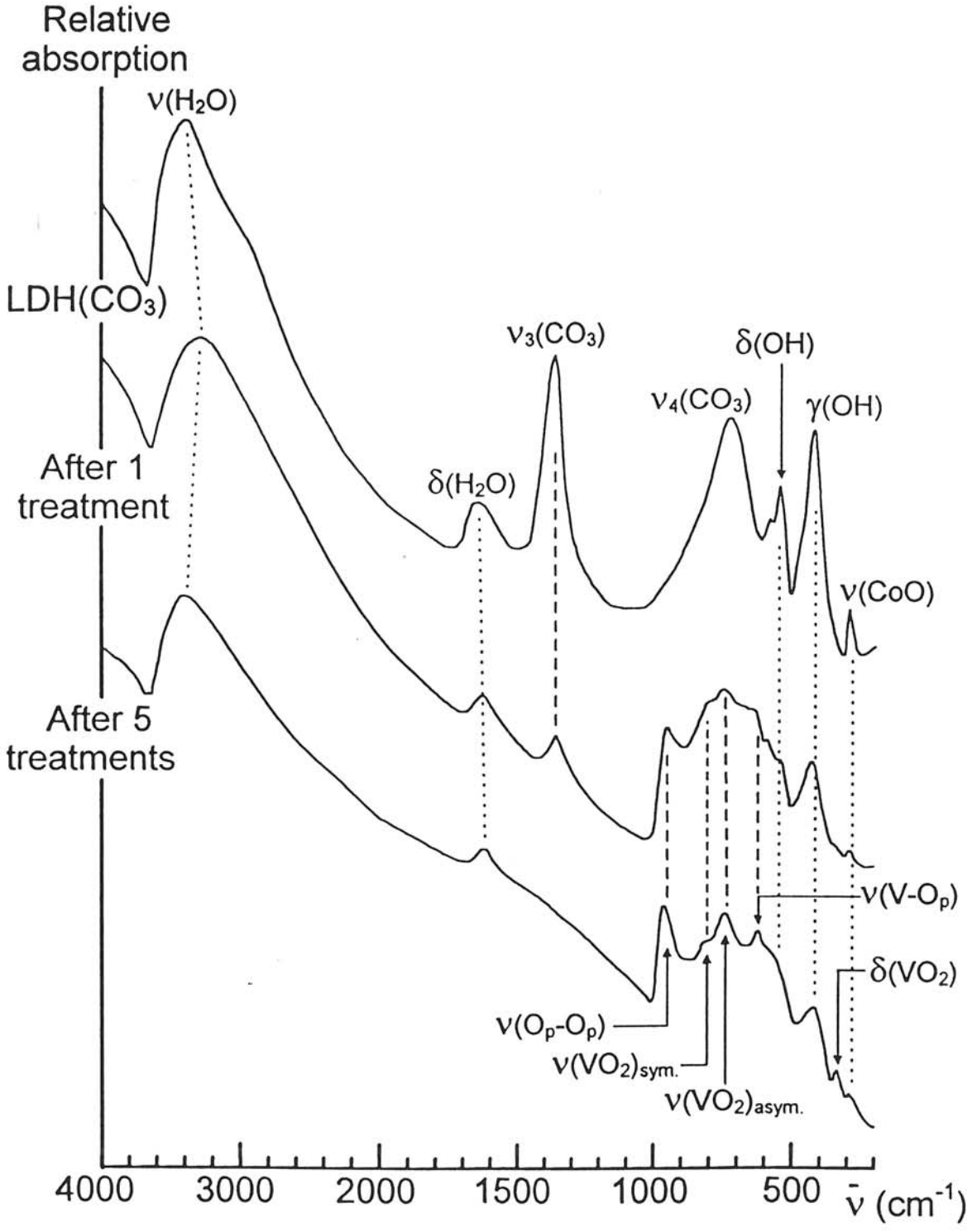

Fig. 6 : Evolution of the infrared spectra during the exchange of peroxovanadate ions (NH_4VO_3 solution at pH = 4) for carbonate ions starting from an LDH(CO_3) phase.

reported by numerous authors [3,28,29]. The successful exchange of the carbonate ions may be attributed to the concentration effect of peroxovanadate ions as well as to the pH of the reaction medium (pH = 4) which is unfavorable to the presence of carbonate ions. This is supported by works performed by Besse et al., Mendiboure et al. and F. Kooli et al., who report success in exchanging carbonate ions for sulphate, nitrate, acetate [28,30] and decavanadate [21,22] in suitable acidic media.

3. 5. General discussion

Assuming that the diperoxovanadate ions are the species first inserted into the freshly obtained LDH, the process of their polycondensation into $(VO_3)_n^{n-}$ metavanadate chains can be represented by the following reaction :

$$n\,[V(OH)_2(OO)_2]^- \rightarrow (VO_3)_n^{n-} + n\,H_2O + n\,O_2$$

Such an assumption has been validated by experiments which showed that 3.8 dm^3 of oxygen was released within 10 days from one mole of the freshly obtained LDH. This volume of oxygen must be compared to the value calculated on the basis of the variation of the $\frac{(O-O)^{2-}}{Ni+Co}$ molar ratio, which decreases from 0.46 for the freshly obtained LDH to 0.10 after 10 days in air, as indicated in Table III. The calculation yields a value of n equal to 0.18 mole per mole of LDH. The polycondensation of n moles of diperoxovanadate ions leads, according to the above written reaction, to the release of 4.0 dm^3 of oxygen. The relatively good agreement between this value and that experimentally observed validates again the hypothesis of a polycondensation of the diperoxovanadate ions into metavanadate chains.

The decrease of the interslab distance of the LDH exposed to air can be directly related to the size of the interlamellar vanadate species present within the interslab space. A calculation based on the ionic radius of oxygen (1.34 Å) and on the average bond distances reported for $(NH_4)_4[O(VO(OO)_2)_2]$ by Svensson [31], leads to a value for the thickness of $[V(OH)_2(OO)_2]^-$ peroxovanadate ions in the 5.9-6.2 Å range. In the case of the $(VO_3)_n^{n-}$ metavanadate chains, the value of the thickness was evaluated to lie in the 4.7-5.0 Å range [4]. Provided that the interslab distance can be very simply considered as

the sum of the thicknesses of the intercalated species and of the $Ni_{0.70}Co_{0.30}(OH)_2$ slab, which is approximately 4.6 Å, the calculation yields interslab distances in the 10.5-10.8 Å range for the freshly obtained LDH and 9.3-9.5 Å for the final LDH. The evolution experimentally observed through the X-ray diffraction patterns shows a decrease from 10.1 Å for the freshly obtained LDH to 8.2 Å for the material exposed to air for one month. The fact that the experimental value observed for the aged material is smaller than the calculated distance may be attributed to a phenomenon of spontaneous grafting of the interlamellar vanadate species to the slabs, which proceeds via the establishment of a V-O bond between vanadate entities and the slab. Such a behavior is currently observed after a thermal treatment of LDHs and was in particular evidenced in the case of the metavanadate inserted LDH(VO_3) phase thermally treated at 190°C, as reported in a previous paper [4]. In the latter material, each vanadium ion was shown to be linked to a slab metal cation via an oxygen anion, leading to a fragmentation of the metavanadate chains mainly into V_2O_7 entities in order to accommodate the strains. This phenomenon entailed a strong decrease of the interslab distance down to 7.2 Å as well the disappearance in the infrared spectrum of the bands attributed to the $\nu\,(VO_2)_{asym.}$ and $\nu\,(VO_2)_{sym.}$ vibrations. Nevertheless, in the case of the LDH exposed to air for one month, no significant decrease in the intensity of these bands is observed with regard to the infrared spectrum of LDH(VO_3) and the interslab distance (8.2 Å) is higher than that obtained after thermal treatment of LDH(VO_3). This behavior suggests that the grafting may be just partial for the LDH exposed to air for one month whereas it was total after thermal treatment of LDH(VO_3). This hypothesis is supported by the results of a ^{51}V NMR study, which will be reported in a forthcoming paper.

4. CONCLUSION

Investigation by X-ray diffraction, infrared spectroscopy and chemical analysis of the intercalation process of vanadate species into an LDH based on packed $Ni_{0.70}Co_{0.30}(OH)_2$ slabs has evidenced a gradual in situ polycondensation, within the LDH exposed to air, of diperoxovanadate species, primarily inserted, into metavanadate chains. This behavior entails a continuous decrease of the interslab distance with time, from 10.1 Å in the freshly obtained LDH to 8.2 Å after one month in air. However, such an evolution of the interslab distance was shown not to be able to be interpreted exclusively in terms of a polycondensation of the interlamellar species, but may also be attributed to a phenomenon of spontaneous grafting of these species to the slabs, as both phenomena can compete after the intercalation of the diperoxovanadates entities.

ACKNOWLEDGEMENT

The authors would like to thank Dr. M. Ménétrier for fruitful discussions.

REFERENCES

[1] W. Jones and M. Chibwe, "Pillared Layered Structures", IV. Mitchell Ed., Elsevier, London, (1990) 67.

[2] F. Cavani, F. Trifiro and A. Vaccari, Catalysis Today, **11** (1991) 173.

[3] C. Delmas and Y. Borthomieu, J. Solid State Chem., **104** (1993) 345.

[4] K. S. Han, L. Guerlou-Demourgues and C. Delmas, Solid State Ionics, submitted.

[5] J. J. Braconnier, C. Delmas, C. Fouassier, M. Figlarz, B. Beaudouin and P. Hagenmuller, Revue de Chimie Minérale, **21** (1984) 496.

[6] C. Delmas, J. J. Braconnier, Y. Borthomieu and P. Hagenmuller, Mat. Res. Bull., **22** (1987) 741.

[7] L. Demourgues-Guerlou, J. J. Braconnier and C. Delmas, J. Solid State Chem., **104** (1993) 359.

[8] N. J. Campbell, A. C. Dengel and W. P. Griffith, Polyhedron, **8(11)** (1989) 1379.

[9] A. T. Harrison and O. W. Howarth, J. Chem. Soc. Dalton Trans., (1985) 1173.

[10] J. S. Jaswal and A. S. Tracey, Inorg. Chem., **30** (1991) 3718.

[11] G. Kakabadse and H. J. Wilson, J. Chem. Soc., (1960) 2475.

[12] O. W. Howarth and J. R. Hunt, J. Chem. Soc. Dalton Trans., (1979) 1388.

[13] M. Orhanovic and R. G. Wilkins, J. Amer. Chem. Soc., **89(2)** (1967) 278.

[14] F. Secco, Inorg. Chem., **19** (1980) 2722.

[15] H. T. Evans, Jr. and R. M. Garrels, Geochimica et Cosmochimica Acta, **15** (1958) 131.

[16] N. Ingri and F. Brito, Acta Chemica Scandinavica, **13** (1959) 1971.

[17] M. T. Pope and B. W. Dale, Rev. Chem. Soc., **22** (1968) 527.

[18] M. A. Ulibarri, F. M. Labajos, V. Rives, R. Trujillano, W. Kagunya and W. Jones, Inorg. Chem., **33** (1994) 2592.

[19] M. A. Drezdon, Inorg. Chem., **27** (1988) 4628.

[20] T. H. Kwon, G. A. Tsidinos and T. J. Pinnavaia, J. Am. Chem. Soc., **110** (1988) 3653.

[21] F. Kooli, V. Rives and M. A. Ulibarri, Inorg. Chem., **34** (1995) 5114.

[22] F. Kooli, V. Rives and M. A. Ulibarri, Inorg. Chem., **34** (1995) 5122.

[23] C. Faure, C. Delmas, M. Fouassier and P. Willmann, J. Power Sources, **35** (1991) 249.

[24] F. P. Kober, J. Electrochem. Soc., **112** (1965) 1064.

[25] F. P. Kober, J. Electrochem. Soc., **114** (1967) 215.

[26] S. Onodera and Y. Ikegami, Inorg. Chem., **19** (1989) 615.

[27] P. Schwendt, Coll. Czech. Chem. Comm., **48** (1983) 248.

[28] A. Mendiboure and R. Schöllhorn, Revue de Chimie Minérale, **23** (1986) 819.

[29] W. T. Reichle, Solid State Ionics, **22** (1986) 135.

[30] K. El Malki, Thesis, University of Clermont-Ferrand II (France) (1991).

[31] I. B. Svensson, Acta Chemica Scand., **25** (1971) 898.

Publication n°4

^{51}V NMR INVESTIGATIONS OF VANADATE-INSERTED LAYERED DOUBLE HYDROXIDES

M. MENETRIER, K. S. HAN, L. GUERLOU-DEMOURGUES

and C. DELMAS

Institut de Chimie de la Matière Condensée de Bordeaux and Ecole Nationale Supérieure de Chimie et Physique de Bordeaux, Av. Dr A. Schweitzer, 33608 Pessac Cedex, France.

ABSTRACT

During the reduction of mixed nickel-cobalt γ-oxyhydroxides in an NH_4VO_3 / H_2O_2 medium, vanadate species are inserted into the obtained layered double hydroxides in order to compensate for the excess positive charges brought by Co^{III}.

Static ^{51}V NMR is performed at various stages on such materials, showing that the magnetic interaction exerted by single electrons of Ni^{II} on the inserted vanadium nuclei allows to determine whether they are grafted to the layer or not. For materials kept for a long time in the NH_4VO_3 / H_2O_2 solution, a partial grafting of the insered metavanadate chains is evidenced which leads to a full occupancy of the interlayer space by vanadate species. Further grafting and fragmentation of the chains is evidenced under thermal or vacuum treatment, accompanied by a collapse of the interlayer spacing.

For materials removed very early from the reaction solution, the polycondensation of the vanadate species is followed by NMR, which also shows a simultaneous partial grafting.

1. INTRODUCTION

Layered double hydroxides (LDHs) are intensively studied for their well-known anionic exchange properties and their potential use as precursors for new catalytic materials [1,2]. The general formula of these lamellar materials i.e. : $[M^{II}_{1-y}\ L^{III}_{y}\ (OH)_2]^{y+}\ X^{p-}_{y/p}\ [H_2O]_z$ ($X^{p-} = CO_3^{2-}$, NO_3^-, Cl^-, OH^-, SO_4^{2-}, etc.), shows that they consist of stacked brucite-type $\left[M^{II}_{1-y}\ L^{III}_{y}\ (OH)_2\right]$ slabs, with water molecules and X^{p-} anions inserted within the interslab spaces [2]. The role of the interlamellar anions consists in compensating for the excess positive charge due to the partial substitution of trivalent cations (L) for the divalent cations (M) within the slabs. The inserted anions also take part in the stabilization of the structure by acting as pillars.

Amongst our general studies devoted to the preparation of LDH by chimie douce methods [3-5], we have recently reported the preparation and characterization of a new LDH constituted by packed $Ni_{0.70}Co_{0.30}(OH)_2$ slabs with interlamellar $(VO_3)^{n-}_n$ metavanadate chains [6,7]. Investigations of the intercalation process have shown that the metavanadate chains are not directly inserted into the interslab space but rather result from an in situ polycondensation of diperoxovanadate anions within the LDH. Such peroxovanadate species are primarily inserted during the initial preparation of the LDH [6,7]. The changes in the overall chemical properties of the material (as studied by X-ray diffraction, IR spectroscopy, chemical analysis, TGA) cannot be interpreted exclusively in terms of a polycondensation of the interlamellar species and suggest a spontaneous partial grafting of the vanadate interlamellar ions to the slab. Such a behavior, which is generally observed under thermal treatment conditions, was unexpected at room temperature. Since Ni^{II} ions are present within the layers, one can expect that they will exert a magnetic interaction on vanadium nuclei when a Ni-O-V bond exists, as it was demonstrated for lithium in related materials [8,9]. ^{51}V NMR studies were thus performed in order to further investigate the polycondensation and grafting phenomena. The results are discussed in the present paper.

2. EXPERIMENTAL

2. 1. Material preparation

The preparation of the vanadate-inserted LDH by chimie douce was extensively described in previous papers [6,7]. Note that the material is obtained by the reduction of a cobalt substituted γ-oxyhydroxide [10] in an NH_4VO_3 / H_2O_2 medium. Two different sets of materials were obtained, depending on the preparation conditions, as schematized in Fig. 1. The pristine material of one set, which was designated as LDH(VO_3) in a previous paper, was obtained after 15 days in the reducing solution [6]. It was shown to contain interlamellar $(VO_3)_n^{n-}$ metavanadate chains. This material was then either thermally treated at 100°C and 190°C or vacuum treated. The pristine material of the other set, which is designated as freshly obtained LDH, was prepared by pouring the NH_4VO_3 / H_2O_2 solution onto the γ-oxyhydroxide present on a filter. It was dried under vacuum, then exposed to air and characterized vs ageing time [7]. As indicated above, the preparation conditions of the LDH(VO_3) and of the material obtained after an ageing in air of the freshly obtained LDH are different : the ageing was performed in the liquid reaction medium in the former case whereas it was done so in air in the second case. Nevertheless, following the evolution of the freshly obtained LDH vs ageing time in air may allow to improve the knowledge of the intercalation process leading to LDH(VO_3).

2. 2. NMR

^{51}V NMR (I = 5/2) spectra were recorded on a Bruker MSL 200 spectrometer at 52.6 MHz. $VOCl_3$ was used as an external reference set at 0 ppm. A quadrupolar-type echo sequence with an 8-step phase cycling was utilised. The length of the two pulses was 1.8 μs. Indeed, a 90° pulse length would have corresponded to 3.3 μs and resulted in too narrow an irradiated zone, owing to the width of the spectra recorded. The echo sequence used therefore results in a selectivity of the central transition vs the quadrupolar satellites. No analysis of the quadrupolar part of the spectra was therefore performed. Even with such short pulses, the width of the spectra prevents any quantitative analysis. Only qualitative evolutions are therefore discussed from these data.

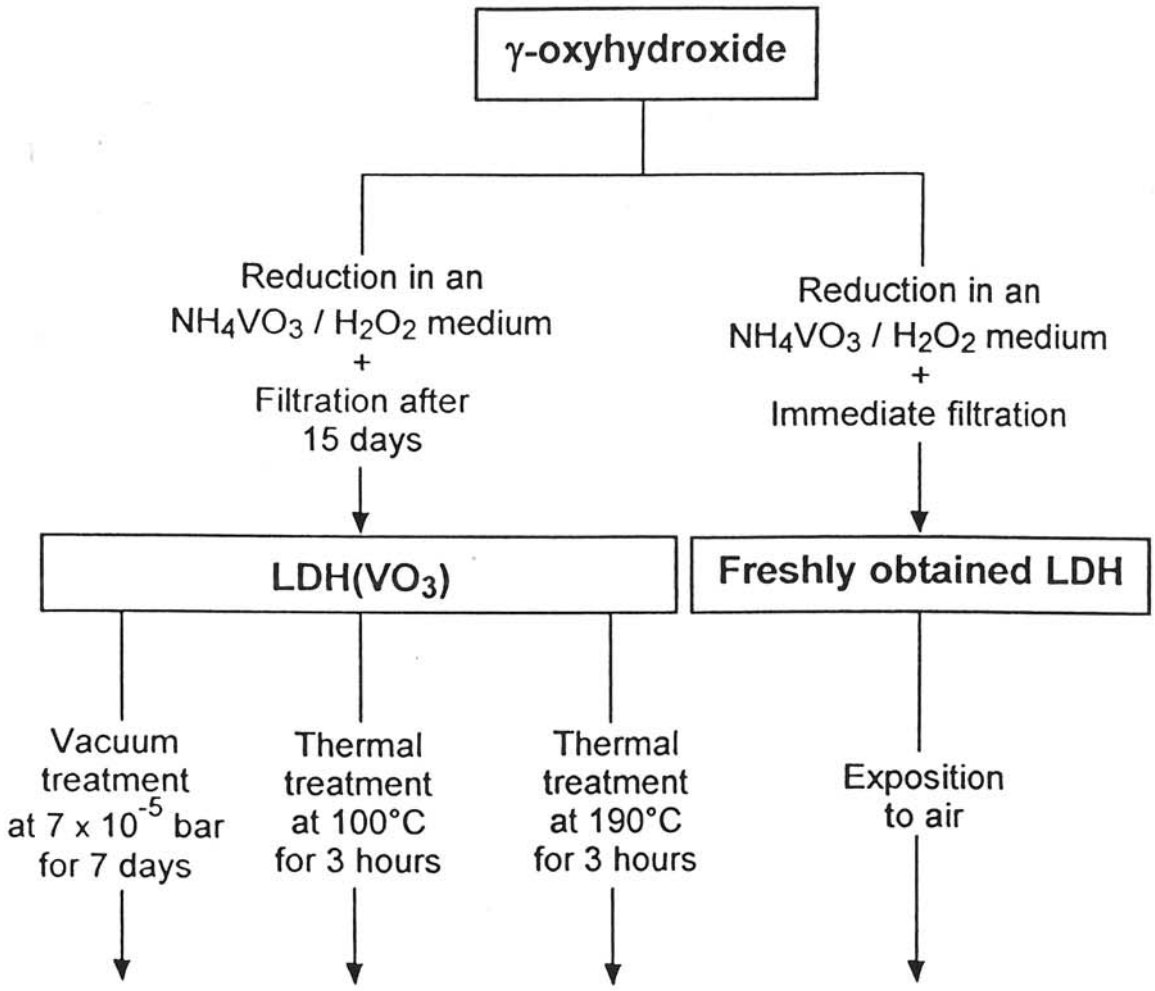

Fig. 1 : Preparation scheme of the two sets of materials characterized by ^{51}V NMR.

3. RESULTS AND DISCUSSION

3. 1. Evolution of LDH(VO_3) upon vacuum or thermal treatment

Two different compositions of LDH(VO_3) were investigated. One corresponds to an $Ni_{0.69}Co_{0.31}(OH)_2$ slab formula while the other corresponds to $Ni_{0.62}Co_{0.38}(OH)_2$. For simplicity, an LDH(VO_3) type material with a given y cobalt composition will be designated hereafter as $LDH_y(VO_3)$. The X-ray diffraction patterns of $LDH_{0.31}(VO_3)$ after the various treatments are reported in Fig. 2. They show a significant decrease of the interslab distance (diffraction line in the 5-15° $2\theta_{Cu}$ range) when a thermal or vacuum treatment is performed. Although not reported here, the evolution observed for $LDH_{0.38}(VO_3)$ is quite similar. This behavior, already discussed in a previous paper, is assigned to a grafting / fragmentation of the metavanadate chains to the slabs, which proceeds via a slab dehydroxylation and deprotonation [6]. Actually, the overall reaction consists of a water release. A similar grafting has previously been observed in the case of inserted sulfate ions by Besse et al. [11] and in our laboratory [10]. In addition, the changes of the X-ray diffraction patterns show also a strong modification in the shape of the diffraction bands located in the 30-45° and 60-70° $2\theta_{Cu}$ ranges. The broad asymmetric diffraction bands observed for the starting $LDH_{0.31}(VO_3)$ material are replaced by separate diffraction lines after thermal or vacuum treatment so that the X-ray diffraction patterns of the variously treated materials can be indexed in the hexagonal system. The broad bands have been attributed to local structural distortions within the slab of the pristine $LDH_{0.31}(VO_3)$ rather than to a turbostratic character which would correspond to a misorientation of the slabs stacked along the c axis [6]. The local structural distortions have been assumed to arise from strains due to electrostatic interactions between the chains and the slabs. During the thermal or vacuum treatments, the grafting of the chains to the slabs entails a partial fragmentation of the chains for steric reasons, which leads to a decrease of the intraslab local structural distortions [6].

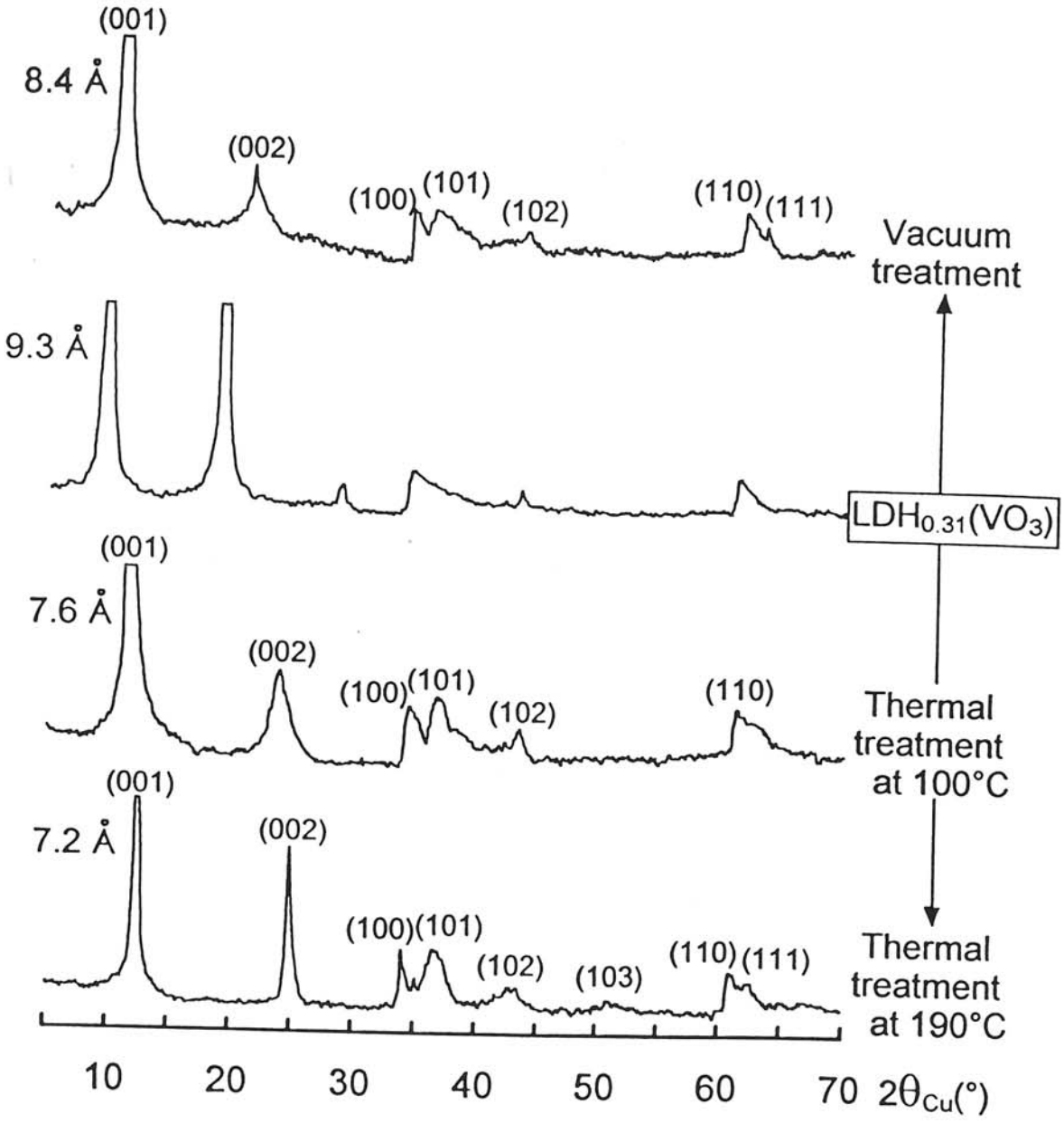

Fig. 2 : X-ray diffraction patterns of $LDH_{0.31}(VO_3)$ and after the various treatments.

The ^{51}V NMR spectra of these various materials are presented in Fig. 3 and 4 for $y = 0.31$ and $y = 0.38$, respectively. The pristine materials spectra (particularly the $y = 0.38$ one) are dominated by a narrow signal at -600 ppm with quadrupolar satellite transitions at the base. Upon vacuum or thermal treatment, another signal at 850 ppm grows at the expense of the former. This new signal is less defined (both in the quadrupolar base and the central peak which seems to contain two contributions) and broader than the former one. Its relative magnitude correlates well with the decrease in interlayer spacing from XRD. It is attributed to vanadium atoms which are grafted via oxygen to the nickel atoms of the $Ni_{1-y}Co_y(OH)_2$ slabs [6]. Indeed, the existence of V-O-Ni bonds allows the transfer of a density of presence probability of unpaired electrons from the Ni^{II} ($t_2^6\ e^2$) to the vanadium atoms. This so-called Fermi contact shift interaction, which is magnetic in nature, causes a broadening and shift of the NMR signal vs that due to vanadium atoms with no V-O-Ni bond at -600 ppm. The grafting is thus seen by NMR through the unpaired electrons of Ni^{II}, while no magnetic interaction is expected for vanadium atoms grafted to an oxygen which would be bonded only to diamagnetic Co^{III} ions. The disappearance of the narrow signal at -600 ppm in the NMR spectra recorded after thermal treatment at 190°C suggests that virtually all vanadium ions are grafted. This is in agreement with TGA results [6]. Fig. 3 and 4 show that the $\frac{\text{nongrafted vanadium}}{\text{grafted vanadium}}$ ratio is higher for the vacuum treated material than for the thermally treated ones. This is in agreement with their respective interslab distances, as shown in the X-ray diffraction patterns of Fig. 2.

Comparing the NMR spectra of the pristine $LDH_{0.31}(VO_3)$ and $LDH_{0.38}(VO_3)$ materials from Fig. 3 and 4 respectively reveals that the relative magnitude of the two signals is significantly different in the two materials. Indeed, the relative magnitude of the 850 ppm signal grows with the Ni / Co ratio, as shown in Fig. 5 for $y = 0.38$, $y = 0.31$ and $y = 0.25$. Since vanadium ions grafted to an oxygen ion with only Co as neighbors would contribute to the -600 ppm signal, the changes observed might be influenced by the number of nickel atoms present, in addition to representing a genuine change in the grafted / nongrafted vanadium ratio.

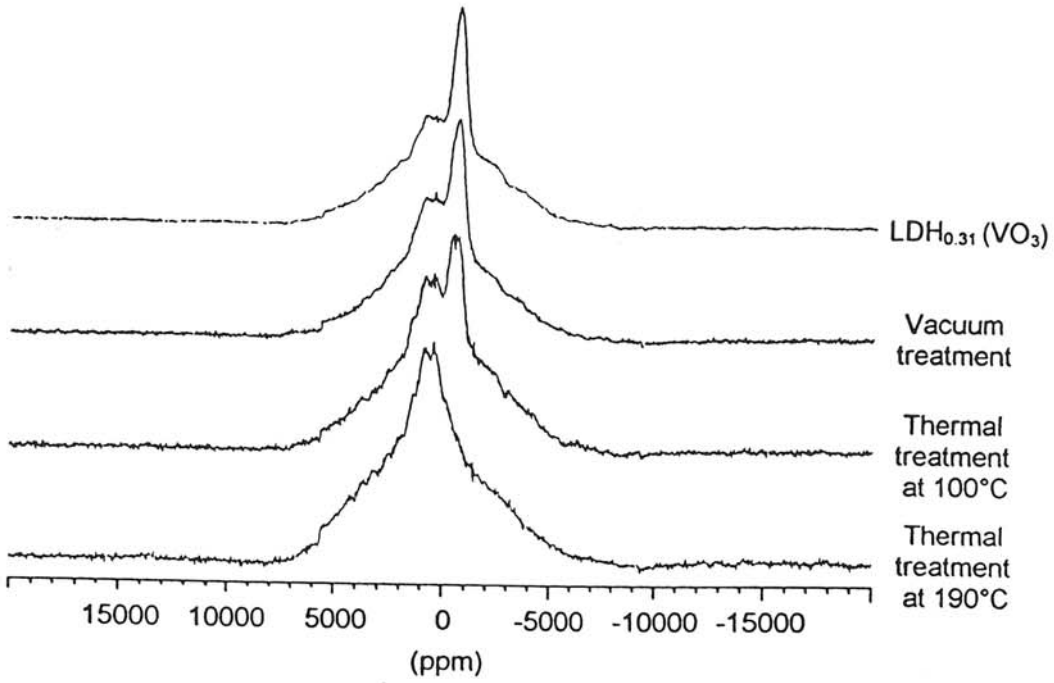

Fig. 3 : Static ^{51}V NMR spectra of $LDH_{0.31}(VO_3)$ and after the various treatments (Reference is $VOCl_3$).

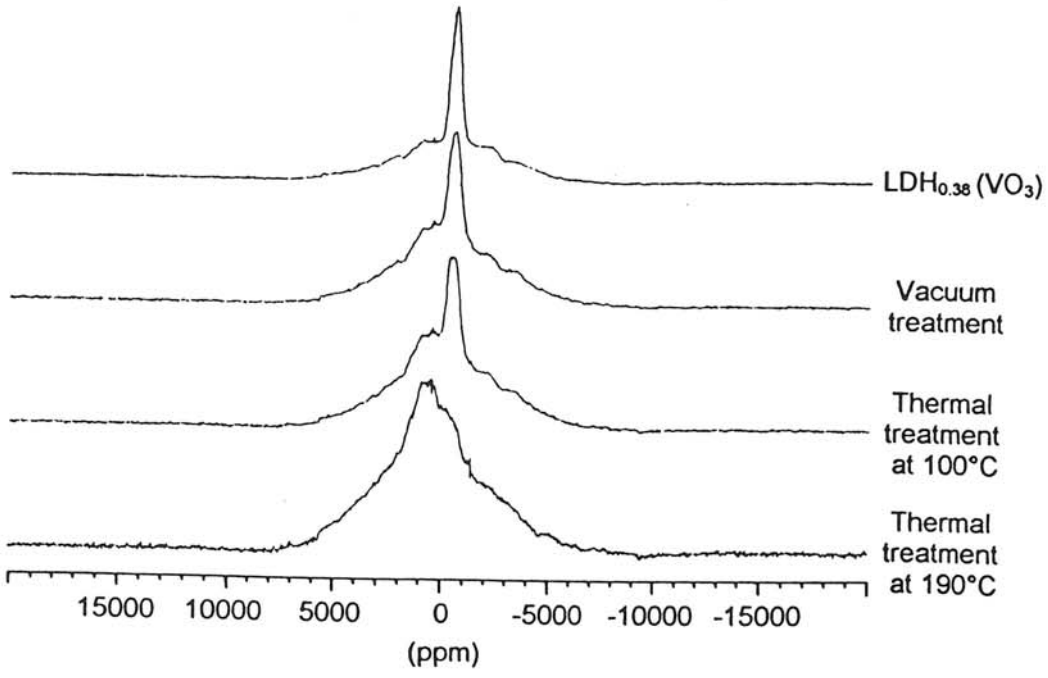

Fig. 4 : Static ^{51}V NMR spectra of $LDH_{0.38}(VO_3)$ and after the various treatments.

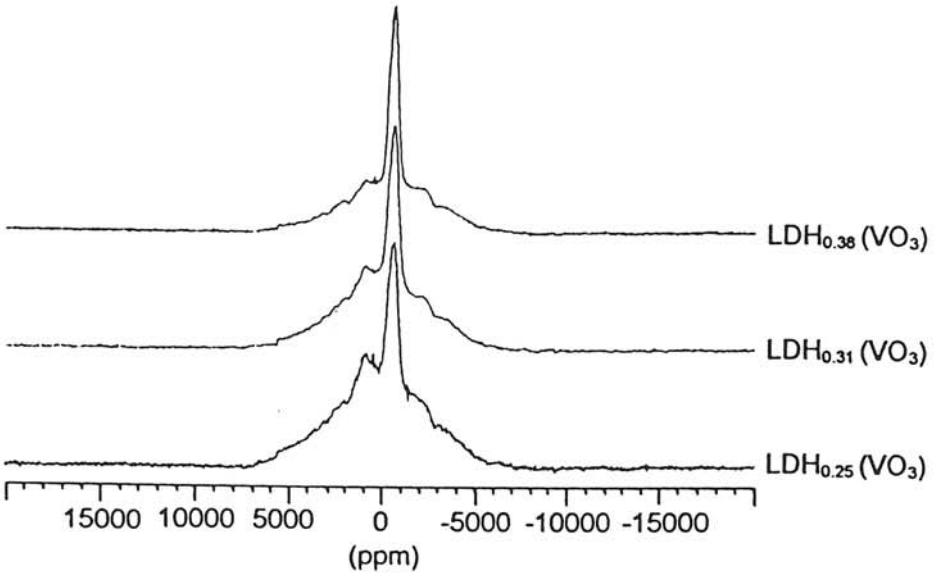

Fig. 5 : Static ^{51}V NMR spectra of various $LDH_y(VO_3)$ phases (y = 0.25, 0.31, 0.38).

In order to eliminate that ambiguity, chemical analyses have been carried out and are reported in Tab. I. If all vanadium ions present were in the form of nongrafted $(VO_3)_n^{n-}$ chains, the achievement of the charge compensation would require the presence of one vanadium ion per cobalt ion. Instead, the values of the V / (Ni + Co) molar ratio, which are quite similar (close to 0.4) whatever the cobalt content (Table I), imply that not all inserted vanadium atoms bring a negative charge, i.e. that some of them must be grafted to the slab, and that a corresponding number of OH^- have been released into the acidic medium, their charges being compensated for by the insertion of additional vanadate species from the solution. This process seems to go on until the whole interslab space is occupied by vanadate anions i.e. approximately 0.4 vanadium ion per (Ni + Co) ion, as indicated by the chemical analyses. Thus, 0.16 VO_4 groups per (Ni + Co) ion would be grafted for $y = 0.25$, 0.07 for $y = 0.31$ and 0.01 for $y = 0.38$, leading to the presence of 1.84, 1.93 and 1.99 OH groups per (Ni + Co) ion respectively, against 2 in the case of the $(Ni,Co)(OH)_2$ nickel hydroxide. This is in good agreement with the increase in relative magnitude of the signal observed for vanadium grafted to nickel ions when y decreases in Fig. 5.

3. 2. Evolution of the freshly obtained vanadate-inserted LDH exposed to air

The X-ray diffraction patterns upon ageing in air of the freshly obtained vanadate-inserted LDH are shown in Fig. 6. Their changes have already been discussed in details in a previous paper [7] and correlated with the results of various techniques (IR spectroscopy, chemical analysis). The large decrease of the interslab distance from 10.1 Å for the fresh LDH to 8.6 Å after 4 days in air must be related to the polycondensation of primarily inserted diperoxovanadate ions to metavanadate chains, as stated in the introduction of the present paper. The modification of the inserted vanadate species also shows up through a change in the shape of the (10ℓ) and (11ℓ) lines, which are well-separated for the freshly obtained LDH and tend to broaden into large asymmetric bands upon ageing in air. This behavior, which was characterized as a loss of the local structural order within the slab, is due to the evolution of the large isolated diperoxovanadate species into metavanadate chains, which tend to create strains within the slab lattice [7]. Nevertheless, some points worthy of note remain.

	$\frac{A}{(Ni + Co)}$ molar ratio		
A	**$LDH_{0.25}(VO_3)$**	**$LDH_{0.31}(VO_3)$**	**$LDH_{0.38}(VO_3)$**
Ni	0.75	0.69	0.62
Co	0.25	0.31	0.38
V	0.41	0.38	0.39
H	3.20	3.38	3.26

Table I : Chemical analyses results of various $LDH_y(VO_3)$ phases (y = 0.25, 0.31, 0.38).

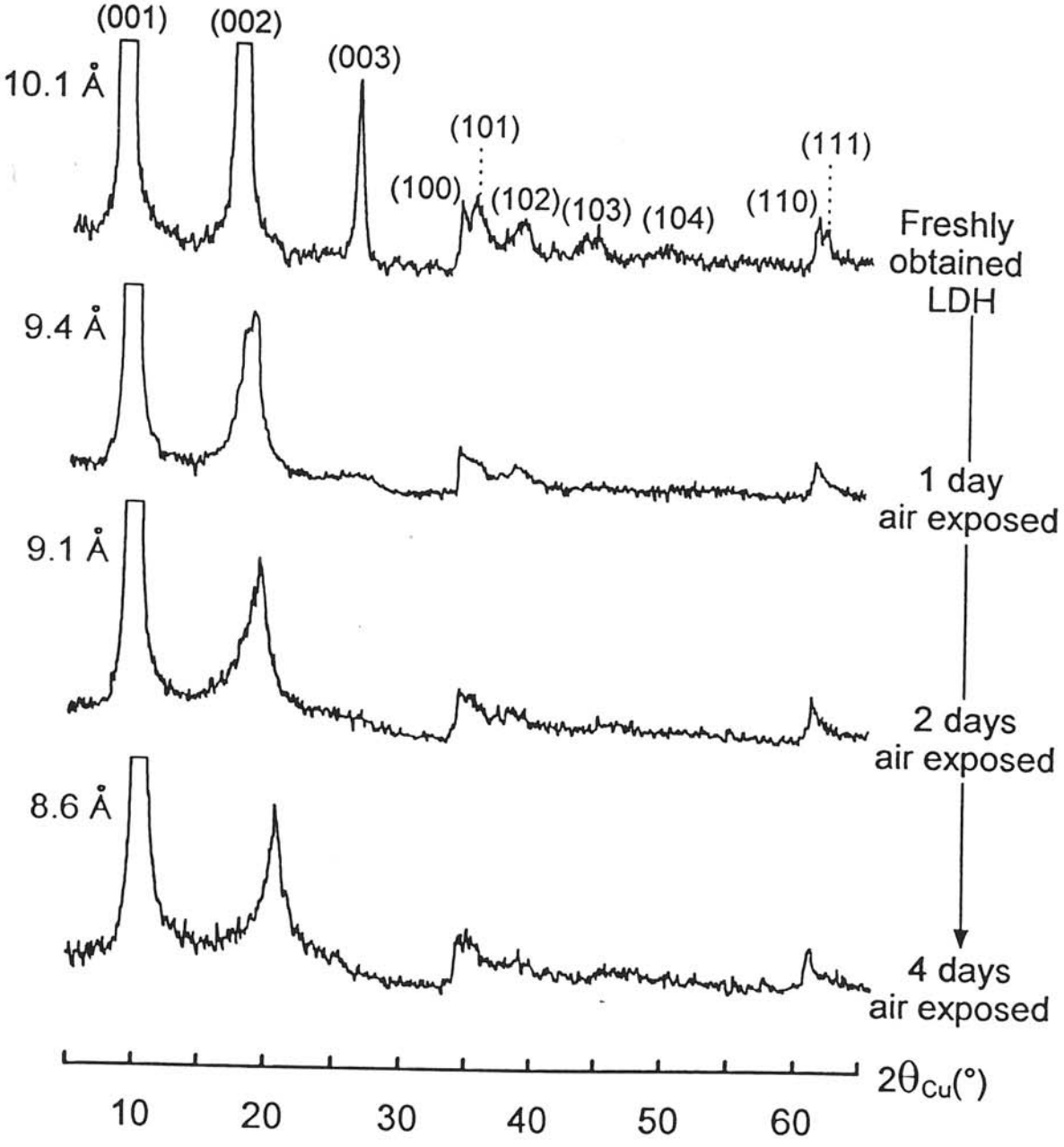

Fig. 6 : X-ray diffraction patterns of the freshly obtained LDH and after ageing in air.

As suggested in the previous section, it appears that grafted vanadium ions coexist with nongrafted ones within the $LDH_y(VO_3)$ materials even before any thermal or vacuum treatment. In order to study the very beginning of the polycondensation and grafting process, the reduction reaction to yield the LDH and the filtration were simultaneously carried out and the material was dried under vacuum as quickly as possible. This material was then exposed to air and NMR spectra were periodically recorded ; they are shown in Fig. 7. Right after the filtration, the signal at -600 ppm is rather broad and ill-defined with a negligible contribution at 850 ppm, which may correspond to the presence of several vanadate species not grafted to the layers : peroxovanadate ions and also intermediate species arising from partial and gradual polycondensation of the diperoxovanadate ions to metavanadate chains [7]. That asymmetric broad line, centered around -600 ppm, tends to loose its feature upon ageing and to give rise after 4 days of exposure in air to a narrow line identical to that of $LDH_y(VO_3)$, which can therefore be attributed to vanadium ions from metavanadate chains. Simultaneously, the signal at 850 ppm which was attributed in the previous section to vanadium atoms grafted to the slab, grows in relative magnitude (this is not clearly apparent at first sight on the figure because of the narrowing with time of the line at -600 ppm). This shows that a grafting phenomenon simultaneously occurs during the polycondensation step. After the initial modification of the NMR spectra during the first 4 days just described, no more modification of the -600 ppm signal shape occurs. However, the relative magnitude of the signal at 850 ppm increases slowly with time in the same way as it does for the $LDH_y(VO_3)$ materials, showing that the grafting of the metavanadate chains goes on spontaneously. In this case, the polycondensation and grafting occur while the material is kept outside the medium containing vanadate species. Therefore, the grafting must proceed differently from that discussed in the first section, i.e. the OH^- ions extracted from the slab cannot be replaced by more vanadate species. Indeed, the total amount of V is 0.23 per (Ni + Co) whereas it was around 0.4 for the first case.

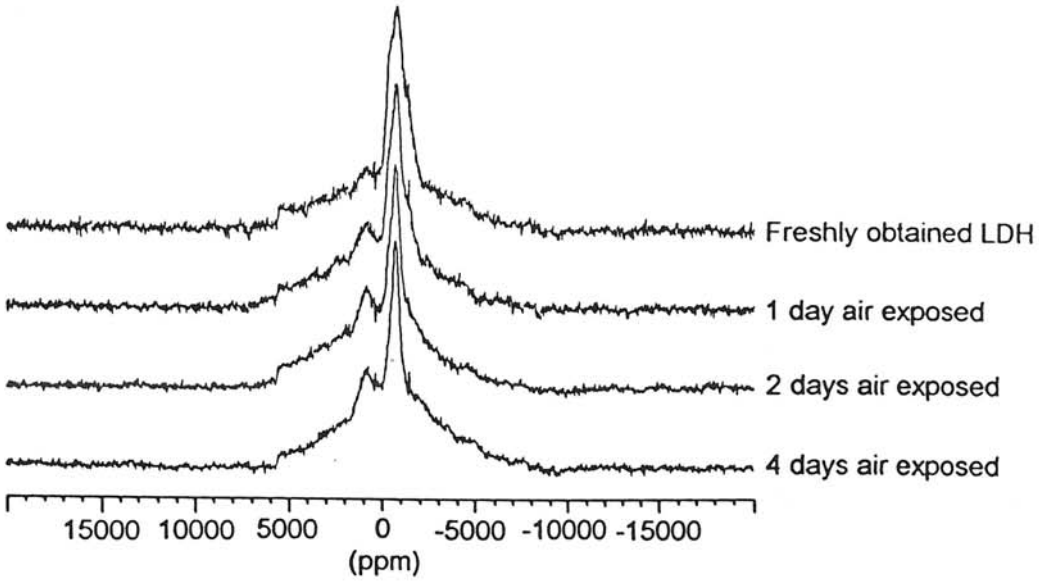

Fig. 7 : Static ^{51}V NMR spectra of the freshly obtained LDH and after ageing in air.

4. CONCLUSION

During the reduction of mixed nickel-cobalt γ-oxyhydroxides in an NH_4VO_3 / H_2O_2 medium, rather complex phenomena seem to occur.

Through the magnetic interaction exerted by Ni^{II} ions, ^{51}V NMR is able to distinguish vanadium atoms which are grafted to the layer from those which are not. It thus appears that, as soon as they are inserted for compensating the excess positive charges due to the presence of Co^{III}, the isolated diperoxovanadate ions undergo a competition between polycondensation and grafting processes.

When the material is kept in the reducing solution containing vanadate species, a partial grafting occurs during the polycondensation and causes a dehydroxylation of the slab. In order to maintain the required charge compensation, more vanadate ions are inserted until the interslab space is filled.

When it is removed and filtered very early from the solution, only as many vanadate ions are inserted as are necessary for the charge compensation. The polycondensation then occurs in air and can be followed by NMR, which in addition shows again a partial simultaneous grafting.

In both cases, after the polycondensation step, partially grafted metavanadate chains seem to be present. Then, further grafting and fragmentation occur, which involve both a dehydroxylation and a deprotonation of the slab, and thus lead to the formation of water. This process is very slow under ambiant conditions, but is much faster and even brought to completion by heating or applying vacuum (i. e. helping to remove the water produced). Such a grafting causes a collapse of the interlayer spacing.

REFERENCES

[1] W. Jones and M. Chibwe, "Pillared Layered Structures", IV. Mitchell Ed., Elsevier, London, (1990) 67.

[2] F. Cavani, F. Trifiro and A. Vaccari, Catalysis Today, **11** (1991) 173.

[3] J. J. Braconnier, C. Delmas, C. Fouassier, M. Figlarz, B. Beaudouin and P. Hagenmuller, Revue de Chimie Minérale, **21** (1984) 496.

[4] C. Delmas, J. J. Braconnier, Y. Borthomieu and M. Figlarz, Solid State Ionics, **28/30** (1988) 1132.

[5] C. Delmas, Y. Borthomieu, C. Faure, A. Delahaye and M. Figlarz, Solid State Ionics, **32/33** (1989) 104.

[6] K. S. Han, L. Guerlou-Demourgues and C. Delmas, Solid State Ionics, submitted.

[7] K. S. Han, L. Guerlou-Demourgues and C. Delmas, Solid State Ionics, submitted.

[8] M. Menetrier, A. Rougier and C. Delmas, Solid State Com., **90** (1994) 439.

[9] C. Marichal, J. Hirschinger, P. Granger, M. Menetrier, A. Rougier and C. Delmas, Inorg. Chem., **34** (1995) 1773.

[10] C. Delmas and Y. Borthomieu, J. Solid State Chem., **104** (1993) 345.

[11] K. El Malki, A. de Roy and J. P. Besse, Eur. J. Solid State Inorg. Chem., **26** (1989) 339.